

The University of Wisconsin Library
Manuscript Theses

Unpublished theses submitted for the Master's and Doctor's degrees and deposited in The University of Wisconsin Library are open for inspection, but are to be used only with due regard to the rights of the authors. Bibliographical references may be noted, but passages may be copied only with the permission of the authors, and proper credit must be given in subsequent written or published work. Extensive copying or publication of the thesis in whole or in part requires also the consent of the Dean of the Graduate School of The University of Wisconsin.

This thesis by PAUL M. PALUCH
has been used by the following persons, whose signatures attest their acceptance of the above restrictions.

A Library which borrows this thesis for use by its patrons is expected to secure the signature of each user:

NAME AND ADDRESS

DATE

**DEVELOPMENT OF A SYSTEM TO AUTOMATICALLY CONTROL
THE APPLICATION RATE OF WASTE SPREADERS**

by

PAUL M. PALUCH

A thesis in partial fulfillment of the requirements for the degree of

MASTERS OF SCIENCE

(Mechanical Engineering)

at the

UNIVERSITY OF WISCONSIN - MADISON

1997

HEU
AWO
P181
P385

AW39049

ACKNOWLEDGEMENTS

This thesis was made possible only with the guidance and assistance of many people. I would like to especially thank Dr. Richard Straub for being an excellent mentor who always took an active role in my academic and professional growth. Dr. Brian Holmes and Dr. Kevin Shinnars aided me with their expert tutelage and commitment to the project. Chuck Shaeffer, Hal Bohne, and Michael Boettcher, were always giving of their time and skills which greatly improved the quality of the research. The contributions of Fred Kuhn and the Gehl Company, and Bruce Johnston of Digi-Star were integral to the success of the research.

The University of Wisconsin Biological Systems Engineering Department and the United States Dairy Forage Research Lab warrant recognition for providing the facilities and equipment for the design and testing of my research project. Those providing valuable assistance included: Brad Igl, Karl Struckmeyer, and Jeff Nelson.

I would also like to bestow a special gratitude to my wife Jennifer for her never ending understanding and selflessness that allowed me to obtain my goal. Most importantly, I would like to thank my Mom and Dad for their encouragement and all encompassing support.

ABSTRACT

Livestock producers do not feel sufficiently confident about the quantity of manure they are applying to take full credit for the plant nutrients applied. Consequently, excess commercial fertilizer is being applied to insure good crop yields. Excessive manure and fertilizer nutrients are contributing to surface and ground water contamination. A system is needed to improve the accuracy of manure application rates which will increase producers' confidence about the applied plant nutrient application rate.

A side discharge spreader has been modified to include a weighing system which employs five load cells and a signal conditioning unit. The weighing system was statically calibrated and tested. The machine's spread pattern was quantified by collecting its discharge on plastic sheets as it was operated through the field. From these tests, a correlation between moisture content of the manure and the spread pattern's spread width was derived. Also, an overlap dimension was statistically determined to insure an uniform application when spreading.

A ground speed sensor, discharge gate position detector, microprocessor, and large digit display unit were incorporated into the spreader to measure and monitor the spreader's discharge. A hydraulic directional control valve was introduced into the spreader's hydraulic system and linked to the microprocessor to automatically control the manure discharge rate. With an operator-entered spread width, the system will control the discharge gate height automatically to achieve the desired discharge rate based upon the desired application rate. This system was tested and proved to be effective with an error of 20.0%.

TABLE OF CONTENTS

CHAPTER 1 INTRODUCTION AND LITERATURE REVIEW

1.1 Introduction.....	1
1.2 Nutrient Management.....	6
1.3 Crediting.....	9
1.4 Current Manure Spreader Technology Introduction.....	15
1.5 Current Methods of Determining Application Rates.....	18
1.6 Current Spreading Technology and Application Research	20

CHAPTER 2 OBJECTIVES.....25

CHAPTER 3 DESIGN CRITERIA AND SYSTEM COMPONENT DESCRIPTION

3.1 Design Criteria.....	27
3.2 System Component Description.....	34

CHAPTER 4 SPREADER MODIFICATION AND FABRICATION DETAILS

4.1 Spreader Specifications.....	44
4.2 Weighing System.....	44
4.3 Speed Sensing System.....	59
4.4 Position Sensing System.....	65
4.5 Directional Control Valve.....	69

CHAPTER 5 CONTROLLER SPECIFICATIONS AND ELECTRICAL SUBSYSTEMS

5.1 Controller Specifications.....	73
5.2 Controller Configuration.....	75
5.3 Electrical Subsystems.....	77

5.4 The Complete Control System.....	91
CHAPTER 6 PRELIMINARY SYSTEM RESPONSE AND OVERLAP TESTING	
6.1 Load Cell Calibration.....	95
6.2 Static Weight Test.....	95
6.3 Dynamic Weight Test	98
6.4 Dynamic Discharge and Overlap Testing.....	99
CHAPTER 7 CONTROLLER THEORY, DESIGN AND TEST RESULTS	
7.1 Controller Theory.....	117
7.2 Controller Design.....	119
7.3 Controller Programming Logic.....	125
7.4 Controller Test Results.....	131
7.5 Controller Precision.....	151
CHAPTER 8 CONCLUSIONS	
8.1 Spreader Performance.....	153
8.2 Controller Performance.....	155
CHAPTER 9 RECOMMENDATIONS FOR FUTURE RESEARCH	
9.1 Spreader Recommendations.....	157
9.2 Controller Recommendations.....	158
REFERENCES.....	162
APPENDIX A.....	164
APPENDIX B.....	166
APPENDIX C.....	169

APPENDIX D.....171

LIST OF FIGURES

Figure 4.1: Digi-Star's standard cylinder end load cell.....	46
Figure 4.2: Digi-Star's tapered cylinder end load cell.....	46
Figure 4.3a: Top view of spreader's original hitch design.....	47
Figure 4.3b: Side view of spreader's original hitch design.....	47
Figure 4.4: Load cell sleeve assembly.....	48
Figure 4.5a: Exploded top view of the spreader's modified hitch with load cell.....	49
Figure 4.5b: Exploded side view of the spreader's modified hitch with load cell.....	49
Figure 4.6: Isometric view of original tandem beam axle assembly.....	50
Figure 4.7: Isometric view of modified tandem beam axle assembly.....	50
Figure 4.8: Top view of load cell with resistor and wiring layout.....	51
Figure 4.9: Schematic of the full Wheatstone Bridge circuit used on the load cells.....	53
Figure 4.10: Digi-Star's five input junction box.....	56
Figure 4.11: Front view of Digi-Star's EZ 210 Scale Indicator.....	57
Figure 4.12: Bottom view of Digi-Star's Scale Indicator interface panel.....	59
Figure 4.13: FSI model RSE-3/8 optical shaft encoder.....	60
Figure 4.14: Optical encoder support and pivot assembly.....	62
Figure 4.15a: Isometric view of encoder assembly positioned on the tandem axle.....	63
Figure 4.15b: Side view of encoder assembly positioned on the tandem axle.....	63
Figure 4.16: Isometric view of the original and new pin design.....	66
Figure 4.17: Isometric view of cylinder end cap.....	67
Figure 4.18: Isometric view of the HPL 350 mounted onto the spreader's cylinder.....	68

Figure 4.19: Original tractor-spreader hydraulic schematic.....	69
Figure 4.20: Revised tractor-spreader hydraulic schematic with DCV.....	72
Figure 5.1: PARALLAX BASIC Stamp Computer.....	74
Figure 5.2: Schematic of MAXIM MAX233ACPP 20 DIP TTL/RS232 driver/receiver.....	76
Figure 5.3: Wiring Diagram of PARRALAX Computer network with MAXIM IC chip.....	76
Figure 5.4: Schematic of load cell weighing system with the PARRALAX computer.....	80
Figure 5.5: Schematic of Zener diode voltage circuit.....	82
Figure 5.6: Schematic of speed system with the PARRALAX computer.....	83
Figure 5.7: Nation Semiconductor's ADC0831 A/D converter IC chip.....	84
Figure 5.8: Schematic of position system with PARALLAX computer and A/D IC chip.....	85
Figure 5.9: Schematic of DCV with voltage circuit and PARALLAX computer.....	87
Figure 5.10: Schematic of controller circuit board.....	88
Figure 5.11: Schematic of display interface with PARALLAX computer.....	90
Figure 6.1: Static weight test results of the spreader's weighing system.....	97
Figure 6.2: Illustration of dynamic and overlap test.....	101
Figure 6.3: Plot of spread pattern for tested manures at a gate height of 10 inches.....	104
Figure 6.4: Plot of spread pattern for tested manures at a gate height of 8 inches.....	105
Figure 6.5: Plot of spread pattern for tested manures at a gate height of 6 inches.....	106
Figure 6.6: Plot of spread pattern for tested gate height at a moisture content of 35.0%.....	107
Figure 6.7: Plot of spread pattern for tested gate height at a moisture content of 61.2%.....	108
Figure 6.8: Plot of spread pattern for tested gate height at a moisture content of 61.2%.....	109
Figure 6.9: Plot of generalized spread pattern for a moisture content of 61.2%.....	113

Figure 6.10: Plot of generalized discrete spread pattern for a moisture content of 61.2%....	114
Figure 6.11: Plot of discrete overlap pattern when overlapped twice.....	115
Figure 6.12: Plot of resulting spread pattern distribution when overlapped twice.....	116
Figure 7.1: Block diagram illustration of closed-loop control system.....	120
Figure 7.2: Complete closed-loop block diagram.....	125
Figure 7.3a: Flow chart for Stamp #1 computer.....	127
Figure 7.3b: Flow chart for Stamp #2 computer.....	128
Figure 7.4a: Test #1: System response to static control test using a K_c of 0.017 inch/lb.....	136
Figure 7.4b: Test #2: System response to static control test using a K_c of 0.017 inch/lb.....	136
Figure 7.5a: Test #1: System response to static control test using a K_c of 0.016 inch/lb.....	137
Figure 7.5b: Test #2: System response to static control test using a K_c of 0.016 inch/lb.....	137
Figure 7.6a: Test #1: System response to static control test using a K_c of 0.014 inch/lb.....	138
Figure 7.6b: Test #2: System response to static control test using a K_c of 0.014 inch/lb.....	138
Figure 7.7a: Test #1: System response to static control test using a K_c of 0.013 inch/lb.....	139
Figure 7.7b: Test #2: System response to static control test using a K_c of 0.013 inch/lb.....	139
Figure 7.8a: Test #1: System response to static control test using a K_c of 0.012 inch/lb.....	140
Figure 7.8b: Test #2: System response to static control test using a K_c of 0.012 inch/lb.....	140
Figure 7.9a: Test #1: System response to static control test using a K_c of 0.010 inch/lb.....	141
Figure 7.9b: Test #2: System response to static control test using a K_c of 0.010 inch/lb.....	141
Figure 7.10: Plot of static control test results.....	142
Figure 7.11a: Test #1: System response to dynamic test using a K_c of 0.013 inch/lb.....	146
Figure 7.11b: Test #2: System response to dynamic test using a K_c of 0.013 inch/lb.....	146

Figure 7.12a: Test #1: System response to dynamic test using a K_c of 0.012 inch/lb.....	147
Figure 7.12b: Test #2: System response to dynamic test using a K_c of 0.012 inch/lb.....	147
Figure 7.13a: Test #1: System response to dynamic test using a K_c of 0.011 inch/lb.....	148
Figure 7.13b: Test #2: System response to dynamic test using a K_c of 0.011 inch/lb.....	148
Figure 7.14a: Test #1: System response to dynamic test using a K_c of 0.011 inch/lb.....	149
Figure 7.14b: Test #2: System response to dynamic test using a K_c of 0.011 inch/lb.....	149
Figure 7.15: Plot of dynamic control test results.....	150
Figure A-1: Performance of a voltage regulator.....	164
Figure B-1: Plot of spread patterns used for developing the overlap dimension.....	168
Figure C-1: Plot of linear regression of average discharge rates for fresh manure.....	170

LIST OF TABLES

Table 1.1: U.S. daily manure and nutrient production for various farm animals.....	6
Table 1.2: Nitrogen recommendations for corn.....	7
Table 1.3a: Corn fertilization recommendations for phosphate (P_2O_5).....	9
Table 1.3b: Corn fertilization recommendations for potassium (K_2O).....	9
Table 1.4a: Average nutrient content from various manures.....	11
Table 1.4b: Average nutrient content from various manures (First Year Availability).....	11
Table 5.1: Complete listing of the three different wire harnesses.....	93
Table 5.2: Complete listing of the wiring diagram for the two computers & voltage circuit..	94
Table 6.1: Dynamic weight test results.....	99
Table 7.1: Linear regression of averaged discharge data.....	118
Table 7.2: Summary of static controller test results.....	142
Table 7.3: Summary of dynamic controller test results.....	150
Table #1 Appendix B: Dynamic weight test results.....	166
Table #2 Appendix B: Correlation of moisture content and spread width.....	167
Table #3 Appendix B: Calculated spread width distances using regression information.....	167
Table #1 Appendix C: Linear regression data from discharge test using fresh manure.....	169

CHAPTER 1

INTRODUCTION AND LITERATURE REVIEW

1.1 Introduction

Every crop removed from the field takes materials from the soil which have been used in building up the plant. Soil that annually bears a crop with no fertility added, must in time become exhausted of its store of available plant food and eventually becomes unfit to produce further profitable crops. Often one constituent of plant food becomes exhausted first and replacement of this constituent would renew the fertility for some time longer. Wastes which are added to the soil to replace the nutrients which have been removed are called *manures*. The oldest and most common form of manure is the excreta from farm animals. Rich in elements such as nitrogen, phosphorus, and potassium, animal manure can be a valued asset to the farmer. Over-application of these elements, however, can result in an environmental hazard. When manures are applied in excess, there is a great risk that nearby bodies of water will be subjected to manure runoff due to rains and thawing snow. This pollutes surrounding waters with organic solids, unneeded nutrients, and acts as a vehicle for disease transmission. Since communities and households place such a high dependence on clean water, it is important to understand the ill-effects that manure runoff can cause to streams, rivers, and lakes.

In assessing water quality, it is important to understand the events and practices that occur in watersheds. A watershed encompasses all the land that drains to a particular body of water.

Therefore, the industrial and farmland practices within a given watershed have a direct impact on water quality.

When manure enters a body of water, the bacterial metabolism consumes the dissolved oxygen in the water. The rate of oxygen consumption can exceed the reaeration rate of the water. In fact, anaerobic conditions could result if oxygen levels decrease dramatically. When sufficient organic matter enters the water, oxygen concentrations will be reduced below the necessary level for fish survival. In some regions of the United States animal wastes have been responsible for a high proportion of fish kills and injury or damage to fish. In Kansas, 15 out of 25 pollution-caused fish kills in 1964, resulted from agricultural waste drainage. In California during 1960-1971 there were five documented fish kills attributed directly to livestock operations (Smith and Willrich, 1972).

In addition to the fish kills, manure runoff can result in large amounts of aquatic plant growth. Nitrogen (N) and phosphorus (P), two of the many elements found in manure, dictate the amount of aquatic plant growth in natural waters. When excess amounts of manure are applied to fields, there is an increased chance that N can leach to the ground or surface water or that P can enter waters through surface runoff. One sign of nutrient enrichment is when green algae and aquatic plants are seen in normally clear water. Although nutrient enrichment is a natural process that takes place within a body of water due to soil weathering and erosion processes, the addition of manure runoff accelerates the rate at which enrichment occurs. When there are high rates of aquatic plant growth, a body of water

is said to be eutrophied. A noted example of nutrient enrichment can be seen by looking at the aging of Lake Erie. Due to years of waste disposal, it has been estimated that Lake Erie has aged 150 years within a 15 year time period (Smith and Willrich, 1972).

A further consideration of over applying manure deals with excessive N levels in groundwater. N not used by the growing crop can leach through the root zone and contribute nitrate to groundwater. Nitrate is the most commonly found contaminant in the nation (NPM, 1993). Nitrate levels in municipal drinking water supplies are monitored regularly by public health services because nitrate has been linked to infantile methemoglobinemia or "blue-baby disease" - so called because of the blue tinge of an affected infant's skin (Smith and Willrich, 1972). The United States Public Health Service has issued a permissible nitrate-nitrogen level of no greater than 10 parts per million (ppm) (Smith and Willrich, 1972). Studies done in Wisconsin have determined that approximately 10% of its drinking water wells contain nitrate levels in excess of this standard, proving that percolation is a concern (NPM, 1993). It should also be noted that high nitrate-nitrogen levels in groundwater can endanger the health of animals as well as humans.

There are other important health concerns involving runoff. As runoff enters waterways, it brings with it a variety of potential diseases. There are more than 150 diseases that can be passed between animals of different species and more than 100 of these can be transmitted from animal to man (Smith and Willrich, 1972). The types of disease that can be spread are: bacterial, rickettsial, fungal, and parasitic. Perhaps the most recent publicized case of

waterborne diseases involving runoff happened in Milwaukee, Wisconsin in 1993. It was estimated that over 400,000 people suffered from a bacterial disease organism called *Cryptosporidium* (Smith, 1994). A more common waterborne disease organism is *Salmonella* which is known to cause typhoid fever and food poisoning (Smith and Willrich, 1972).

Due to the severity of problems caused by runoff, federal and state regulations have been imposed. The Federal Clean Water Act mandates that all states safeguard the nation's waters to meet swimming and fishing designations. In adherence to federal regulations of the Clean Water Act, Wisconsin has chartered a water quality standard, NR 102, in the Wisconsin Administrative Code. The standard supports efforts to maintain clean waters for recreation and ecological purposes. The goal of the standard is to provide waters that are safe for swimming and that support fish and aquatic plant life. An example of a body of water not meeting the legislated standard is of a lake that once supported species of fish like trout or bass, but now can only support a lesser species such as carp (Loehr, 1996).

Although it is important to understand the effects and hazards of runoff, it is equally important to identify where the runoff originates. There are two types of sources for runoff into the watershed: point and non-point. A point source is a single traceable source of runoff such as a factory or sewage treatment plant. Conversely, a non-point source of runoff can be described as having a distributed origin. Non-point sources contribute to the largest impairment of surface water quality (Kurtz and Neher, 1995). In Wisconsin, studies have

shown that 40% of the state's streams and 90% of the states 15,000 inland lakes, major portions of the Great Lakes harbors and coastal waters, and groundwater areas have suffered from non-point runoff (Kurtz and Neher, 1995). A significant factor involved in non-point runoff is incorrect manure handling and application practices.

The Wisconsin Department of Agriculture, Trade and Consumer Protection (WDATCP) statistics indicate there were an estimated 94 million beef cattle, 9.4 million dairy cows, 60 million hogs, 81 million sheep and lambs, 384 million chickens, and 317 million turkeys on our nations farms (WDATCP 1996). By using estimated animal populations and respective daily manure production numbers in Table 1.1, it is calculated that 1996's yearly manure production was approximately 12.9 million tons per year of nitrogen and 7.8 million tons per year of phosphorous. If livestock producers do not handle manure properly, there can be large amounts of manure stockpiled and over-applied to fields to rid themselves of the animal's byproduct. The dilemma facing agriculturists is how to employ the manure as a farm input, while limiting its use so groundwater and surface water are not endangered.

Table 1.1: U.S. daily manure and nutrient production for various farm animals. *

	Animal Population (#) x 1000	Manure from Animal (lb./day)	Total Daily Manure Produced (tons/day)	N (tons/day)	P (tons/day)	K (tons/day)
Beef	103,819	72.0	3,737,484	26,162	16,819	20,556
Dairy Cow	9,412	139.0	654,134	3,271	1,635	3,271
Swine	60,190	7.9	237,751	1,189	713	1,070
Sheep	81,457	5.1	207,715	2,908	415	2,077
Chicken	133,767	0.4	24,078	301	301	144
Turkey	317,468	0.8	125,400	1,567	1,567	752
Total			4,986,562	35,398	21,451	27,871

*Compiled from (Smith and Willrich, 1972), (NPM, 1994), and (WDATECP 1996).

1.2 Nutrient Management

The key to utilizing the fertility potential of manure while protecting the environment from its overuse is called nutrient management. The single most important factor in nutrient management is determining the application rate for the crop. Application rates that exceed the crop needs can be environmentally damaging and economically detrimental. Excess nutrients not used by the crop can leach to groundwater or runoff into surface water. Lost nutrients cannot restore fertility to the soil yielding a lost investment in fertilizer. Conversely, if nutrient levels do not meet crop requirements, there are lower crop yields which correspond to lower profit. Because of the importance of available crop nutrients, it is recommended that farmers have their soil tested regularly either before planting or during periods of initial crop growth (NPM, 1994). This will assure an accurate nutrient level of the soil and allow the farmer to calculate the needed application rate of manure. The two

recommended ways to manage nutrients are based upon managing the individual nutrient levels of N and P.

1.2.1 Nitrogen Management

Managing the amount of applied nitrogen is the best way to guarantee crop demand will be met and little if any nitrogen is dissipated into groundwater. Nitrogen (N) recommendations are based upon soil yield potential, soil organic matter content, soil texture and from N response research done through state agricultural experiment stations (NPM, 1994). For example, Wisconsin N recommendations for corn are shown in Table 1.2.

Table 1.2: Nitrogen recommendations for corn.

Soil Organic Matter (%)	Sands and Loamy Sands		Other Soils	
	Irrigated (lb. N/a)	Non-irrigated (lb. N/a)	Medium and Low Yield Potential (lb. N/a)	Very High and High Yield Potential (lb. N/a)
< 2	200	120	150	180
2.0 - 4.9	160	110	120	160
5.0 - 10.0	120	100	90	120
> 10.0	80	80	80	80

(NPM, 1994)

The lower recommendations for non-irrigated sandy soils reflects the lower corn yield potential and greater tendency of leaching in those soils. For medium and finer-textured soils, the N recommendations are based on soil yield potential and organic matter content. Soil characteristic such as drainage, soil depth, water holding capacity, and length of the growing season are used to determine the yield potential ranking of very high and high. It

should be noted the recommendations given in Table 1.2 are the maximum application rates for an economically and environmentally sound crop yield.

1.2.2 Phosphorous Management

Controlling phosphorous (P) levels limits nutrient enrichment of surface waters. Like N management, P management involves using the same principles of crop requirements. Applying higher P rates than the crop needs can result in a negative environmental and economical practice. As in N management, soil samples must be taken to determine P levels. Knowing the P level and the crop yield goals, a recommended application rate of P can be determined from research done through state agricultural experiment stations. It is interesting to note that at optimum soil test levels, the recommended P and potassium (K) additives are approximately equal to that of the anticipated crop removal. These additives must be returned to the soil for it to regain its optimum nutrient balance of P and K for the crop to yield a profitable return (NPM, 1994). Wisconsin recommendations for corn production can be seen in Table 1.3a and table 1.3b respectively.

Table 1.3a: Corn fertilization recommendations for phosphate (P_2O_5).

Soil Test Interpretation					
Yield Goal (bu/a)	Very Low (lb./a)	Low (lb./a)	Optimum (lb./a)	High (lb./a)	Excessively High (lb./a)
71 - 90	45 - 60	40 - 50	30	15	0
91 - 110	55 - 90	50 - 60	40	20	0
111 - 130	60 - 95	55 - 65	45	25	0
131 - 150	70 - 85	65 - 75	55	25	0
151 - 170	75 - 90	70 - 80	60	30	0
171 - 190	85 - 100	80 - 90	70	35	0
191 - 210	90 - 105	85 - 95	75	40	0

(NPM, 1994)

Table 1.3b: Corn fertilization recommendations for potassium (K_2O).

Soil Test Interpretation					
Yield Goal (bu/a)	Very Low (lb./a)	Low (lb./a)	Optimum (lb./a)	High (lb./a)	Excessively High (lb./a)
71 - 90	35 - 60	30 - 50	20	10	0
91 - 110	45 - 65	35 - 55	25	15	0
111 - 130	45 - 70	40 - 60	30	15	0
131 - 150	50 - 75	45 - 65	35	20	0
151 - 170	55 - 80	50 - 70	40	20	0
171 - 190	60 - 85	55 - 75	45	20	0
191 - 210	65 - 90	60 - 80	50	25	0

(NPM, 1994)

1.3 Crediting

The best way to ensure environmental water quality protection and economic return is by taking into account soil nutrient levels as well as nutrients from farmer inputs. Crediting accounts for nutrient contributions in the manure, previous crop growth in rotation, and land-applied organic wastes before commercial fertilizers are used. When the nutrient levels of

the soil have been determined from the soil tests, farmers can calculate the needed additives based upon the management plan of their choice. To determine the desired manure application rate, the nutrient content of the manure must be evaluated. This can be done using two different methods. The first involves having the manure tested for its nutrients and the second method is to use average values supplied by state agricultural agencies.

The most accurate application rates will be determined by proper manure sampling and by having the nutrient content of the manure tested by a laboratory. The reason that this is the most accurate method is due to large farm-to-farm variation as a result of manure storage, handling, livestock feed, or other farm management differences (NPM 1994). Although manure testing is the best method, it is not always the most convenient or available. When this situation arises, the next best alternative is to use average values of nutrient content. Tables 1.4a and 1.4b list average nutrient contents of various manures.

By referencing Table 1.4b it is obvious that not all of the nutrients in manure are available in the first year after application. For example, there is an organic form and an inorganic form of N. It is only the inorganic form of N that is available for immediate crop intake. The N in organic form is released more slowly.

Table 1.4a: Average nutrient content from various manures.

	Dairy	Beef	Swine	Poultry
	Nitrogen (N)	Nitrogen (N)	Nitrogen (N)	Nitrogen (N)
Solid (lb./ton)	10	14	10	25
Liquid (lb./1000 gal)	28	39	30	69
	Phosphate (P₂O₅)	Phosphate (P₂O₅)	Phosphate (P₂O₅)	Phosphate (P₂O₅)
Solid (lb./ton)	5	9	6	25
Liquid (lb./1000 gal)	14	25	10	69
	Potash (K₂O)	Potash (K₂O)	Potash (K₂O)	Potash (K₂O)
Solid (lb./ton)	10	11	9	12
Liquid (lb./1000 gal)	28	31	10	33

(NPM, 1994)

Table 1.4b: Average nutrient content from various manures (First Year Availability).

	Dairy	Beef	Swine	Poultry
	Nitrogen (N)	Nitrogen (N)	Nitrogen (N)	Nitrogen (N)
Solid (lb./ton):				
surface applied	3	4	4	13
incorporated	4	4	5	15
Liquid (lb./1000 gal):				
surface applied	8	10	12	35
incorporated	10	12	15	41
	Phosphate (P₂O₅)	Phosphate (P₂O₅)	Phosphate (P₂O₅)	Phosphate (P₂O₅)
Solid (lb./ton)	3	5	3	14
Liquid (lb./1000 gal)	8	14	6	38
	Potash (K₂O)	Potash (K₂O)	Potash (K₂O)	Potash (K₂O)
Solid (lb./ton)	8	8	7	9
Liquid (lb./1000 gal)	21	23	8	25

(NPM, 1994)

Mineralization of some of the organic nitrogen occurs throughout the growing season. The available N from dairy manure is approximately 30-35% of the total N content of the manure

in the first crop year (NPM, 1994). Additional amounts of nutrients are released to the soil in the second and third year following manure applications. Another point of interest evident in Table 1.4b is there are reduced nutrients credits given when the manure is not incorporated into the soil. Reduced crediting recognizes the loss of N from volatilization and runoff. If it is decided the manure is to be incorporated in to the soil, this should be done no more than 72 hours after the application. This is based on the fact that most of the volatilization loss occurs in the first 3 days.

Crediting used in conjunction with nutrient management is being promoted by researchers and extention workers in the area of nutrient management. Extention staffs are making great efforts to educate farmers on the proper practices and techniques that should be exercised in the field. To understand current nutrient management trends in Wisconsin, University of Wisconsin - Madison researchers conducted a study called the Farm Practices Inventory. This study attempted to understand current farmer practices concerning nutrient management and identify what potential obstacles prevent farmers from accepting proper nutrient management schemes. In the first year of the study, 1200 farmers were interviewed at seven sites in various counties, different crop areas, and watersheds. The results of the survey showed that 58% of the farmers applied extra N due to not crediting the manure they applied. Over 40% over-applied N by at least 60 pounds per acre, and 85% applied too much phosphorous to the same field (NPM, 1993).

Statistics from a later survey of 700 Wisconsin farmers showed similar results. Only 2 percent properly credited the nutrients in manure spread on their fields within 10% of the university recommendations (Nowak, 1994). Further results of the survey showed seventy percent of the farmers surveyed relied only on chemical fertilizers and did not credit any of the manure applied to their fields (Nowak, 1994). In fact, it is believed farmers are commonly applying manure at two or more times that recommended under various nutrient management plans (Sturgul, 1996).

In assessing the Farm Practices Inventory survey, it was determined farmers were not aware of the repercussions which occur with over-applying manure. Results of the survey indicated the big challenge for researchers and state agencies is to educate the farmer on water quality management and the environmental hazards that exist (NPM, 1993). Results also showed no statistical difference in manure management practices between farmers who had a cost-shared manure structure and those without structures.

Perhaps one way to convince more farmers to credit the manure they apply is to look at the economics of the issue. Manure does not only supply N, P, and K as effectively as commercial fertilizers, but it also adds organic matter to soil, improves soil structure, tilth, and water-holding capacity. Based on these properties, it is rational to view manure as a farm input with a monetary value rather than a useless byproduct. By considering the nutrient content and the current price of commercial fertilizer, it is easy to estimate the cost savings that could be realized by crediting applied manure. The price per pound of N, P₂O₅, and K₂O

in commercial fertilizers are \$0.20, \$0.24, and \$.12 per lb. respectively (NPM, 1993). To illustrate the point, consider a N surface-applied management plan of 25 tons per acre for a 50 acre plot using dairy manure. Since there are 3 lb./ton of nitrogen available the first year in dairy manure (see Table 1.4b), there will be a credit of 75 lb. per acre. This translates to 3,750 lb. of N over the 50 acre plot. At \$0.20 a lb. this amounts to a cost savings of \$750. This \$750 is a direct savings to the farmer due to needing to buy less commercial nitrogen fertilizer. This analysis presumes at least 75 lb. are needed on the field. If previous crop credits are given, 75 lb./acre may not be needed and the whole \$750 can not be credited.

Results like those from the Farm Practices Inventory survey sparked federal and state agencies to develop nutrient management criteria. The United States Department of Agriculture-Natural Resource Conservation Service (USDA-NRCS) has developed nutrient management standards that prescribe the amount, form, placement, and timing of applications of plant nutrients. In Wisconsin, this standard is called Nutrient Management Standard 590. This standard is based upon the following three main ideas (USDA-NRCS, 1994):

1. Minimum criteria to provide nutrients for crop production and to minimize entry of nutrients to surface water and groundwater.
2. Criteria to minimize entry of nutrients to groundwater.
3. Criteria to minimize entry of nutrients to surface water.

These include some underlying criteria (Loehr, 1996):

- Nitrogen application must not exceed rates pre-determined by university extension specialists as part of the crop requirement plan.

- Application rates cannot exceed 75 pounds of available P_2O_5 per acre (32.8 lb. P per acre) total for a five year period unless incorporated.
- No more than 25 tons per acre of solid dairy manure or its equivalent be applied annually.

Enforcement of the Nutrient Management 590 Standard, will cause farmers who are required to have permits (>1000 animal units) and those receiving cost share moneys and some government payments to follow the bylaws for safe manure handling practices. Although this represents a small fraction of existing livestock producers, it is still progress towards improving water quality in sensitive areas.

1.4 Current Manure Spreader Technology

Through the use of nutrient management practices and standards, farmers can determine the required amount of nutrients needed for their crops. From this, the farmer can determine how much manure to spread on each acre. The next question that arises is how to spread the manure. Typically there are three types of manure spreaders: rear box discharge, side or rear V-bottom discharge, and liquid tank spreader. Each operates on a different principle and is designed to handle a different type of manure.

The rear discharge spreader is designed to handle drier more solid manure. It has a box type configuration that has two functional mechanisms: a live apron and a rotating set of beaters. The apron is similar to a conveyer in the sense that it is a continuous moving bed that is pulled by a set of sprockets. The apron is powered through input to a gearbox from the

power take-off (PTO) of the tractor. When the PTO is engaged and the spreader is loaded with manure, the apron delivers the load to the beaters. The PTO powered beaters, rotate perpendicular to the incoming load and tear manure away from the load, discharging it to the rear and the sides of the spreader. There may be a gate located at the rear end of the spreader in front of the beaters. The gate prevents the load from falling out during transport to the desired field. The application rate is determined by the travel speed of the spreader and the rate manure is delivered on the apron to the beaters.

V-bottom side discharging manure spreaders are intended to spread semi-solid and liquid manures. They can also be used to spread solid manure and are commonly used to broadcasting manure on alfalfa fields. Most side discharging spreaders are designed with an open V-tank shape instead of the rectangular shape of a rear box discharge spreader. Near the bottom of the V-tank is an auger with an axis parallel to the sides of the tank. The auger is powered through a gearbox linked to the PTO of the tractor and moves manure toward the front or rear of the tank as it rotates. As the manure reaches the end of the spreader, it flows toward another rotating mechanism called the expeller. The expeller, also powered through the gearbox, is made up of a shaft with serrated impeller blades attached. With the expeller rotating parallel to the auger and rotating at much faster speeds, the impellers scoop manure from the advancing pile and throw the manure perpendicular to the side of the spreader. The side discharge spreader has a gate that controls the discharge rate. Usually operated hydraulically, the gate moves up and down in a slot located just behind the expeller. As the gate position changes, the area of the delivery opening through which manure passes

increases or decreases. Therefore, the operator can adjust the amount of manure delivered to the expeller by changing the spreader gate height. The application rate is determined by the auger speed, expeller speed, size of the discharge opening, and the travel speed of the spreader.

Liquid manure spreaders are commonly designed with a large horizontal tank mounted on a spreader chassis frame. They are usually equipped with agitation and pumping devices which stir and direct the manure to an outlet port. Less complicated spreaders just pump the liquid to the rear and the side of the machine onto the field. More complicated designs have the outlet ports located behind shanks equipped with chisel tools. This design allows the liquid to be injected and incorporated below the soil. Surface discharge rates are controlled by the ground speed of the spreader and the discharge rate of the pump. The major advantage of this type of spreader are a) application rates can be relatively more precise because liquid manure has a more uniform density than semi-solid and solid manure and b) injection below the soil surface reduces odors and likelihood of nutrient loss to volatilization and runoff.

In terms of spreader popularity, farmers prefer some forms of spreaders over others. In a Wisconsin survey of 350 farmers it was reported that 67.5% owned rear discharge units, 16.0% owned side discharge units, and the remaining 16.5% owned a closed tank liquid spreader (Loehr, 1996). The type of spreader is often usually dictated by the nature of manure generated on the farm and the cost of the spreader.

Spreader manufactures often list two load-size ratings in operating literature: a heaped rating and a struck-level rating. These two ratings are identical for closed-tank spreaders but can vary greatly for box and V-tank spreaders. The accuracy of these values is essential in determining accurate application rates. Studies have shown that manufactures have reported inflated capacity rating of up to 159% for rear and side discharge spreaders and a lesser inflated capacity of 12% for closed tank spreaders (Loehr, 1996). These discrepancies arose because of improper spreader volume designations and highly varying manure densities. Farmers are cautioned by extension agents about the manufacturer listed capacities and urged to determine capacity rating of their own. This can be done by weighing the empty spreader and then weighing several loads to determine an average load capacity.

1.5 Current Methods of Determining Application Rates

With current spreading technology, there are only three methods to estimate an application rate: weighing method, sample method, and calculation method. The weighing method involves four steps. The weight of the empty spreader is recorded. Platform or portable truck scales are used to weigh the spreader. The spreader is filled and weighed to determine the load. Finally, the empty weight is subtracted from the full weight. The load weight is divided by the land area upon which the manure is applied.

The sample method involves laying plastic sheets of known dimensions and weight on a field and applying manure on plastic sheets. The sheets containing the manure are weighed and the net weight of the manure determined. This weight collected should be divided by the area

of the manure on the plastic sheets. This application rate is used to estimate an average overall application rate.

The third method involves calculating or estimating the spreader's heaped volume and multiplying that by a selected density value for a given type of manure. Heaped spreader volumes can be calculated by following the American Society of Agricultural Engineers (ASAE) S324.1 standard. Density values are assumed to be uniform for the entire load and can be found in various handbooks or estimated using calibrated buckets. Knowing the weight and volume of the manure in the bucket will yield an average manure density. Both these methods are not recommended because manure densities are known to be highly variable.

Problems with these methods are that they are either very cumbersome or their level of accuracy is low. The weighing and sampling methods are labor intensive, time consuming, and monotonous. It is very hard to convince farmers to adopt these practices when there are so many adverse circumstances they have to endure. Finally, the calculation method is just too variable to accurately measure how much manure is actually being applied. Also, most farmers have a limited math background which impedes their abilities to do the calculations. Because most farmers do not fully understand the environmental and economical benefits in nutrient crediting, it is hard to persuade them to employ these practices due to the limitations on their accuracy and difficulty. Most farmers view these calculation and prediction methods

as unnecessary and painstaking. This helps to explain why farmers are not taking a more active role in nutrient management.

1.6 Current Spreading Technology and Application Research

Purdue University has worked to develop a manure management system (Ess and Morgan, 1996). Using a liquid tank type manure spreader, they are in the process of incorporating various off-the-self computer based technology to build a system that can: measure the flow rate per unit area, document application rates and locations, and control the application location within a mapped site.

Mounted between the units tank and independent frame are four load cells that measure the instantaneous weight of the spreader. Weight data is collected by a portable computer and processed by a program written in common computer language. This allows the weight of the spreader to be measured and an application rate per unit time to be computed. The data collection system also allows an application map to be generated.

To control the application rate of the spreader there is a gate valve mounted on the units main discharge tube and controlled by a hydro-pneumatic actuator. The actuator is controlled by a directional control valve (DCV) which is controlled by an auxiliary DCV incorporated into the tractor's hydraulic system. The auxiliary DCV is controlled by a solenoid actuated tractor-cab-mounted toggle switch. Activation of the switch is accomplished by interfacing the toggle switch with an isolator circuit electrically linked to the portable computer.

While the liquid manure applicator underwent development into a precision manure application system at Purdue, there was concurrent research being done with V-bottom type manure spreader at the University of Wisconsin - Madison (Loehr, 1996). Work has been done involving research to develop an "on-the-go" weighing system for side discharge manure spreaders.

Specifically, load cells were placed at the main pivot on each of the walking beam undercarriages of a four wheel Gehl Model 1315 spreader. A single load cell was incorporated into the hitch of the spreader. The placement of the individual load cells provided a force measurement at three points on the spreader.

Testing of this system was performed and modifications were made to the spreaders suspension system. Results of the tests indicated there were high variations in weight measurement caused by driving over surface irregularities, tractor vibration, and side loads developed by the dual wheels of the undercarriage system during turns. Attempts to reduce the variability of force measurement include: a) replacing the double wheel walking beam with single wheels, b) installing accelerometers to condition the force signal, and c) mathematical averaging techniques to condition the force signal.

Initial trials with the weighing system and the tandem axle configuration indicated the tandem axles created a weight variation of $\pm 10\%$ during turns (+10% during right turns, -10%

during left turns). The variation in spreader weight while turning proved to be statistically significant. It was decided that fluctuations of up to 20% was unacceptable for this system. Therefore, the spreader was converted to single axle. Conversion to the single axle reduced the variation of spreader weight to about 5% while turning. The accuracy of the system was improved with the single tire configuration. At the time, the goal was set for final system accuracy of 5 - 10%.

In efforts to reduce variability of the data, further testing was performed with the single tire assembly. Even with the single tire configuration, the weight varied appreciably when hitting small stones or ruts in the field. The single tire did not provide the dampening characteristics offered by the tandem walking beam assembly and allowed the spreader to bounce more, creating weight variance while driving.

Initial data indicated a problem with signal interference from electrical sources ranging from the tractor's alternator to residential power lines and other unknown sources. Signal "wandering" also occurred due to vibrations from the PTO, the spreader's impeller, and all the spreader's rotating components. An electric filtering device was then added to the load signal to eliminate interference and instability problems. This reduced the variance in the weight data.

Once the instrumentation was functioning acceptably, several tests were performed to determine the accuracy of the system. The method used to determine the system's accuracy

was to measure the loaded spreader in a static (not moving) condition and to compare that weight to the dynamic weights recorded while driving through the field. At 6 miles per hour (mi/h), the variation was about 14% of the static loaded spreader weight. Incorporating smoothing techniques by averaging 200 weight measurements over 2 seconds reduced the variance to a very respectable 2%. Thus the averaged data is a more accurate representation of the actual weight on the spreader while moving.

Another technique used to eliminate the variation was to record the acceleration of the spreader and correct the force measurement using Newton's First Law. Since the spreader and tractor interface do not serve as perfect rigid bodies, it was very difficult to correlate the recorded forces and acceleration data. The weight of the spreader varied by about 22% using this method.

Finally, an averaging technique for damping out the variation was used in a test of the spreader while it was being discharged. The technique averaged 500 values over 5 seconds. There was a tremendous improvement in the averaged data. The dampened weight values showed a more clear picture of the spreader weight loss as manure is being discharged when compared to the undamped data.

The behavior of the weighing system and spreader was also influenced by: a) the method of loading the manure into the spreader, b) the position of manure in the spreader (spreader

balance, c) the terrain traversed by the tractor and spreader, d) tire inflation pressure, and e) travel speed.

CHAPTER 2

INITIAL OBJECTIVES

The primary objective of this research was to develop a manure measurement and control system for manure spreaders that manufacturers could market to farmers. With current water quality regulations and future nutrient management mandates, farmers will be required to measure and control the amount of manure they apply. Spreader manufacturers expect that these added requirements will lead to new market needs. An automated spreading control system is believed to be the answer that farmers and regulatory agencies are looking for. Manufacturers, however, want a system that can be readily adapted to current spreader technology without excess design and manufacturing changes to existing products. Farmers, on the other hand, want a system that is inexpensive and easy to use. These demands help determine many of the design objectives and criteria for the project.

The general objectives of the project were to develop a system that could be incorporated into current spreader designs without making major changes to the undercarriage. The system should also be manufactured and sold at a low price relative to that of the cost of the spreader. Furthermore, the additional price of the system should be recoverable in the cost savings due to lower commercial fertilizer inputs amortized over the life of the machine.

Specific objectives include providing the machine operator with continuous measurement and control of an applied application rate. The main goal in the initial stages of the research involved simplifying and improving the weight data collection system that had been

previously implemented by Loehr (1996). Other main points of interest included: reduction or elimination of weight data variation due to uneven loading of the spreader, reduction or elimination of weight data variation due to poor ground conditions, and reduction or elimination of delay due to back averaging. Additional improvements were to implement some form of mechanical and or electrical dampening and the addition of a mathematical processor to perform on-the-go calculations.

Once the improvements were made and the additions employed, the objective then was to determine the accuracy of the new weighing system. This was done by comparing discharged manure weight measured by the system verses actual weight of manure collected on plastic sheets.

The end result of this research was to produce a system that would accurately measure and control manure application rates within $\pm 5\%$ of the actual application rate. Development of this system will increase farmer's confidence in manure nutrient management and lower input costs while contributing to the reduction of water pollution.

CHAPTER 3

DESIGN CRITERIA AND SYSTEM COMPONENT DESCRIPTION

3.1 Design Criteria

To establish design criteria for this second phase of the project, there needed to be some investigation into the previous research done by Loehr (1996). Loehr's research provided information about performance and reliability of the load weighing system (load cells), the force measuring system (accelerometers), and the data acquisition system. After evaluating these subsystems and receiving industrial recommendations, there was some refinement of the original project objectives as well as the addition of some new ones. The following is a list of the updated project objectives:

1. Load cells must be incorporated into the tandem axles and the hitch of the spreader. This would facilitate a weighing system as an add-on feature of a conventional spreader.
2. Spreading control system must be completely portable and powered by an external DC power source or tractor battery.
3. System must be unaffected by high frequency vibration caused by rotating components such as the tractor engine, power take-off (PTO) shaft, and the spreader auger and expeller.
4. Sensing technology and control system must be able to withstand rapid abrupt inertial forces due to traveling over rough ground.
5. System must be built without the use of a traditional data acquisition system.

6. System must be built without the use of accelerometers.
7. System must be able to down load application rate information for data retrieval purposes.
8. Control system must operate without the use of any on-board lap or desktop computer.
9. System must be able to display an on-the-go application rate from somewhere on the tractor or spreader.
10. System must be able to operate efficiently and accurately in an agricultural environment, which includes exposure to dust, manure, mud, rain, snow, oil, fuel, etc.
11. System must be able to operate effectively under extreme temperatures in an approximate range from -40° F to 120° F.
12. System must be reliable on a daily basis, since many farmers spread manure every day of the year.
13. System must be user-friendly to farmers and machine operators.
14. Complete system must be constructed and tested within the UW-Madison Agricultural Engineering Lab and Research Stations.

Structured into the design criteria are certain standards or guidelines that the individual system components must meet. Major components included: weighing system, signal conditioning system, speed tracking system, computer processor, hydraulic directional

control valve, and alpha-numeric display. All of these components can be grouped into one or more of the following functional categories: sensing, computing, control, and display.

Perhaps the most vital part of the whole research was in the proper selection and configuration of the spreader's load, speed, and gate position sensing equipment. Careful attention needed to be paid to which technologies to select, how much they cost as well as how they would be interfaced. Therefore, an individual set of criteria was created for all of the different technologies used for measuring various system parameters.

The entire weighing system was comprised of the following: load cells, a junction box, signal conditioning unit, and digital read-out.

Detailed criteria for the **load cells** are listed below:

1. Ability to measure static forces with an accuracy of 2% or less.
2. Ability to withstand and accurately measure dynamic forces with accelerations up to 5 g's.
3. Ability to be easily installed into the spreaders tandem axles with few modifications to existing axles.
4. Must be able to continuously transmit a live signal (voltage) to the signal conditioning system which is linearly proportional to the force applied to the spreader.

Detailed criteria for the **junction box** are listed below:

1. Must be able to input and sum five individual load cell voltages.
2. Must be capable of being mounted directly onto the spreader.
3. Must protect load cell wire terminals from elements common to spreading environments.

Detailed criteria for the **signal conditioning unit** are listed below:

1. Ability to convert the analog output from the junction box into a 16 bit digital signal.
2. Must be capable of adjusting the resolution (smallest increment) of the output.
3. Unit should have built in filtering capabilities and numerical averaging techniques.
4. Unit must have an RS232 interface to retrieve weight data.
5. Must have an output rate of no less than 4 Hz.

The spreader's speed was essential in measuring an on-the-go application rate. Therefore, it was important to measure the ground speed of the spreader as it was traveling through the field.

Detailed criteria for the **speed sensor** are listed below:

1. Must be easily installed on the spreader and incorporated into the drive-line of the spreader.

2. Must be able to withstand elements common to spreading environments.
3. Must transmit an analog (0, +5 Vdc) or (0, +12 Vdc) pulsed output or 16 bit digital signal.
4. Must be powered by an external 12 Vdc source or tractor battery.

Since this research involves the use and modification of a side discharge spreader, the discharge gate plays a significant role in changing the application rate. One way to control the application rate is to develop a relationship between the gate height and the discharge rate. Therefore, it is important to determine the gate position to affect changes in the application rate.

Detailed criteria for the **position sensor** are listed below:

1. Must be easily adapted to the current gate configuration.
2. Must have a linear stroke of at least 15.75 inches.
3. Must be able to operate on a supply voltage of +5 Vdc.
4. Must be able to output an analog voltage within a range of 0 - 5 Vdc.
5. Must be able to interface with an analog-to-digital (A/D) computer chip.
6. Must be able to continuously transmit a live signal (voltage) to the computer.
7. Must withstand elements common to spreading environments.

Once the weight, speed and gate position were quantified, it is necessary to process the data and perform calculations based upon the measured values to estimate an application rate.

This is accomplished through the use of a computer processor. The processing and input/output capabilities are a major concern when selecting computer processors.

Detailed criteria for the **computer processor** are listed below:

1. Must be able to perform addition, subtraction, multiplication, and division.
2. Must be able to be programmed in a common programming language such as:
Basic, C, or Fortran.
3. Ability to transmit and receive RS232 communication.
4. Possess at least 8 input/output channels for data input/output.
5. Ability to read and count analog (0, +5 Vdc) or (0, +12 Vdc) pulsed input signals.
6. Ability to measure varying input voltages ranging from 0 to +5 Vdc.
7. Ability to sink or source +5 Vdc at 20mA.
8. Capability of processing numbers of at least 16 bit word lengths.
9. Process at a speed of at least 20 MHz.
10. Possess a random access memory (RAM) of at least 64K.
11. Must be powered by a +5 to +15 Vdc source.

Since the gate position has such a large effect on the application rate, there should be some consideration given to how the position is controlled. Like most V-bottom manure spreaders, the Gehl Scavenger 1315 side discharge unit uses the tractors hydraulic system with a hydraulic cylinder on the spreader to activate the discharge gate opening. The addition of a

servo-controlled valve into the hydraulic circuit controlling the cylinder on the spreader, provides an opportunity to control the gate position with a control system.

Detailed criteria for the **directional control hydraulic valve** are listed below:

1. Must be able to handle pressures up to 3000 pounds per square inch (psi).
2. Must be able to handle flow rate up to 12 gallons per minute (gpm).
3. Must be a 4 way, 3 position valve, with a spring centered open center configuration.
4. Must be a dual activated solenoid valve (12 Vdc).
5. Must be easily mounted on the spreader.
6. Must have a useful life of at least 10^6 cycles.
7. Must withstand elements common to spreading environments.

Finally, the last functional category of the system that needed to be assessed was the display unit of the system. The purpose of the display unit was to allow spectators to witness the controlled application output during educational demonstrations.

Detailed criteria for the **display unit** are listed below:

1. Ability to output at least 5 alpha-numeric characters.
2. Characters had to be a minimum of 3 inches tall for easy viewing.
3. Ability to receive and output RS232 serial communication.
4. Must be powered by a 12 Vdc or 120 Vac source.

3.2 System Component Description

Once all the criteria had been established, individual components needed to be identified, evaluated, and compared. It was imperative to learn more about the individual components. Selection and evaluation of all the components was founded on a solid understanding of their form and function.

3.2.1 Load Cells

Load cells are usually hand crafted instruments that come in many sizes, shapes, and configurations. Load cells employ the principle of strain to measure such properties as force and torque. Strain is a resulting elongation or deformation in a material that arises from a load acting on a mechanical member. Using strain gages placed on the surface of the member, the load cell can measure the load by measuring the strain of the surface. A strain gauge is a precision resistor that changes its resistance proportionally with changes in its length and or width. In a Wheatstone Bridge, the strain gage produces an output voltage when an excitation voltage is applied to it and when its resistance changes. The output voltage will vary as the resistance of the gage varies due to strain from tension, compression, or bending moment. When these strain gages are calibrated correctly and wired in a Wheatstone Bridge, the output voltage of the gage will be proportional to the applied load.

There are many different load cells that are used to measure many different types of loads. For example, there are shear beam, bending beam, tension, and compression load cells. Shear beams have a high tolerance of dynamic forces and allow for good sealing and

environmental protection. Bending beam load cells are easy to manufacture and inexpensive. Tension and compression load cells work best in applications in which the loading is primarily in one direction. All of the different types of load cells perform accurately throughout a very wide range of forces, environmental conditions and loading applications (Loehr, 1996).

3.2.2 Junction Box

The junction box is used in the weighing system with the load cells. It takes the input voltages from multiple load cells and sums them in parallel to provide a single output voltage equal to the sum of the forces on the load cells. Summing is a common practice in industry as most tanks, bins, hoppers, and platforms are often supported by 2, 3, or 4 load cells which when summed give the total weight being monitored. All of the load cells should have the same capacity and have interchangeable rated outputs.

3.2.3 Signal Conditioning Unit

Signal conditioners are devices that accept raw voltage inputs from sensors such as: strain gauges, load cells, pressure transducers, and thermocouples. The signal conditioners take the raw signal and then process the input according to signal magnitude or frequency. The conditioner needs to have as many channels as there are raw input signals and are usually sold on a per channel basis. Additionally, conditioners can process the channels in a multiplexing fashion or a batch processing fashion. Less expensive conditioners process the input signals in a multiplexing fashion, conditioning one channel at a time sequentially.

Conversely, more expensive conditioners perform batch processing which means the unit conditions all of the input signals simultaneously. The advantage to batch processing conditioners is that the inputs are read at the same time, which corresponds to a more accurate representation of input sampling. The major disadvantage of batch processing conditioners is the added cost for speed and accuracy relative to the multiplexing signal. The application must warrant a high level of accuracy to justify the extra cost.

One of the most important functions of a signal conditioner is the ability to filter the raw input signal. Filtering can be accomplished through the use of many different types of filters. The following are typical types of filters used in signal conditioners: passive, active, bandpass, lowpass, and highpass filters.

A passive filter is a frequency-selective network consisting of passive resistors, inductors and capacitors. Passive filters do not require an additional power source and can be inserted into the positive (+) side of the signal line, but have the potential to attenuate a portion of the input signal. An active filter is one that incorporates amplifiers. An active filter requires a power supply, but does not attenuate much of the input signal. Passive filters use large expensive inductors, while active filters are designed using low cost op-amps which make them less expensive (Smith and Dorf, 1992).

When it is desired to filter at specific frequency ranges, a bandpass filter is used. A bandpass filter passes frequencies within a specified range and attenuates frequencies above and below

the specified range. A lowpass filter uses a special series circuit made up of capacitors, inductors, and a rectifier to block the ac components and pass dc components (Smith & Dorf, 1992). Lowpass filters are sometimes referred to as anti-aliasing filters. Finally, highpass filters perform the opposite function of lowpass filters. They use a special series circuit made up of capacitors, inductors, and a rectifier to block the dc components and pass ac components. The selection of filters should be based upon the application and presence of frequencies that are to be avoided.

3.2.4 Speed Sensor

Much of today's agricultural equipment use speed sensors to monitor and control everything from ground speed to individual component drive-line speeds. Although there are many different sensors that could be used to measure speed, the most common to agricultural equipment are the magnetic pick up and the optical encoder.

The magnetic pick-up works by supplying power to the permanent magnetic coil of the device, which in turn induces a magnetic field around the pick-up. There is usually a symmetric rotating gear, sprocket, or perforated disk that is located a certain perpendicular distance away from the pick up. The air gap between the pick-up and the rotating object changes due to the tooth or bolt circle profile. The change in the air gap changes the reluctance of the magnetic circuit. The flux established by the permanent magnet changes and a voltage is induced in the pick up coil. The generated electromotive force (emf) is proportional to the velocity of the rotating disk attached to the rotating object. (Smith and

Dorf, 1992). This resulting voltage is usually in the form of a pulsed square-wave of (0, +5 Vdc) or (0, +12 Vdc) depending on the supply power. The pulses of the square-wave are counted and a speed is calculated depending on the profile of the rotating object.

Just as a magnetic pick-up uses current to produce a pulsed output, an optical shaft encoder uses voltage to produce a pulsed output. Encoders are usually directly linked to the rotating member through some type of coupler or universal joint. Optical encoders transmit light through an evenly slotted or ruled disk on a rotating shaft onto a photo-detector that converts the transmitted light into an electrical voltage via a photo-sensitive transformer. The voltage produced is also a pulsed square-wave of (0, +5 Vdc) or (0, +12 Vdc). Again, the pulses are counted and calibrated to the corresponding rotating disk to which it is coupled. The resolution of the encoder depends on the number of slots or rulings on the rotating disk. There are magnetic encoders that use magnetic pick-ups to create an electrical pulsed output, but they are less common and not used as extensively as optical encoders because the resolution of optical encoders is much greater.

3.2.5 Position Sensor

Position sensors are by far the most common type of sensor in machine control systems because of the obvious need to control the position of various moving parts of machines (Bollinger and Duffie, 1988).. Position sensors are also commonly used for measuring other physical quantities that can be converted into positional changes. There are many different

devices used to measure linear position, but the two most commonly used are the linear variable differential transformer (LVDT) and the linear potentiometer.

The LVDT is an inductive position-sensing device typically consisting of one central primary winding and two secondary windings on a hollow cylinder. The central winding is excited by applying a sinusoidal voltage. Each of the outer secondary windings have an equal number of turns and are positioned on either side of the central winding. A ferro-magnetic core moves axially within the hollow cylinder causing the magnetic flux linking the primary and secondary windings to change. This change in flux is detected to measure position. When the core is centered, the magnetic flux and induced voltages in both secondary windings are equal resulting in the voltage difference of zero. As the core moves toward one secondary winding, the induced voltage in that winding increases and the induced voltage in the other winding decreases resulting in a voltage difference. LVDTs can be obtained with ranges of motion from 1 to 50 mm with resolution of $1\mu\text{m}$ or smaller. Although LVDTs possess great accuracy, they are relatively expensive and only very useful when axial movement in either direction away from a central location is to be detected (Bollinger and Duffie, 1988).

When absolute position must be measured, the best device is a linear potentiometer. With a linear potentiometer voltage is applied across a resistive element. An output voltage is proportional to the position of a brush that slides along the resistive element. The brush is connected mechanically to the mechanical component whose transitional position is to be measured. The potentiometer will yield a zero voltage potential when it is fully retracted and

yield the supply voltage when it is fully extended. The resistive element is normally either wire-wound or coated with a conductive film. The resistance per unit length is usually constant along the element. Accuracy better than 0.1% of the measurement range at a relatively low cost can be obtained, but wear of the resistive element can be a problem (Bollinger and Duffie, 1988).

3.2.6 Computer Processor

Much of today's machine monitoring and control is done with the use of computer processors. More specifically, microprocessors are being incorporated into new products that can measure, calculate, and control complicated machine movement. The invention of microprocessors has led to the development of new technologies and industries. The success of the microprocessor is due to the integration of the following three components with the programmability of a common computer language: central processing unit (CPU), memory, and input/output (I/O) devices.

The CPU of the processor transfers data and instructions from one part of the processor to the other, controls the order in which processing instructions are executed, decodes instructions, and executes the instructions by using logical comparisons and evaluating chronological commands. Instructions and data are transferred in and out of memory under direction of the CPU. Data is transferred to and from the I/O devices by the CPU. The CPU also contains logic circuits that perform arithmetic and logic operations (Bollinger and Duffie, 1988).

Since the CPU cannot store all of the necessary information, it must rely on the memory of the processor to hold data and other important information. In most cases, the processor's memory is of the random access (RAM), read/write type, but parts of it may be of the read-only (ROM) type. Addresses specifying locations of data in memory are selected by the CPU as a function of the retrieved addresses with instructions or addresses computed by the CPU. Once a memory address has been selected by the CPU, data can either be transferred from the CPU to that address by a write operation or transferred to the CPU from that address by a read operation.

Sometimes the CPU will need to store a value in memory or output a value from memory. This is accomplished through the use of input/output devices. The most basic of these devices are monitors for display and keyboards for data entry. These devices allow the user to input programs and data into the processor. The programs can be executed and the results displayed. Other I/O devices include digital-to-analog converters, analog-to-digital converters, encoders, and potentiometers.

3.2.7 Directional Control Hydraulic Valve

A directional control valve consists of a body with internal passages which are connected and disconnected by a moveable spool. Spool valves are by far the most common type of directional valve used in industrial hydraulics. Most spool valves consist of a pump passage, tank passage, and one or two actuator passages. If the valve has one actuator passage, it is called a three-way valve (3 ports). Likewise, if the valve has two actuator passages, it is

called a four-way valve (4 ports). The purpose of the of a directional valve is to reverse motion of a cylinder or hydraulic motor. For example, in a three-way valve the valve pressurizes an actuator port when the spool is in on extreme position. When the spool is shifted to the other extreme, the valve exhausts the same port. On the other hand, a four way valve uses the spool to direct flow from the pump passage to one actuator passage when it is in one extreme position. At the same time, the spool is positioned so that the other actuator passage is exhausted to tank. If the spool position is reversed to the other extreme position, then the actuator passages become reversed and the port that was pressurized becomes exhausted and the port that was exhausted becomes pressurized.

3.2.8 Display Unit

Since the display unit needed to be seen from great distances and withstand relatively large forces and vibrations due to rough ground conditions and tractor vibration, a traditional display unit such as a computer monitor or television screen could not be used. Also the display had to be capable of accepting computer based language since it would display information calculated and sent by the microprocessor. This type of outdoor field and computer-based application called for an industrial display. Industrial displays are commonly used at sporting events, on factory floors, and at construction sites. This type of display usually has a high alpha-numeric annunciation with dot matrix characters. The characters are made up of a matrix of light emitting diodes (LED). They employ a plug-in communication board that determines the type of serial data it receives and transmits. Displays can be operated in a direct mode where each character is displayed as soon as it is received, or in a

mode where the display is updated after it receives a line termination. Software commands control scrolling and scroll rate, flashing and flash rate, brightness level, cursor position, and more. Data formats and baud rates are field selectable with internal switches. Units are typically available in character heights from one to six inches and display two to ten characters.

CHAPTER 4

SPREADER MODIFICATIONS AND FABRICATION DETAILS

4.1 Spreader Specifications

The Gehl Company donated a Scavenger Model 1315 spreader that has a liquid capacity of 1,620 gallons and a solid struck capacity of 217 ft³. The spreader has a weight of 5224 lb. (less load and tires) with the following overall dimensions: 264 inches in length (spreader tank is 192 inches in length), 94.5 inches in width, and 65 inches in height. The spreader's PTO is driven at 540 RPM and operated by a tractor of 70 horsepower. For safety considerations, the spreader should not weigh more than 23,500 lb. based upon manufacturer recommendations.

4.2 Modified System

The spreader's weighing system consists of five load cells, a junction box, and a scale indicator with signal conditioning capabilities. The spreader's load is measured at five different locations by using Digi-Star bending beam load cells, model 2.5 DIA, 10,000 lb. capacity. The individual load cell signals are summed using a five input Digi-Star junction box. Finally, the summed load measurement is conditioned and displayed using a Digi-Star EZ 210 Electronic Scale Indicator. For this project, the load cells and junction box are incorporated into the spreader, while the scale indicator is mounted in the cab of a 1494 Case tractor.

4.2.1 Load Cells

The selected load cells each had a manufacturer's rating of 10,000 lb. and were made from elevated temperature drawn (ETD) 150 steel. The load cells were placed in the hitch and suspension system of the spreader. Although all the load cells had the same mechanical and electrical properties, two different types of load cells were needed to measure the spreader's load. A standard cylinder end shown in Figure 4.1 was incorporated into the hitch, while a typical wheel spindle shown in Figure 4.2 was included in the running gear of the spreader.

Modifications to the spreader's original hitch were made to incorporate the standard cylinder load cell and are shown in Figures 4.3a and 4.3b. The major change to the hitch was to include a sleeve to accommodate the load cell. To do this the existing hitch assembly was removed 12 inches past the hitch mounting plate. This left enough space to insert the sleeve assembly and allow the hitch to be reworked to its original tractor mounting dimension. The sleeve assembly must fit within the channel shaped tongue of the hitch as well as tightly hold the load cell in place. To do this, the sleeve assembly, shown in Figure 4.4, was used. By design, the sleeve forces the load cell to be symmetrically positioned within the hitch's tongue. This design was used so that the load cell could meet the manufacturer's mounting specifications of being parallel within 0.020 of an inch over 10 inches and mounted horizontally within 0.032 of an inch over 10 inches. To insure a tight fit of the load cell in the sleeve, the tube in the assembly was machine to 0.003 inches over the 2.5 inch diameter dimension of the load cell. A hole was drilled perpendicular to the tube's

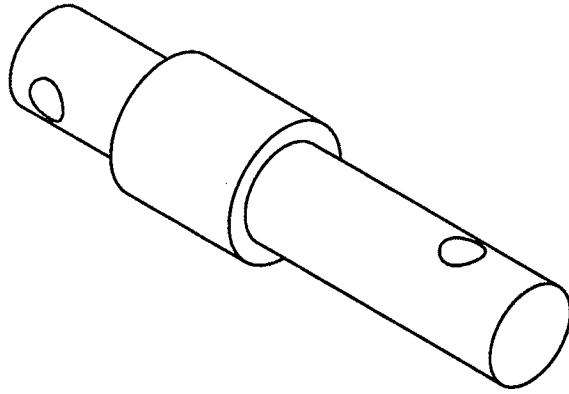


Figure 4.1: Digi-Star's standard cylinder end load cell.

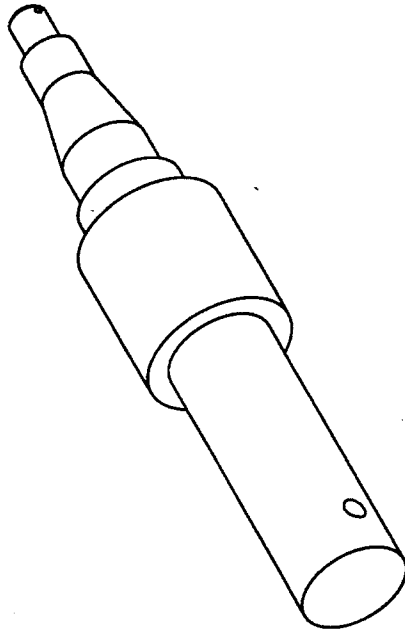


Figure 4.2: Digi-Star's wheel spindle load cell.

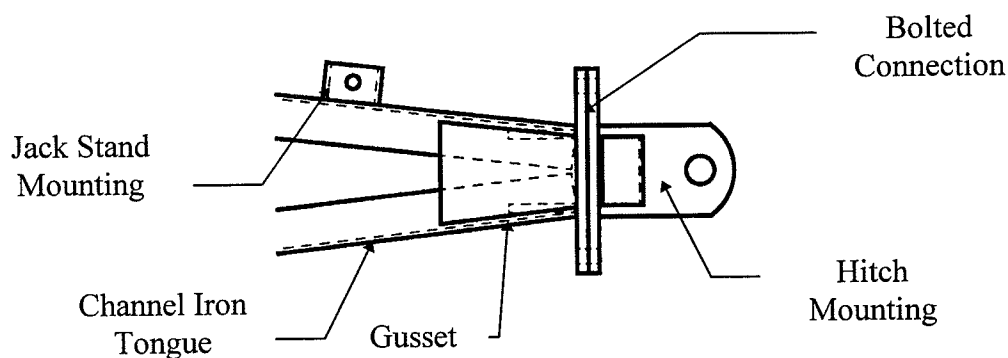


Figure 4.3a: Top view of spreader's original hitch design.

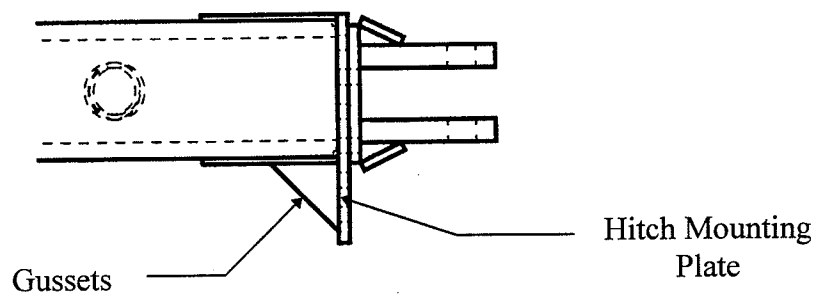


Figure 4.3b: Side view of spreader's original hitch design.

circumference and cylindrical axis so that a 1 inch grade 8 bolt could be used to lock the load cell within the sleeve (see Figure 4.4).

After the sleeve assembly was welded in place inside of the spreader's tongue (see Figure 4.5a & 4.5b), panels were welded onto the sides of the channels to compensate for the removed material. A mounting plate much like the original, but with a 4.0 inch hole where

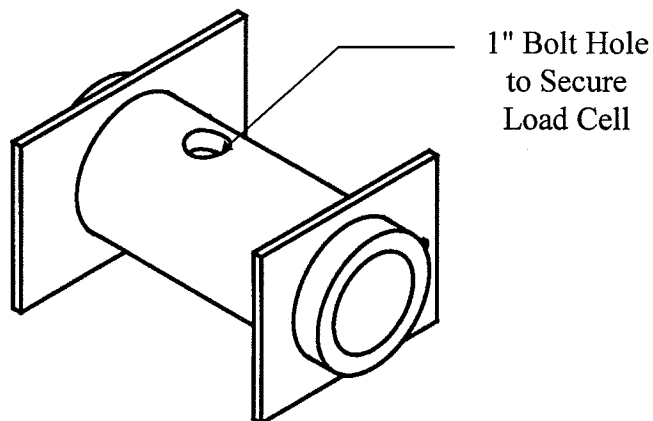


Figure 4.4: Load cell sleeve assembly.

the load cell would pass, was welded perpendicular to the side panels. This was done for removal and installation of the load cell as well as for the future use of the spreader without the load cell. Support plates and gussets similar to that of the original hitch were included in the modified hitch design. To connect the load cell to the hitch mounting bracket, a face plate with a cylindrical adapter had to be made to connect to the other end of the load cell. Another 1 inch bolt was used to connect the load cell and face plate assembly. The hitch mounting was bolted to the face plate assembly using $3/4"$ - 10 x 1.5 inch long grade 8 bolts to allow the spreader to connect to the tractor's hitch.

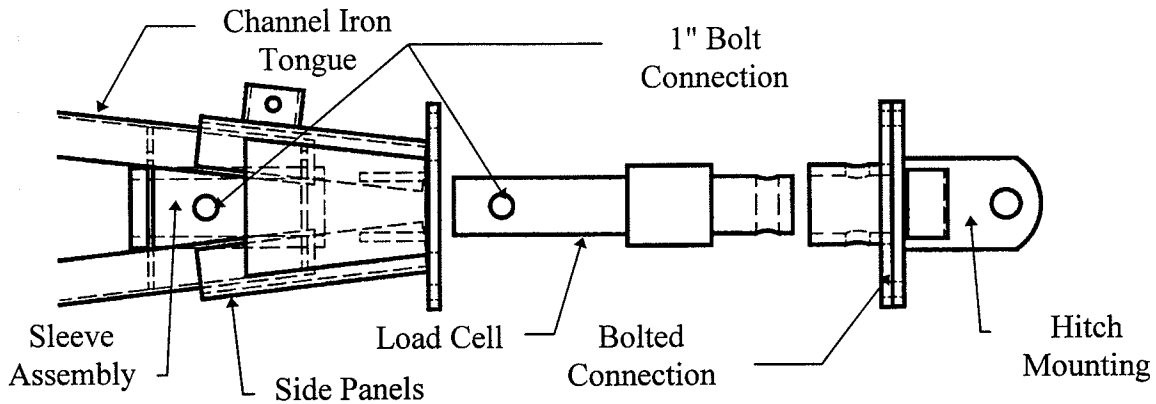


Figure 4.5a: Exploded top view of the spreader's modified hitch with load cell.

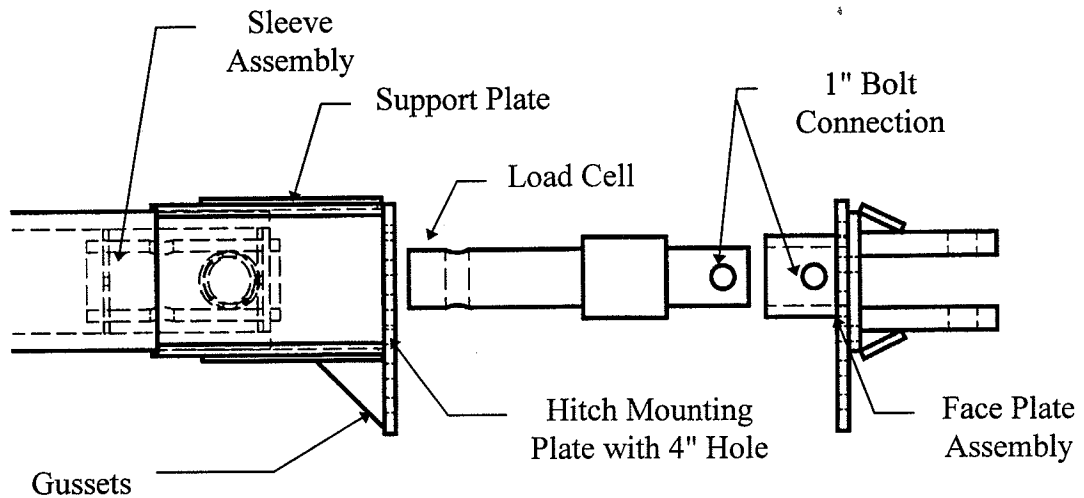


Figure 4.5b: Exploded side view of the spreader's modified hitch with load cell.

The next step in completing the spreader's weighing system was to modify the existing tandem beam axles shown in Figure 4.6. The spindles were removed and replaced with sockets that could hold the wheel spindle load cells. The sockets were made from 3.5 inch diameter (0.5 inch wall thickness) drawn over mandrel (DOM) tube steel machined to 0.003 inches greater than the 2.5 inch diameter dimension of the load cell. A hole was drilled perpendicular to the circumference and cylindrical axis of the tube so a 0.5 inch diameter

retaining pin could hold the load cell in place. The pin chronologically passes through the side wall of the axle, socket, load cell, and socket again with the head of the pin being fastened to side wall of the axle. Figure 4.7 is a drawing of the modified axle.

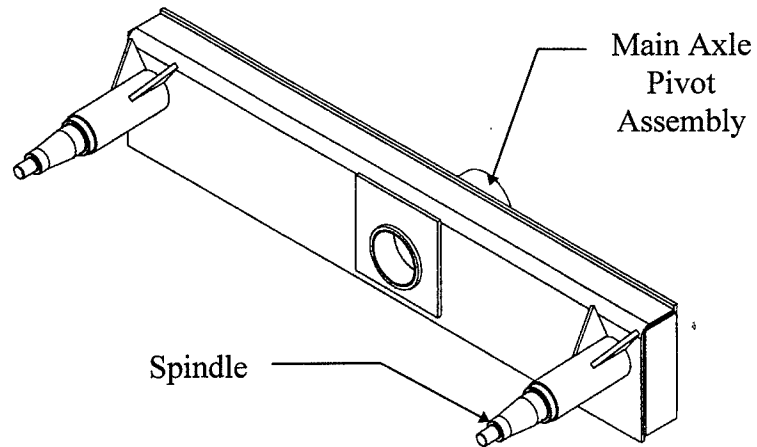


Figure 4.6: Isometric view of original tandem beam axle assembly.

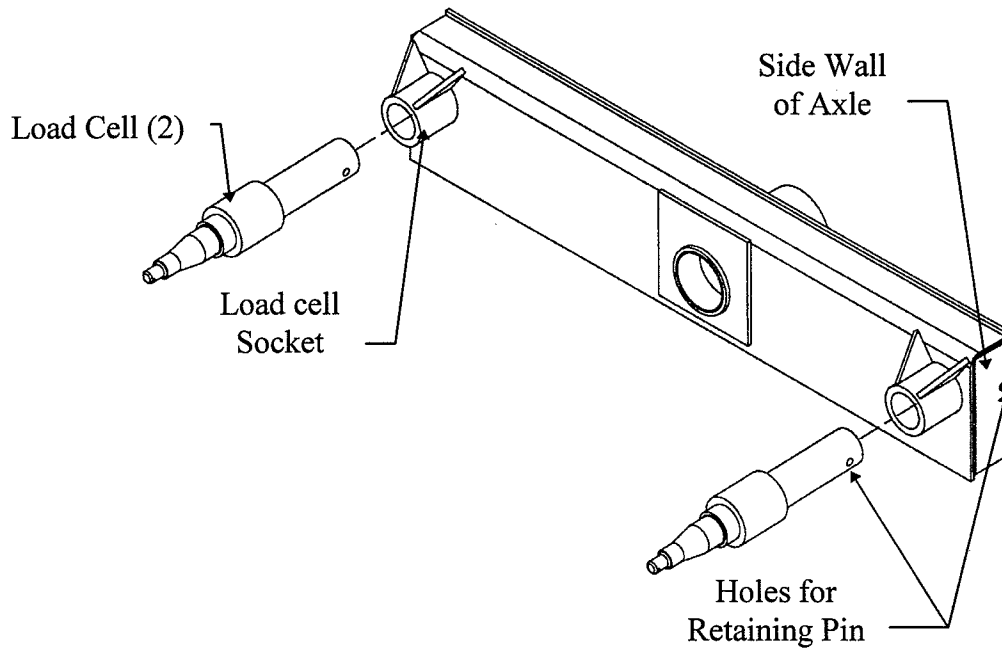


Figure 4.7: Isometric view of modified tandem beam axle assembly.

The load cell's circuitry required the precision machining and placement of the sleeve and sockets on the spreader and axles. For accurate measurement, the load cell must be held firmly in place in the proper direction of the acting load or the strain gauges will give false readings. For most bending beam load cells, four strain gauges are equally placed on the radial surface of the of the beam. In Figure 4.8, the two strain gauges illustrated as R_2 and R_4 are located on the top surface, while strain gauges illustrated as R_1 and R_3 are located on the bottom surface. The strain gauges are hermetically sealed to the beam by a steel shell. Sealing the strain gauges prevents them from being damaged and maintains their high sensitivity.

The red and black wires (power and ground respectively) supply the load cell its excitation voltage. The white and green wires (signal and signal ground respectively) provide the measured output signal to the junction box. Refer to Figure 4.8 for an illustration of a placement and wiring diagram of the load cell.

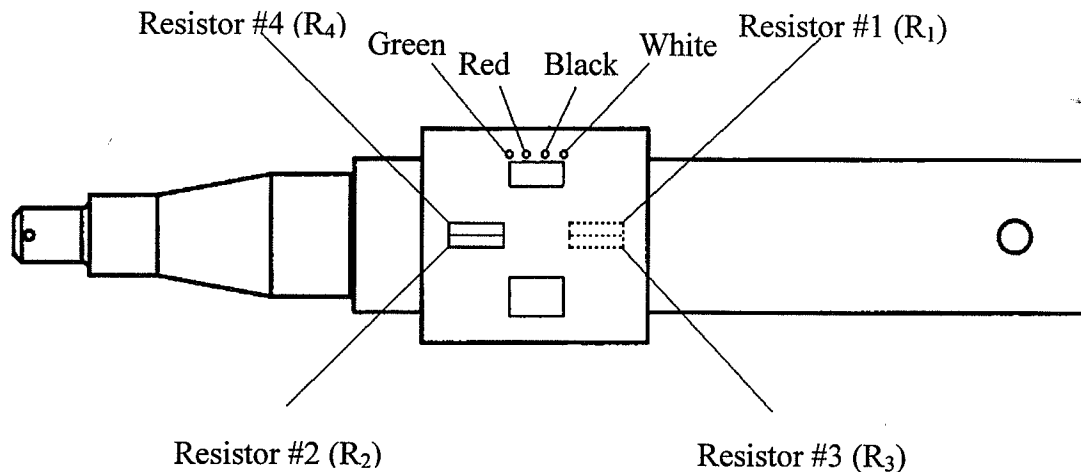


Figure 4.8: Top view of load cell with resistor and wiring layout.

Load cells usually indicate the location of the strain gauges by labeling the top of the load cell. If the load cell is positioned with the "TOP" label up, then a positive voltage will occur when an upward force acts on the bottom of the load cell. This occurs because the resistance of the strain gauge changes when the surface material of the load cell is stressed. The resulting strain of the load cells surface deforms the gauges and changes the resistance. Since the resistance change is exactly proportional to the strain due from stress and the stress is proportional to the applied force, then the resistance change in the gauge is directly proportional to the applied load of the beam.

The strain gauges are wired together in a Wheatstone Bridge configuration. The Wheatstone Bridge is the common wiring configuration used with strain gauge load cell applications because of its high accuracy of strain measurement under static and dynamic conditions. The inherent mathematical capabilities of the bridge exist because of the way it measures the electrical properties of the circuit. The bridge measures voltage or current by comparing other elements in the circuit. Figure 4.9 is an illustration of a common Wheatstone Bridge circuit. The two principal ways of operating a bridge are as a null detector and as a device that reads a difference in voltage or current.

To construct a null detector, a number of fixed resistance resistors are used in the circuit. When $R_1/R_4 = R_2/R_3$ the bridge is said to be null or balanced regardless of the magnitude of excitation or the mode of read out. Therefore, if the ratio of R_2/R_3 is fixed at a value (K), then the null bridge will balance when $R_1 = K \cdot R_4$. If R_1 is unknown and R_4 is known, then

R_1 can be determined by varying the resistance of R_4 until the bridge is balanced. Null-type detector bridges are usually used in feedback systems involving electromechanical elements (Sheingold, 1980).

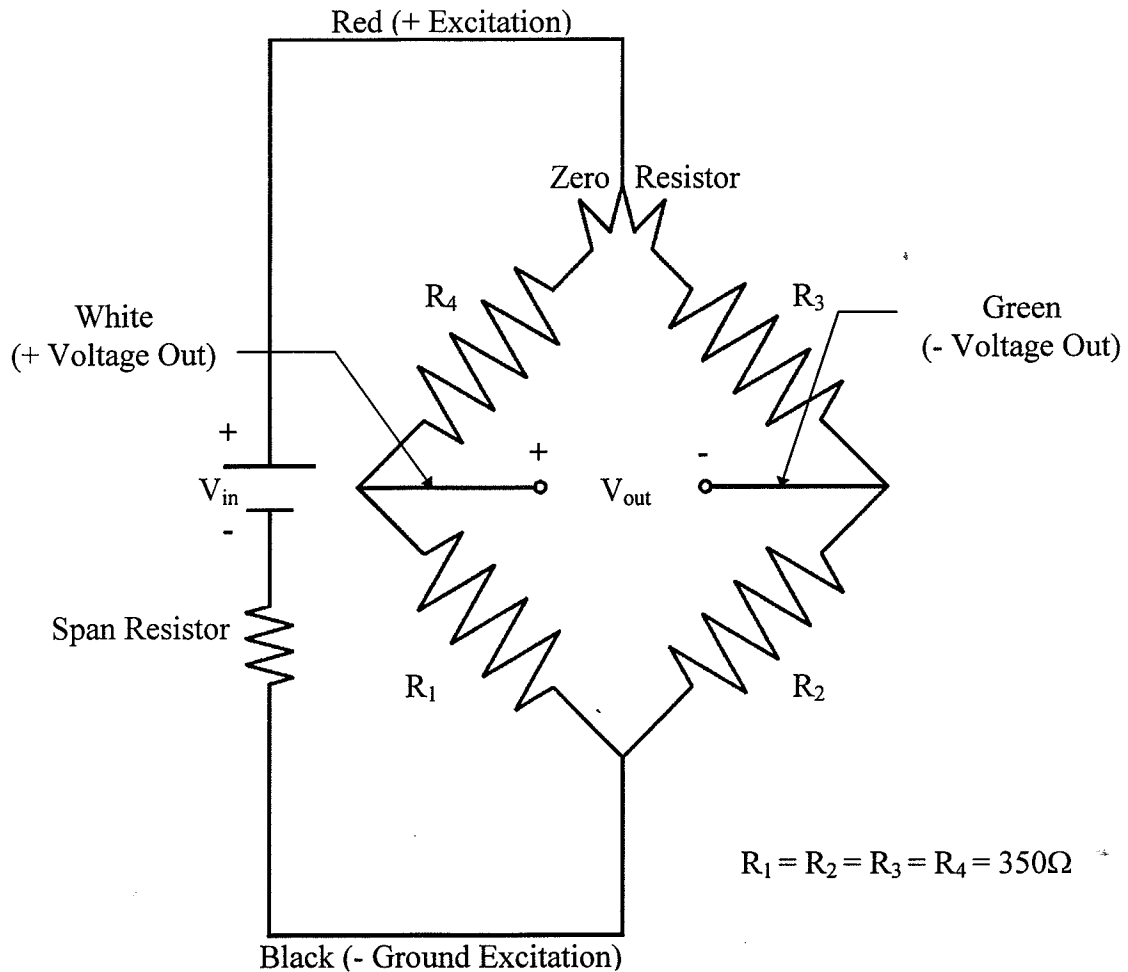


Figure 4.9: Schematic of the full Wheatstone Bridge circuit used on the load cells.

When a voltage or current difference is to be measured, variable resistors are used instead of fixed resistance resistors. Initially, all of the variable resistors are set equal. As the individual resistors are changed, the output of the bridge deviates from the balanced state yielding an output other than zero. This type of bridge is used for many transducer applications because it allows one or more variable resistors to be used for such things as strain measurement.

For either bridge configuration, the relationship between the excitation voltage supplied to the bridge and the output voltage from the bridge is based upon the following relationship:

$$V_{out} = V_{in} \left(\frac{R_1}{R_1 + R_4} - \frac{R_2}{R_2 + R_3} \right)$$

The sensitivity of the bridge is the ratio of the maximum expected change in the value of the output to the excitation voltage. An example of this can be seen by looking at the sensitivity of the load cells used in the weighing system of the spreader. All the load cells had a sensitivity of 0.0004 Vdc per 1 Vdc of excitation at the rated load of 10,000 lb. This means that for 1 Vdc of excitation and an applied load of 10,000 lb., there will be an output of 0.0004 Vdc. Likewise, 2.0 Vdc of excitation at the rated load would produce an output of 0.0008 Vdc. The manufacturer's recommended excitation voltage is between 5.0 to 10.0 Vdc.

In addition to the four 350 Ω strain gauges in Figure 4.9, there are also zero and span resistors. The zero resistor is included in the bridge to compensate for any small resistance

changes in the strain gauges due to temperature fluctuations or creep occurring in the load cell. The zero resistor corrects for the small fluctuations and allows the bridge to be balanced. The span resistor is usually a foil resistor which is used to adjust the bridge so the output is consistently linearly proportional to the excitation voltage.

An element not shown in the circuit in Figure 4.9 is a fifth wire called a shield wire. A shield wire is used to protect the circuit from current leakage which can degrade the performance of the load cell. The shield is nothing more than a wound strand of conducting material that is wrapped around the inner surface of the load cell and bridge. The shield is driven at low impedance to a potential that is very close to the voltage being protected. When the shield is properly used on the load cell it protects the bridge by absorbing stray currents (Sheingold, 1980). The use of the shield along with the Wheatstone Bridge's high efficiency renders an extremely accurate load cell. The expected accuracy range of the Digi-Star load cells is $\pm 1\%$ for static conditions. The expected accuracy range of the load cells under dynamic conditions is $\pm 3\%$, but can vary depending on the application.

4.2.2 Junction Box

A five input Digi-Star junction box is used to interface with the five load cells used on the spreader. Mounted on the rear wall of the spreader's enclosed gearbox, the junction box distributes the supply voltage from the indicator to the load cells as well as sums the signal from the load cells to the indicator. Consisting of a total of six main wire banks (five for the load cells and one for the scale indicator) which lead to an on-board circuit, the junction box

acts as a mediator between the load cells and scale indicator. The five screw terminals located on each wire bank are for each of the load cell wire bundle ends: signal (+), signal (-), excitation (+), excitation (-), and shield. The terminal ends of each wire bank are wired into the circuit board. The circuit board adds the individual load cell signals in parallel, breaks down the power input from the indicator, provides equal excitation to each load cell, and delivers the summed measured voltage to the indicator. Figure 4.10 is an illustration of a five input Digi-Star junction box.

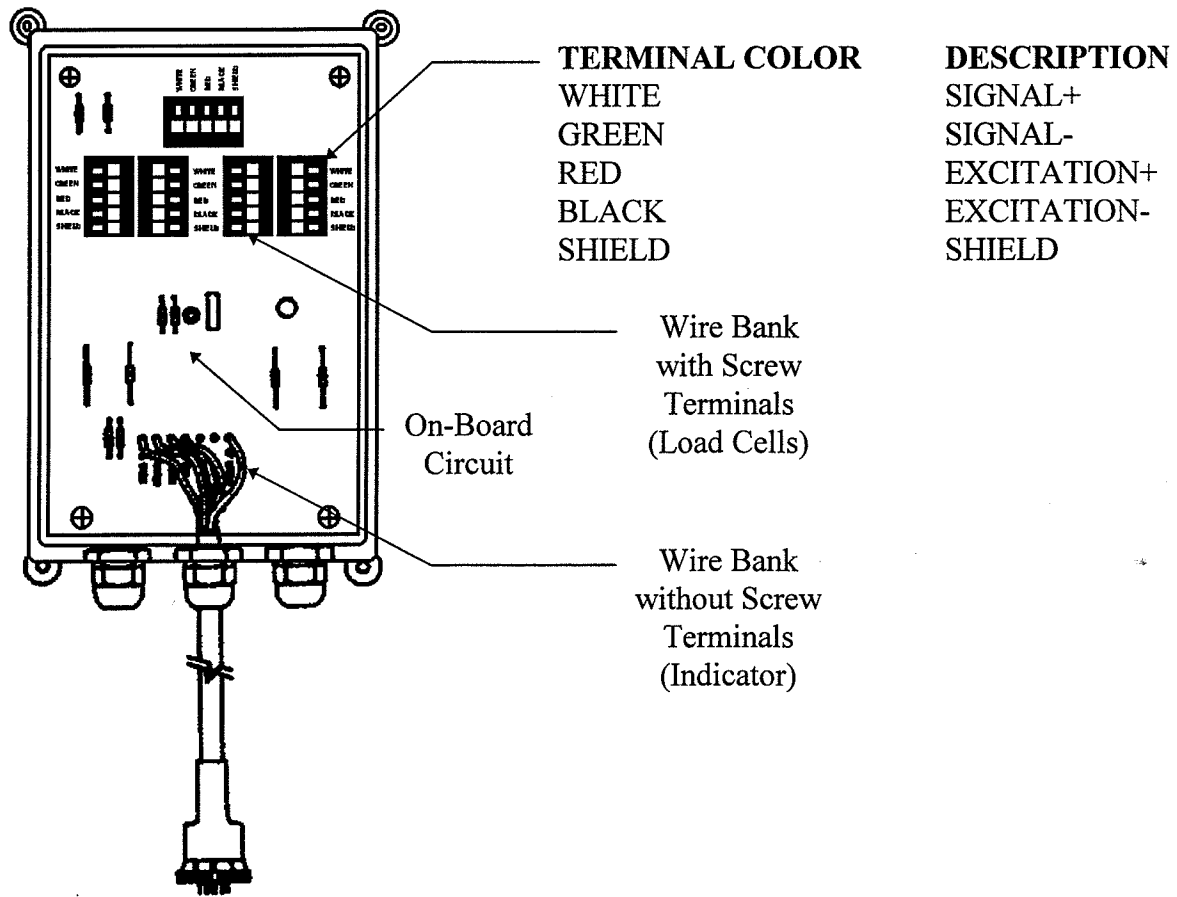


Figure 4.10: Digi-Star's five input junction box.

4.2.3 Electronic Scale Indicator

The Digi-Star EZ-210 Electronic Scale Indicator shown in Figure 4.11 is a multipurpose unit that acts as a signal conditioner and alpha-numeric display that provides the following: on-board weight and error message display, front panel calibration of load cells, a one button zero-balancing, and a choice of standard or metric weight units.

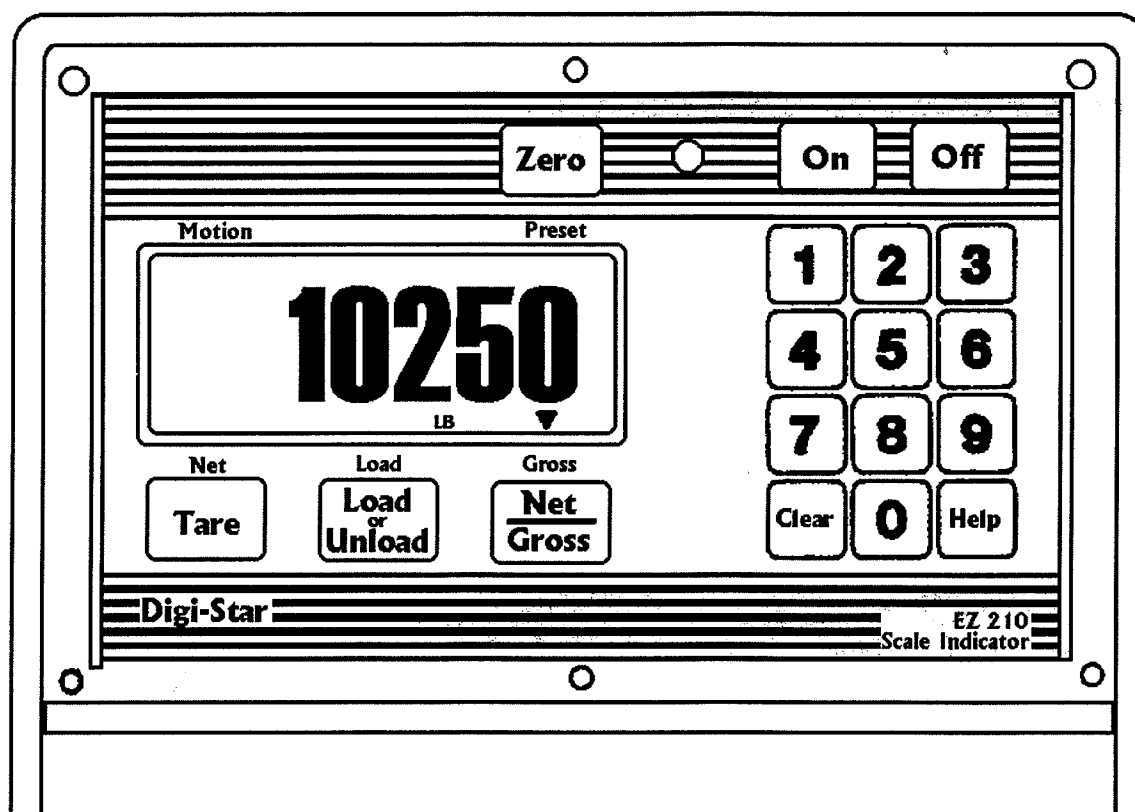


Figure 4.11: Front view of Digi-Star's EZ 210 Scale Indicator.

The indicator processes the summed analog voltage signal into a 16 bit digital weight value under user-specified conditions such as: amplification of the load cell signal (gain), smallest

weight increment (e.g. 1, 2, 5, 10 lb., etc.), system load capacity, data filtering method (tolerance), data averaging method (little - great), and the output rate of weight data (1 - 4 Hz). All of the user-specified parameters are entered into the indicator through the keypad on the front panel.

Once the analog weight signal has been received through the load cell port (see Figure 4.12) and internally processed, the digital weight value is displayed on the front panel of the unit as well as sent to the printer port (see Figure 4.12) as a RS232 serial communication string. RS232 is a standard that designates the form of the communication signal. Specifically, it is a +5 to +15/-5 to -15 (1/0) voltage requirement on transmitted signals and a +3 to +13/-3 to -13 (1/0) on received signals. This alpha-numeric string can be printed, displayed, or written to a file by any device that can accept and decipher RS232 serial communication.

The indicator's power requirements are between 10.5 to 16 Vdc. It uses a portion of its supply voltage to deliver 8 Vdc of excitation voltage to the individual load cells. The unit has an optional remote port (see Figure 4.12), which allows users of the system to calibrate and input user-specified parameters into the indicator from remote locations. The indicator has an operating temperature range of -20° to 140° F and has a system accuracy of $\pm 0.25\%$ or $\pm 0.5\%$ depending on the type of Digi-Star load cells used.

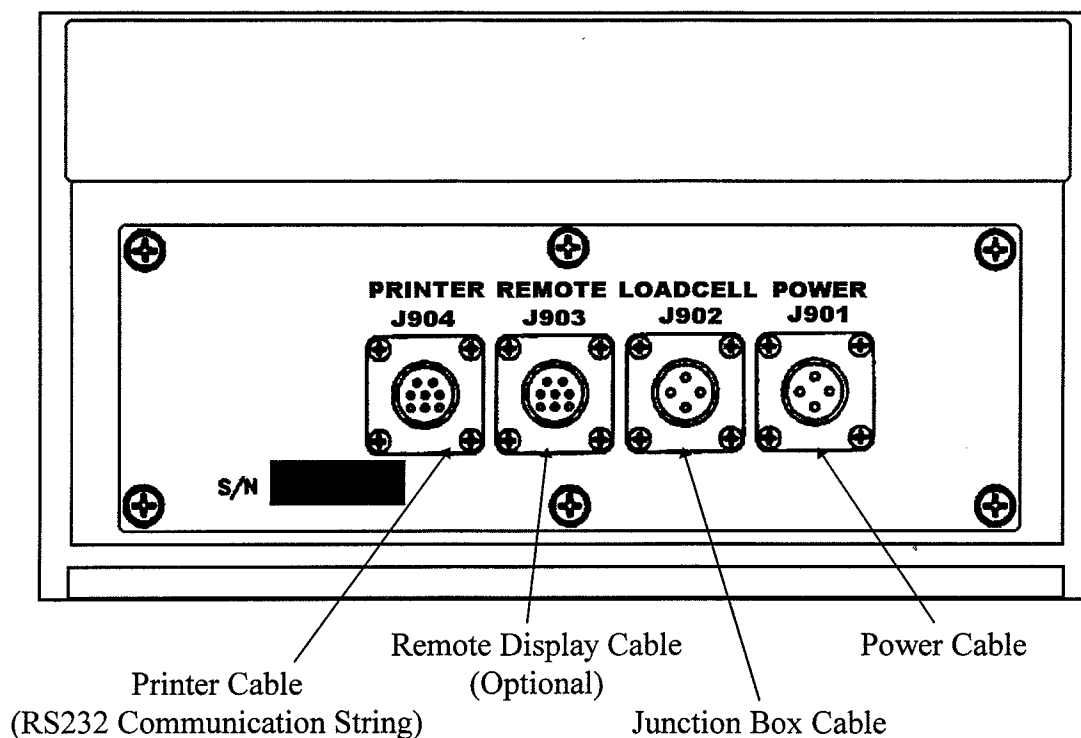


Figure 4.12: Bottom view of Digi-Star's Scale Indicator interface panel.

4.3 Speed Sensing System

With the weighing system in place, the next step was providing instrumentation to measure the speed of the spreader. Because the Case 1494 tractor does not come equipped with a true ground speed indicator, the ground speed of the spreader had to be determined in some other fashion to calculate an on-the-go application rate. A Fork Standards Inc. (FSI) rotary shaft encoder was selected to measure the speed of the spreader. The FSI model RSE-3/8 (see Figure 4.13) was chosen.

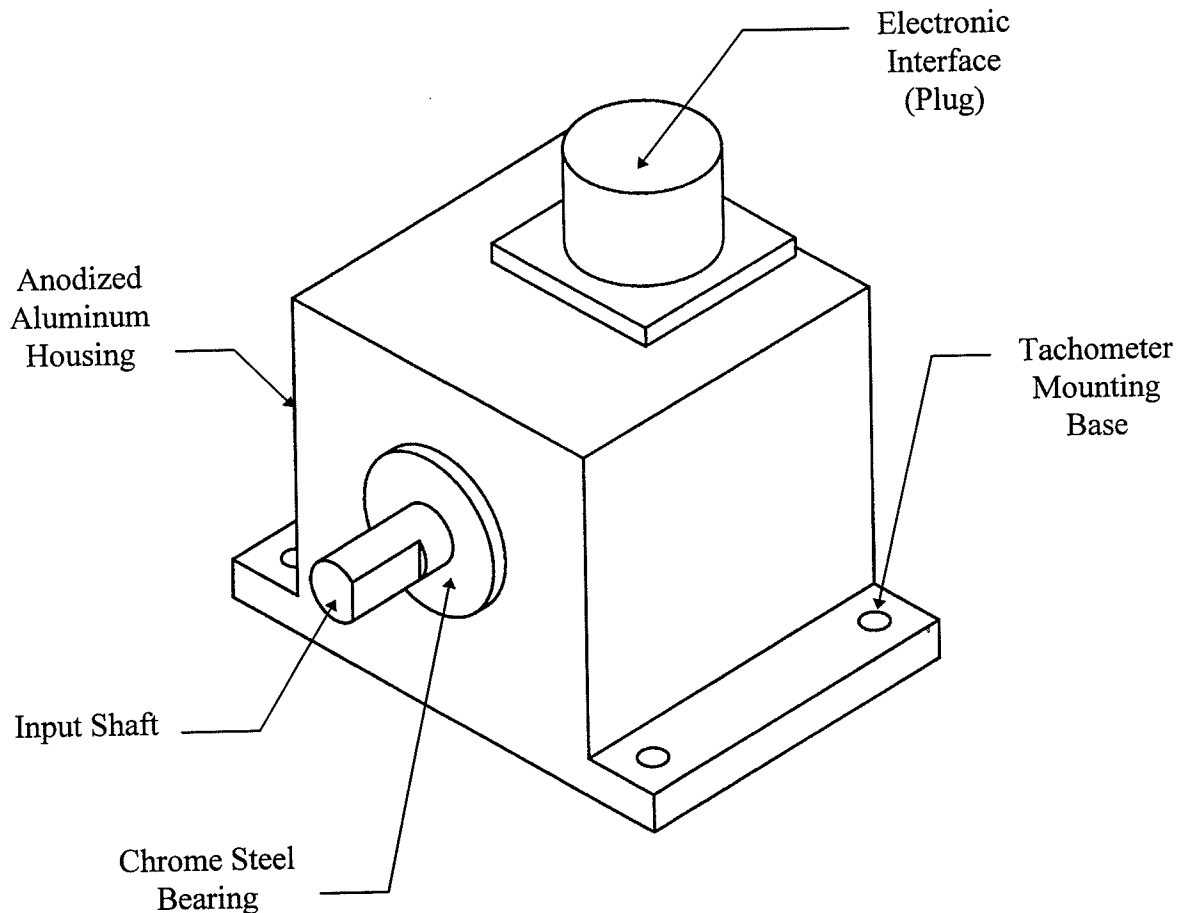


Figure 4.13: FSI model RSE-3/8 optical shaft encoder.

The RSE-3/8 sends out a square wave 50/50 duty cycle or an indexed pulse output that ranges from 0 to 20,000 pulses/sec. The magnitude of the square wave or pulsed output is equal to the input voltage. The range of input voltages is 5 Vdc or 12 - 28 Vdc. The encoder operates under low power consumption (45 milliamps @ 15 Vdc) and has reverse polarity and output short circuit protection.

The encoder's internal circuitry is protected by an anodized aluminum housing with an optional tachometer mounting base. The encoder's input shaft is supported by heavy duty

chrome steel bearings that can withstand radial loads up to 30 lb. and axial loads up to 10 lb. The input shaft can rotate in either direction and can handle speeds up to 6,000 revolutions per minute.

The tractor battery was used to provide the input power to the encoder. With this configuration and choice of output, the encoder will deliver a +13.2 to +15 Vdc indexed output pulse depending on the charge of the battery. The pulses can be counted by an analog counter which can determine the number of pulses per unit time. To build an effective ground speed detection system, the input shaft of the encoder had to be directly or indirectly linked to the wheel of the spreader.

The support system shown in Figure 4.14 was designed to indirectly link the encoder's input shaft to the wheel of the spreader. It is mounted on top of the spreader's left hand side tandem beam axle between the two tires (see Figures 4.15a and 4.15b) using the three slotted holes. The three slotted holes match up with three 1/4" - 20 tapped holes machined in the tandem beam axle. The support system uses the cantilevered mounting plate to hold the encoder in place, while allowing the rest of the spring-loaded input wheel assembly to pivot. All of the rotation occurs at the universal-joint that connects the input shaft of the encoder to the shaft of the input wheel. The spring applies the proper tension to hold the input wheel against the spreader's wheel. The spring also allows the input wheel to deflect off of the spreader's wheel if any dirt or debris gets stuck on the tire. The angular deflection of the

input wheel assembly is controlled by a small rod welded to the bottom of the largest telescoping square tube riding in the slot of the main mounting bracket.

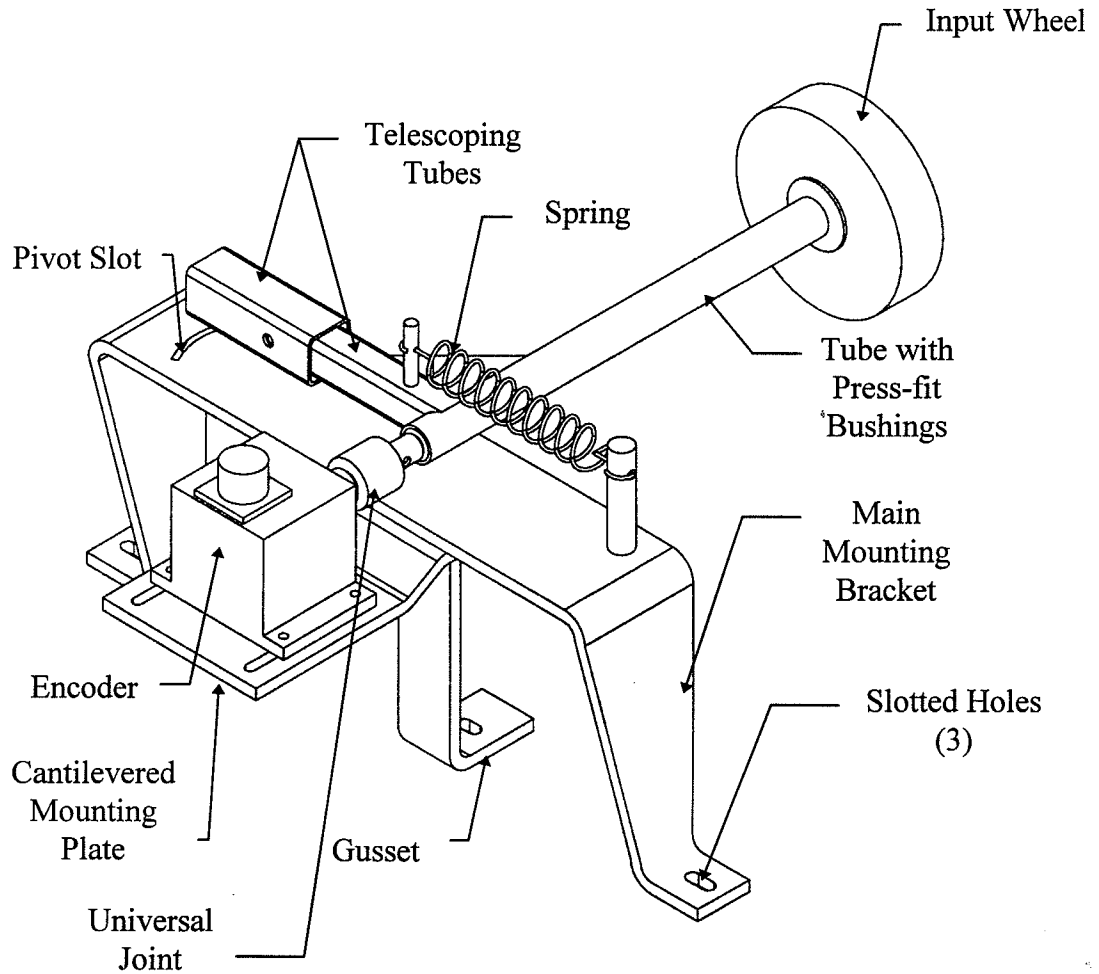


Figure 4.14: Optical encoder support and pivot assembly.

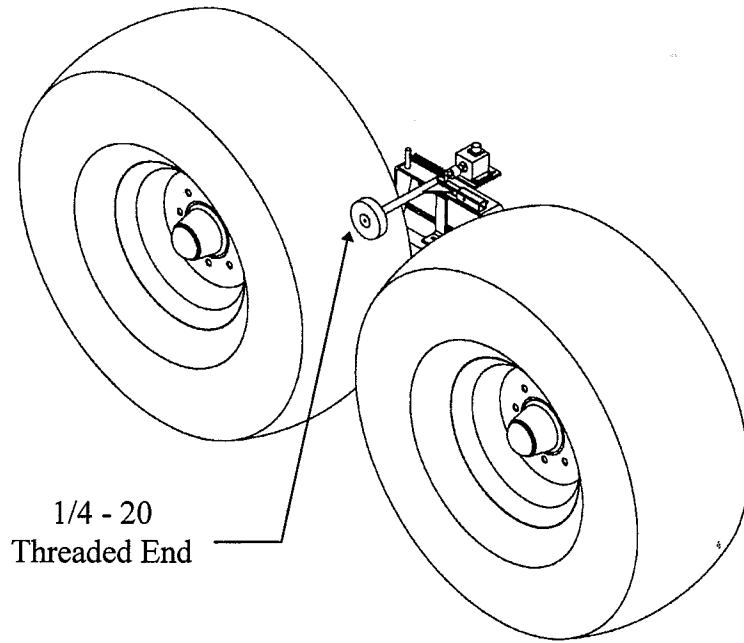


Figure 4.15a: Isometric view of encoder assembly positioned on the tandem axle.

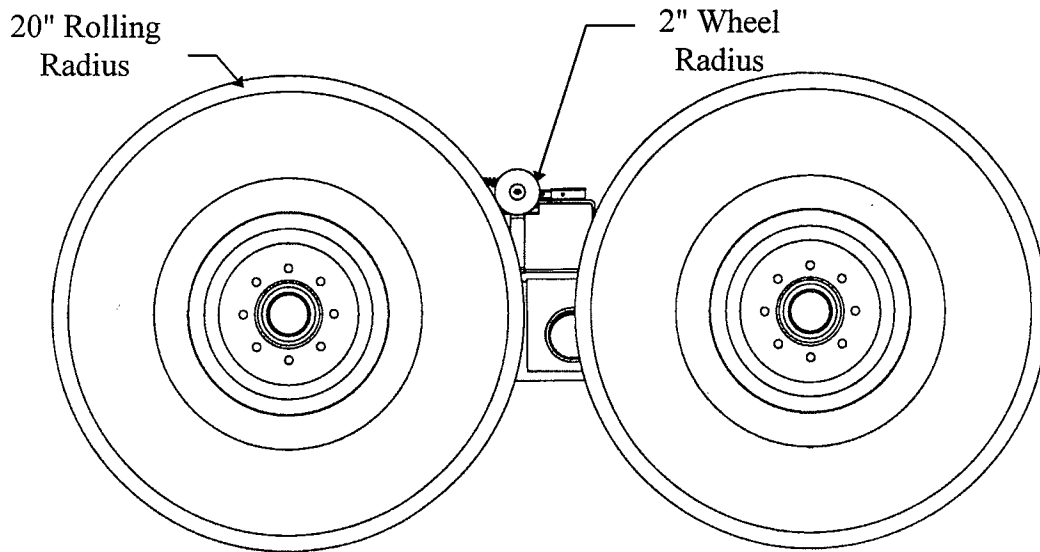


Figure 4.15b: Side view of encoder assembly positioned on the tandem axle.

Since the shaft encoder is indirectly linked to the spreader, it is important to size the connection between the spreader's tire and the encoder's input wheel. To develop a proportional relationship between the two, the spreader's average rolling radius was used as a basis. Using the tire manufacturer's specified rolling radius and Gehl Company's suggested rolling radius, a twenty inch rolling radius was used. This value accounted for dimensional fluctuations due to loading, tire pressure, and temperature. A two inch radius input wheel was used to yield a convenient 10 to 1 ratio. For example, for every ten rotations of the encoder wheel there is one complete rotation of the spreader's drive wheel. The input wheel has a black hard rubber stain-resistant, nonmarking, tread molded to a hard rubber core. Built for light to medium duty commercial or industrial applications, the hard rubber wheel rolls easily, resists oil and water, and handles high load capacities on hard surfaces. It also features a self-lubricating plastic insert roller wheel bearing.

The input wheel is held fixed onto the rotating shaft connected to the universal joint by a screw tightened into the 1/4" - 20 threaded end of the shaft. That rotating shaft is supported by two oil impregnated, bronze bushings press-fit into each end of the machined tube. Although the frictional contact between the input wheel and the spreader wheel is large enough not to be affected by such elements as water or a light layer of mud, it is important to prevent any debris build-up on the input wheel. Any build-up on the input wheel will alter the desired 10 to 1 speed ratio.

4.4 Position Sensing System

The Gehl Scavenger Model 1315 side discharge spreader uses a vertical gate located behind the expellers to control the discharge rate. It employs a hydraulic cylinder connected to the tractor's hydraulic system to raise and lower the gate. The cylinder is attached between the top of the gate and an upper portion of the spreader's reinforced side wall. Because changes in gate height cause changes in the application rate, it was necessary to know the position of the gate for control purposes.

A Penny+Giles Hybrid Linear Potentiometer (HLP) was selected to measure the gate's position because it ensured the required level of accuracy as well as being economical. The HLP, model 350, has a stroke of 15.75 inches (400 millimeters) and two self aligning bearing mountings to accommodate the 15.68 inch stroke and mounting parameters of the hydraulic cylinder. The potentiometer works on a proportional volts-in/volts-out principle using a linear wiper resistance of 16 k Ω which has a maximum power dissipation of 8 watts. It can handle input voltages ranging from 0 to 74 Vdc and has an independent linearity of $\pm 0.15\%$. It can accurately track position at speeds up to 1000 millimeters/second and has a rated life of 50 million cycles at 250 millimeters/second.

To insure the in-line action of the cylinder was being measured, the potentiometer was mounted parallel to the hydraulic cylinder: the pin connection of the gate and cylinder and at the very top of the cylinder. To mount the bottom portion of the potentiometer, a new pin had to be designed that would join the gate and cylinder together as well as act as a mounting

device to attach the potentiometer (see Figure 4.16). The original pin was a 5.0 inch solid piece of 1 inch diameter steel. The new pin design was 3.375 inches longer than the original and had one end with a reduced diameter of 0.375 inches at one end to accommodate the self aligning bearing mounting of the potentiometer. The 0.375 inch diameter end on the pin was 0.375 inches in length. A 1/4" - 20 hole was tapped into the end with the 0.375 inch diameter so the bottom of the potentiometer could be held on the shaft by a bolt. The cotter pin holes for holding the pin in place on the original design were adapted to the new pin design.

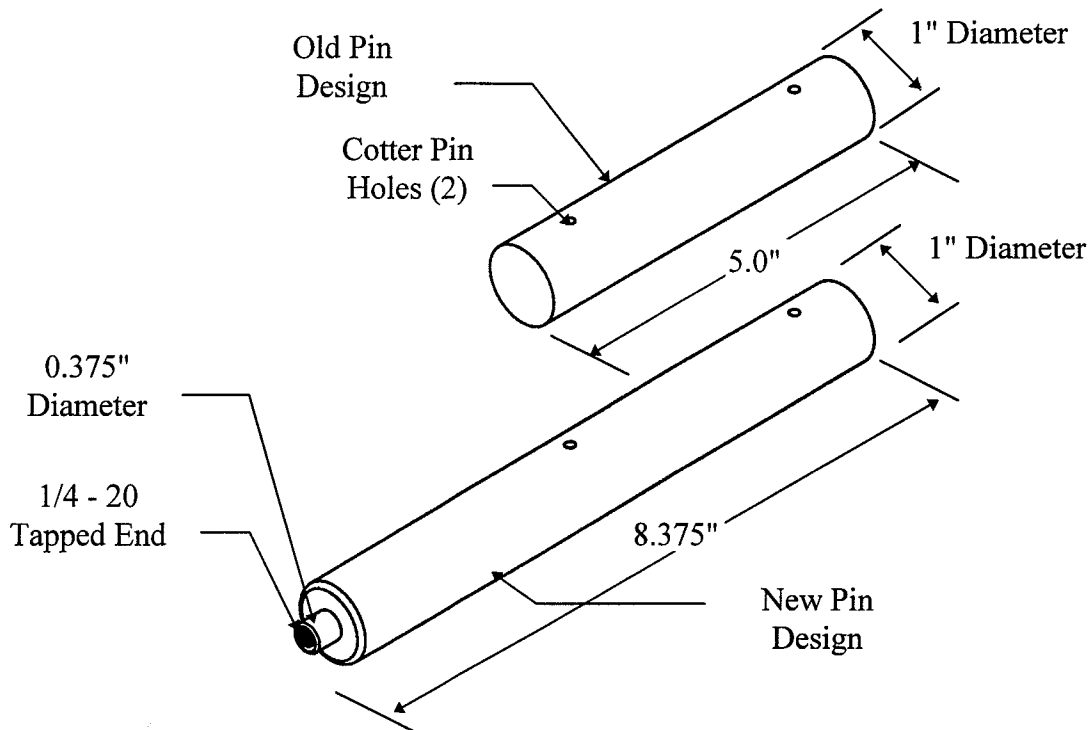


Figure 4.16: Isometric view of the original and new pin design.

To mount the top portion of the potentiometer, a cylinder end cap was designed (see Figure 4.17). It consisted of a 7.25 inch by 0.5 inch diameter rod and an 8 inch by 3.5 inch diameter (with a 0.5 inch wall thickness) DOM tube. At one end of the rod, there is a 0.375 inch long section machined down to 0.375 inches in diameter. A 1/4" - 20 hole was tapped into the

0.375 inch diameter rod end so the top of the potentiometer could be held on the shaft by a bolt. A 2 inch portion inside tube was machined to 0.005 inches over the outside diameter of the cylinder. A 1.125 inch slot was milled into the side wall of the tube to fit over the hydraulic cylinder port. At the opposite end, a 0.5 inch diameter hole was drilled perpendicular to the tube's circumference. The rod, with the non-machined end, was placed in the drill holes flush to one end of the outer tube and then welded. The welded assembly was positioned over the end of the cylinder with the machined groove resting on the top end of the cylinder and welded into place. Refer to Figure 4.18 to see a drawing of the HLP 350 mounted on the spreader's cylinder.

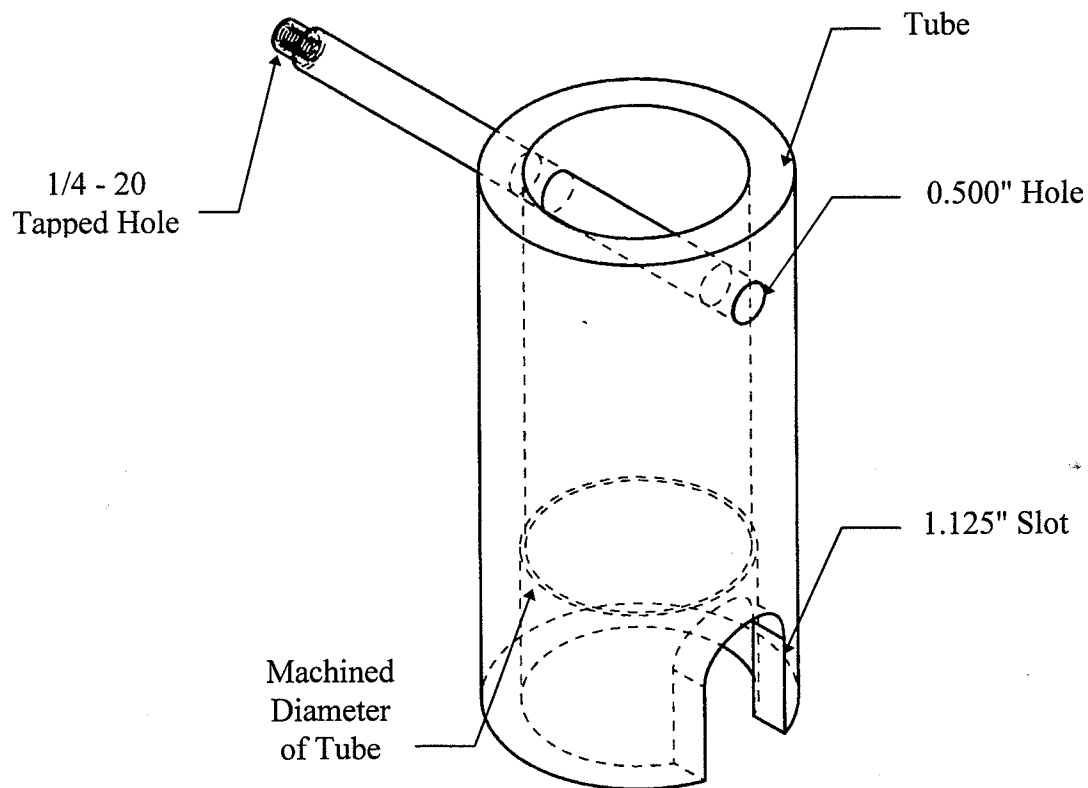


Figure 4.17: Isometric view of cylinder end cap.

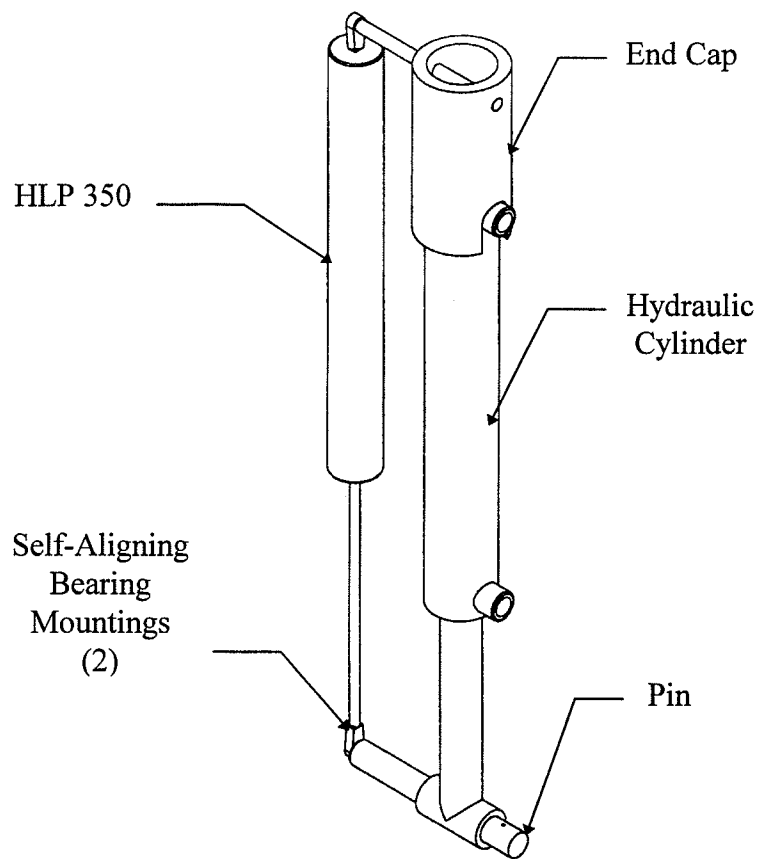


Figure 4.18: Isometric view of the HPL 350 mounted onto the spreader's cylinder.

Since the potentiometer was going to be exposed to moisture and other potentially damaging elements, it was enclosed in a set of telescoping polyvinyl chloride (PVC) tubes. A 2.25 inch outer diameter (O.D.) tube was machined so that its inner diameter (I.D.) was 0.005 inches over the O.D. of the thickest portion of the potentiometer. A 2.50 inch O.D. tube was machined so that its I.D. was 0.005 inches greater than the 2.25 inch O.D. tube. Two corresponding PVC end caps were used to enclose the potentiometer inside the telescoping tubes. Holes were cut in the end caps to accommodate self-aligning bearing mounting

dimensions. The end caps were glued (using PVC epoxy) onto the ends of the tubes with the potentiometer inside. With the protective shell caps butted up to the end of the mountings, small metal brackets were placed on each mounting to prevent any relative motion between each tube and the potentiometer.

4.5 Directional Control Valve

With the spreader's original hydraulic configuration, the gate is raised or lowered by moving the lever of the tractor's 4-way, 3-position, open-center, hand-operated directional control valve (DCV) to one extreme or the other. A schematic of the original tractor-spreader hydraulic system is shown in Figure 4.18. Changes had to be made to the spreader's existing hydraulic system to build a feedback control system that will measure and manipulate the application rate.

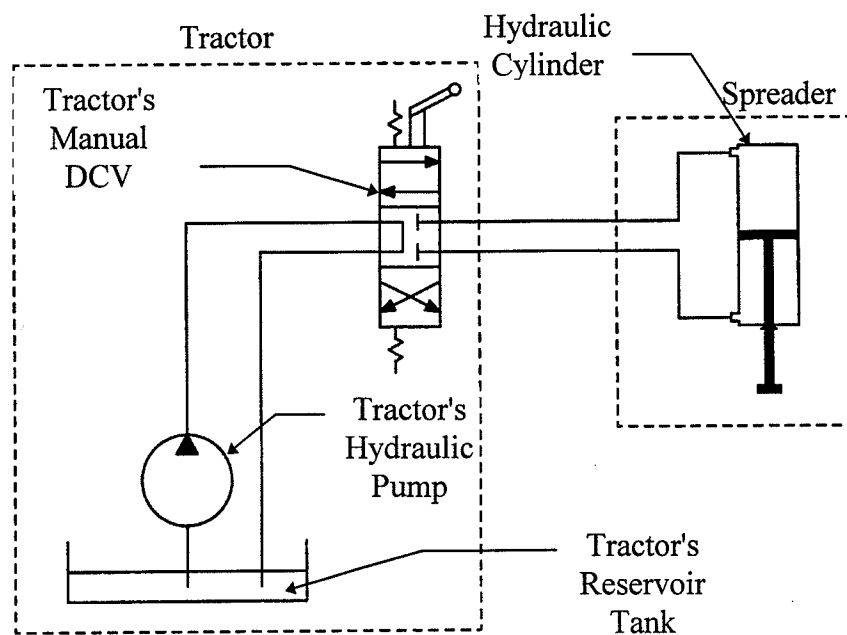


Figure 4.19: Original tractor-spreader hydraulic schematic.

A Fluid Power Systems (FPS) DCV, model MV4-43K-12LA, was selected and incorporated into the spreader's hydraulic system. This 4-way, 3-position, open-center, spring centered, DC solenoid operated valve is designed to handle flow rates up to 12 gallons per minute (GPM) at pressures of 3000 pounds per square inch (psi). This valve features a hardened steel spool which is precision fit into a high strength alloy cast iron body. It has 3/4" - 16 thread O-ring boss female ports which make the valve easy and versatile to plumb. The weather-resistant solenoid coils are epoxy-encapsulated with Class H magnetic wire and crosslinked polyethylene coated lead wire. The solenoids operate on 12 Vdc and draw a maximum of 3.4 amps.

The inclusion of this valve in the spreader's hydraulic system allows the gate position to be electronically controlled by activating one of the two solenoids. If neither solenoid is activated, flow is sent back to the tractor's reservoir tank. To activate one of the solenoids on this valve, 12 Vdc must be applied across the two lead wires. These lead wires interface with a wire winding around a ferromagnetic core within the solenoid. The current derived from the applied voltage is sent through the winding producing a magnetic flux. The magnetic flux production in turn produces a magnetic field intensity which attracts a moveable iron armature attached to the valve's spool (Smith and Dorf, 1992). As long as there is current flowing through the winding, the armature will be attracted to the core and the spool will be held in place allowing fluid to flow into one end of the cylinder. Once the applied voltage is terminated, current through the winding stops and a spring placed between the spool end and

solenoid core will force the spool back to its original position allowing the fluid to flow back to the tractor reservoir.

A schematic of this closed-loop circuit can be seen in Figure 4.20. It should be noted that to operate the gate electronically without any operator input the tractor's DCV must be placed in the forward position which corresponds to the spool position shown in Figure 4.20.

To mount the DCV to the spreader, four 3/8 inch holes were drilled into the side wall of the enclosed drive. The DCV, equipped with mounting brackets, was fastened to the inside wall by four 3/8" - 16 x 3/4 inch long grade 8 bolts. An additional 3 inch hole was drilled into the end support plate to pass the hydraulic hoses leading to and from the cylinder to reach the valve. A rubber grommet was placed around the perimeter of the hole to prevent damage to the hoses.

To connect the four hoses to the valve, four 90° 3/4" - 16 O-ring boss male to 9/16" - 18 Joint Industrial Conference Standard (JIC) male fittings were used. The 3/4" - 16 O-ring boss male ends were threaded into the female valve ports. A set of 6 and 10 foot hoses were used to make all the connections. The 6 foot set used Gates 3/8 inch diameter high pressure hoses (rated @ 2500 psi) with JIC female fittings on both ends. The 10 foot set used the same hose type with two JIC female fittings on one end and 1/2 inch National Pipe Thread (NPT) at the other. A Parker Pioneer male nipple was placed on the 1/2 inch NPT end of the 10 foot hoses for coupling to the tractor remote ports.

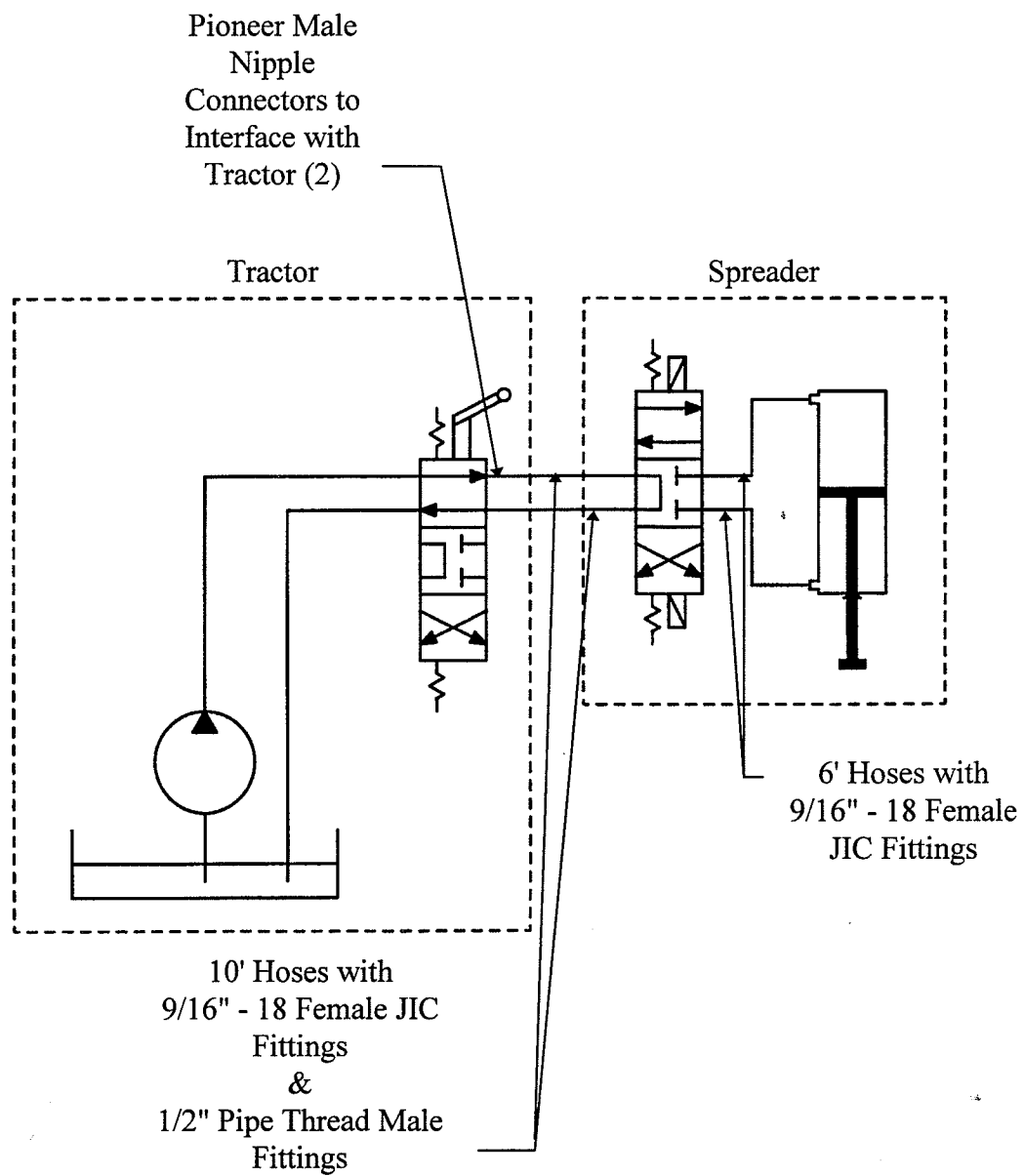


Figure 4.20: Revised tractor-spreader hydraulic schematic with DCV.

CHAPTER 5

CONTROLLER SPECIFICATIONS AND ELECTRICAL SUBSYSTEMS

5.1 Controller Specifications

The application of a digital computer for control may take many forms and entail a wide range of ideas and principles. The simplest approach is to use a computer for a data collector and calculator. To completely automate a process it is necessary to develop a computer system that is capable of comparing desired results with actual results and then taking corrective action. The computer relies on sensors for its input data and actuators to carry out its system manipulation. To build an efficient and effective control system the computer must be able to receive various forms of inputs as well as transmit various forms of output. It must also be capable of performing mathematical and logic operations at a high speed. In addition, it must be compact, easily powered, reliable and durable. These computer control demands warrant the use of a microcomputer.

The central core of the controller is a pair of microcomputers. Two PARALLAX BASIC Stamp Computers are used to collect input data, perform calculations, and control the system output. Each computer is a 24 dual in-line package (DIP) integrated circuit (IC) mounted on a 2.625 x 3.125 inch carrier board with a prototyping area. Each one has 16 input/output (I/O) lines and is programmed in BASIC. They have the ability to perform integer math and Boolean logic operations. Each hold up to 600 lines of programming code and operate at a clock speed of 20 MHz. All control code is downloaded to the IC through the female DB 9

pin serial port hardwired on the carrier board. The computers come with their own BASIC interpreter and EEPROM program memory. There is a reset switch on each carrier board that restarts the BASIC interpreter allowing the computer to reboot itself without power termination. They are individually powered by a +9 Vdc source (9 volt battery or electric 9 volt battery adapter). They have a regulated +5 Vdc output capability for controlling logic devices such as servos and stepper motors. They also have the ability to receive and transmit transistor to transistor logic (TTL) communications as well as perform pulse recognition and counting operations. They can be interfaced with liquid crystal displays (LCD's), analog to digital converters (A/D), keypads, serial communication drivers, and infrared communication equipment. A schematic of the PARALLAX BASIC Stamp Computer is shown in Figure 5.1.

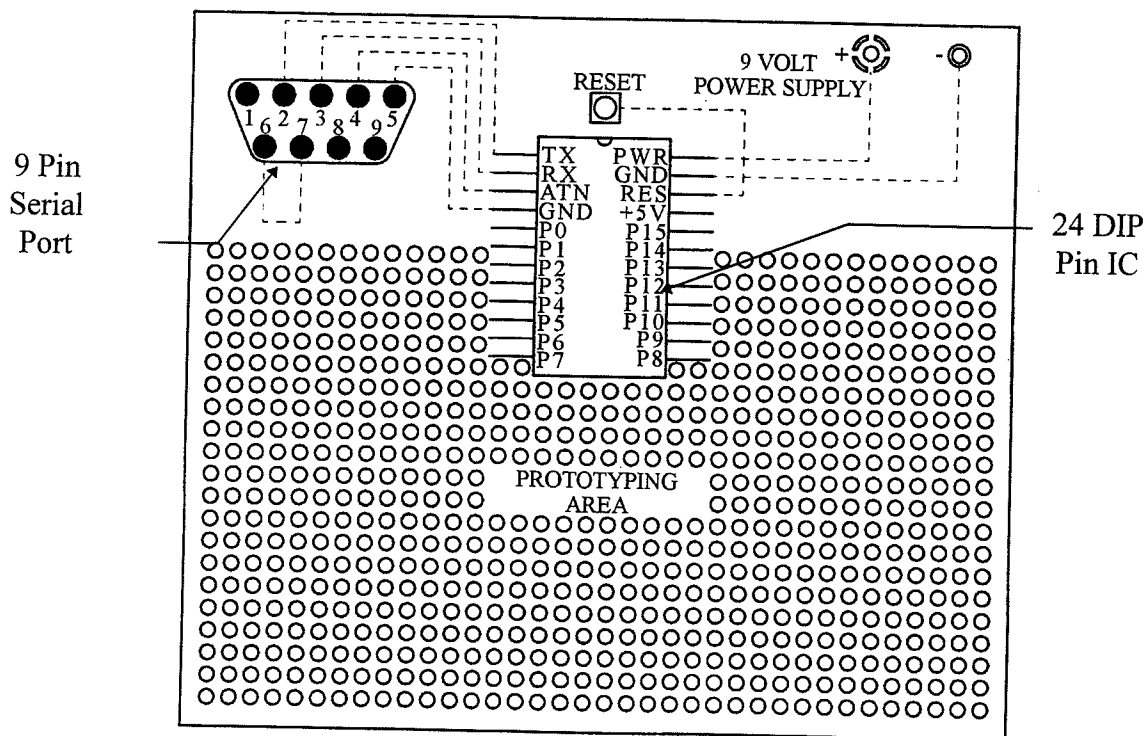


Figure 5.1: PARALLAX BASIC Stamp computer.

5.2 Controller Configuration

Two computers are used to increase the overall speed of the control system by dividing the required work between two units. The first unit is dedicated to reading the weight and speed as well as calculating an application rate based upon those values and user-specified information. The second unit is responsible for measuring the spreader gate position and manipulating the spreader's hydraulic DCV.

The key to passing information from one computer to another lies in the RS232 communication abilities. The computers are designed to handle TTL communication, but can be easily adapted to handle RS232 serial communication. RS232 serial communication is preferred over TTL communication because it has a variable transmission speed and can be received and transmitted faster than TTL. By using a TTL/RS232 communication driver/receiver in conjunction with each computer, the two units can exchange digital information.

A MAXIM MAX233ACPP 20 DIP IC, Figure 5.2, is used to perform the information exchange. It operates by accepting TTL communication and converting it into RS232 serial communication and vice-versa. It can handle two TTL and two RS232 inputs for a total of four inputs and four outputs. Data is sent from one computer on an I/O line in TTL form to the on-board MAXIM IC chip. The MAXIX chip converts the TTL to RS232 and then sends the RS232 data to the second MAXIM chip on the second computer. The second MAXIM

chip receives and converts the RS232 back to TTL and then sends it to one of the second computer's I/O lines where it is processed. Refer to Figure 5.3 and Table 5.2 for a complete explanation of the wiring diagram of the PARRALAX BASIC Stamp computer network with the MAXIM driver/receiver chips.

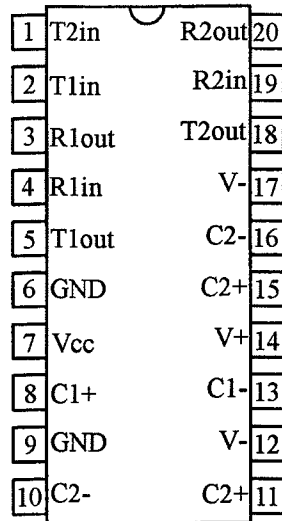


Figure 5.2: Schematic of MAXIM MAX233ACPP 20 DIP TTL/RS232 driver/receiver.

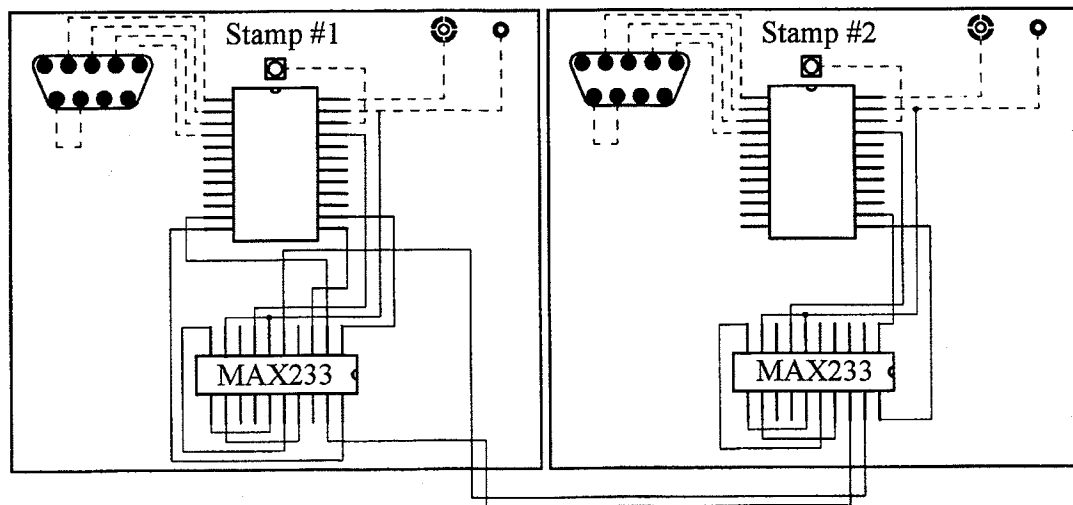


Figure 5.3: Wiring Diagram of PARRALAX Computer network with MAXIM IC chip.

5.3 Electrical Subsystems

Once the foundation of the controller was setup, proper electrical connections had to be made to accommodate the weight, speed, position, hydraulic, and display systems. Each of these subsystems required a different form of electrical input and sent out various forms of electrical output. The subsystems were laid out individually and then collectively wired into the controller.

5.3.1 Weighing System

The main idea behind wiring the Digi-Star weighing system was to supply power to the EZ 210 Electronic Scale Indicator and then make the proper connections between the five input junction box and the five bending beam load cells. Since the indicator has a power specification range of 10.5 to 16 Vdc, the Case 1494 tractor battery was used.

To connect the battery to the indicator, a power line was constructed using two 16 American Wire Gauge (AWG) wires (one red and one black). Insulated ring tongues (3/8 inch) were crimped onto one end of each wire and used to transmit power from the battery. The ring tongues are fastened onto the bolts of the tractor battery terminals ((+) to red and (-) to black). A 3 amp fuse was inserted between the two lines. The other ends of the wire assembly are soldered to the battery (+12Vdc, red wire) and ground (-, black wire) terminals of a four pin male circular plastic connector. The power transmission from the battery to the indicator through the wire assembly is accomplished by connecting the four pin male plug to the four pin female socket on the bottom interface panel of the Electronic Scale Indicator (see Figures

4.12 and 5.4). The Scale Indicator is internally protected from power surges which might occur when the power connection is made.

To supply the junction box with excitation voltage for the load cells, a connection is needed between the indicator and the junction box . This is done by connecting the junction box cable to the indicator. The junction box cable consists of a shielded wire connected to a four pin socket at the end. This socket interfaces with the four pin plug on the bottom interface panel of the Electronic Scale Indicator (see Figures 4.12 and 5.4).

A series of critical connections exist between the individual load cells and the junction box. The five load cell wires: signal +, signal -, excitation +, excitation -, and shield must be securely tightened in the five screw terminals of the five load cell wire banks. This is done by placing the wire end in the terminals and tightening the screw between the two metal plates until the wire end is fastened in place. See Figures 4.11 and 5.4 for a wiring diagram of the wire terminals and load cells.

Finally, the last connection is between the printer port and the controller. This is done by interfacing with the 8 pin plug on the bottom interface panel of the Electronic Scale Indicator (see Figure 4.12) with a 8 pin socket. A wire assembly consisting of two 30 AWG wires, one soldered to pin #4 (signal data, red) and the other to pin #7 (signal ground, black) of the socket, carries the RS232 signal sent from the indicator. The signal data wire is soldered to the #4 pin of the MAXIM IC. This signal is converted to TTL by the IC and sent out on pin

#3 of the IC to the P8 I/O line of the computer. The signal ground wire is soldered to the computer's ground pin (GND). See Figure 5.4 and Table 5.2 for a complete explanation of the complete electrical schematic of the load cell weighing system with the PARRALAX computer and MAXIM IC .

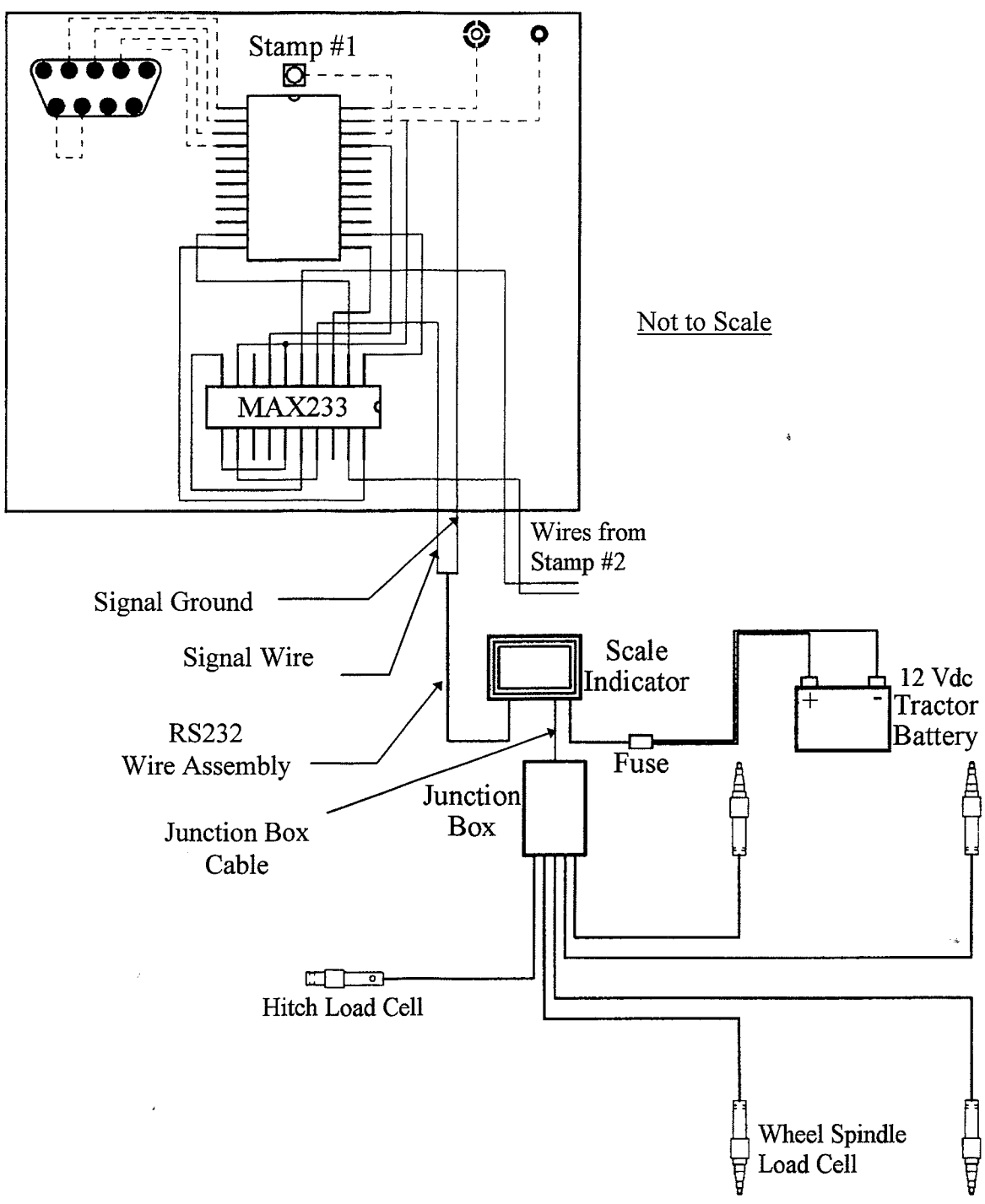


Figure 5.4: Schematic of load cell weighing system with the PARRALAX computer.

5.3.2 Speed Sensing System

Since the computer's pulse counter uses a +5 Vdc pulse detection system, it is necessary to correctly power the encoder to obtain the desired output. Because the encoder's output is a pulsed form of its input, there is a problem in using the tractor battery to power the encoder. If the encoder were powered by the tractor battery, the pulsed output would be somewhere in the range of +12 to +15 Vdc depending on the charge of the battery. This would render a problem with the output signal because the threshold voltage on the computer's pulse counter is +5 Vdc. On the other hand, it would be very cumbersome to use an external +5 Vdc power source to power the encoder. It was decided to use the tractor battery with a voltage regulator to power the encoder and regulate the output voltage to the pulse counter of the computer.

A simple voltage regulator can be built by using a series resistance and a Zener diode in parallel with the load. The function of the regulator is to keep the load voltage nearly constant with changes in supply voltage (V^+) or current load (I_L). The operation is based on the fact that, in the Zener diode breakdown region, small changes in diode voltage are accompanied by large changes in diode current (I_Z). The large current flowing through the series resistor (R_S) produce voltages that compensate for changes in load voltage (V_L^+) or current (Smith and Dorf, 1992). See Figure 5.5 for a description of the Zener diode voltage regulator circuit. See Appendix A for voltage regulator calculations.

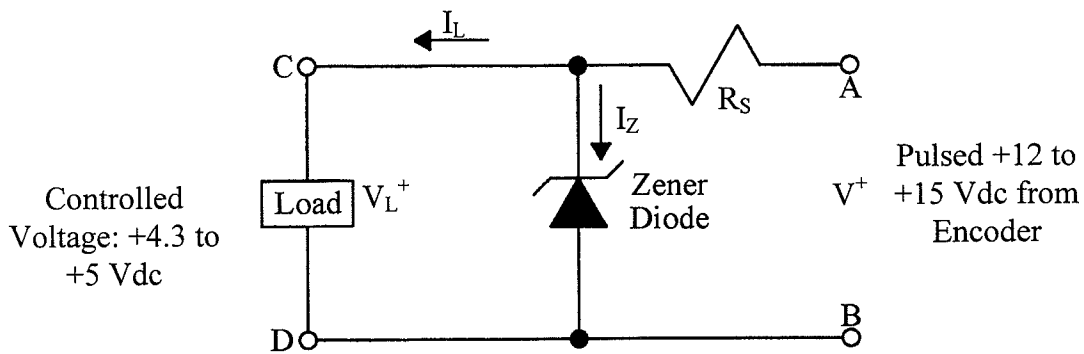


Figure 5.5: Schematic of Zener diode voltage circuit.

With a way to control the encoder's output, the tractor battery is used to supply power to the encoder. Two 16 AWG wires (one red and one black) with 3/8 inch insulated ring tongues on one end are bolted to the tractor battery terminals ((+) to red and (-) to black). The other end of the wire set is soldered to the input voltage (red wire) and ground (black wire) terminals of a 5 pin metal circular socket. This 5 pin socket interfaces with the 5 pin plug located on top of the encoder (see Figure 4.13 for encoder interface). The output signal from the encoder is sent through a wire soldered to the five pin socket of the encoder interface that is connected to location A in Figures 5.5 and 5.6. A second ground wire soldered to the 5 pin socket connects the ground line of the encoder to the ground line, location B in Figures 5.5 and 5.6, of Zener diode voltage regulator circuit.

When a pulsed voltage potential ranging from +12 to +15 Vdc from the encoder occurs between locations A and B, the Zener diode voltage regulator circuit produces an output voltage potential between +4.3 and +5 Vdc at locations C and D in Figures 5.5 and 5.6. This

pulse is sent to the computer's P10 I/O line and grounded to the computer's GND pin. Refer to Figure 5.6 for a complete schematic of the speed system.

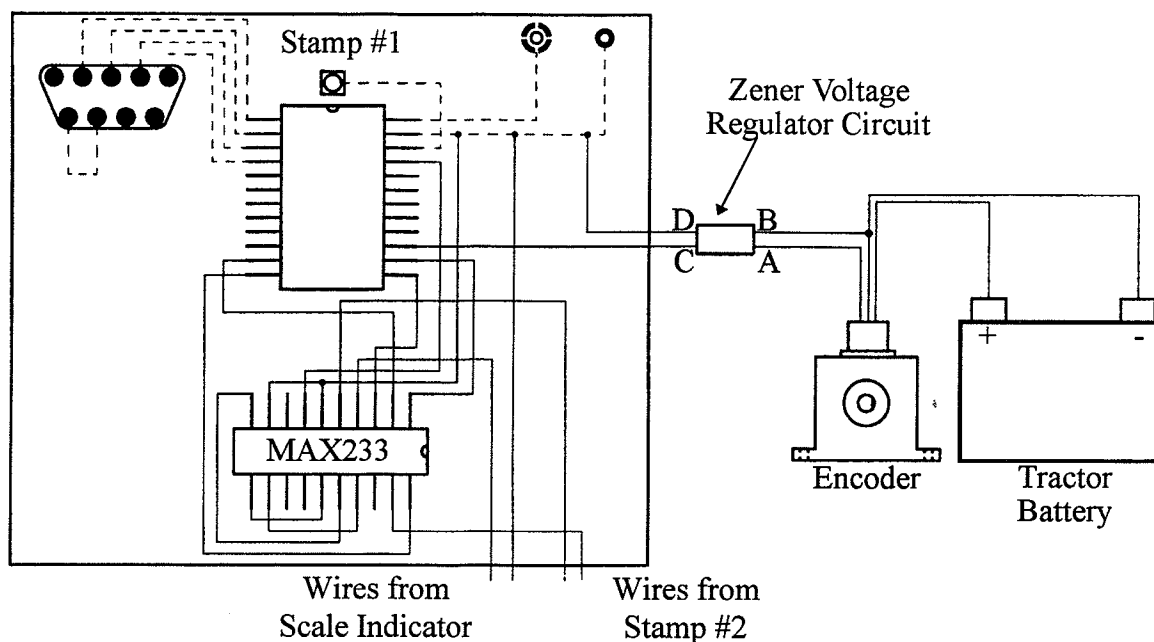


Figure 5.6: Schematic of speed system with the PARRALAX computer.

5.3.3 Position Sensing System

Since the linear potentiometer works on a proportional volt-in/volts-out principle, the selection of the supply voltage was critical when interfacing the potentiometer with an 8 bit A/D converter. Because a traditional A/D converter was too expensive and large to incorporate into a hand held controller, an 8 bit A/D logic converter IC chip was used. A National Semiconductor ADC0831 A/D logic IC (see Figure 5.7) is used to measure voltages on a scale of 0 to 256 based on a maximum input voltage of +5 Vdc. This in turn requires there be a supply voltage of +5 Vdc to the linear potentiometer.

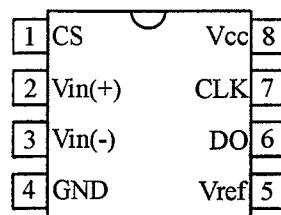


Figure 5.7: Nation Semiconductor's ADC0831 A/D converter IC chip.

This prompted the use of a +5 Vdc fixed voltage regulator. This device is an IC chip that takes a range of input DC voltage from +5 to +35 Vdc and outputs a fixed +5 Vdc. In this application, the +12 Vdc from the tractor battery is used to supply the input voltage to the fixed voltage regulator. The regulator uses the tractor supply voltage and delivers +5 Vdc to the linear potentiometer where it is converted to a voltage between 0 to +5 Vdc depending on the potentiometer wiper location.

The output signal from the potentiometer is input to the 8 bit A/D IC on pin #2. The IC converts the input voltage from the potentiometer into a 8 bit digital signal sent to the P7 I/O line of the Stamp #2 computer. The 8 bit A/D IC uses a series of computer I/O lines (P5-P7) to shift the digital signal using the computer's TTL capabilities. A schematic of the entire position system is shown in Figure 5.8.

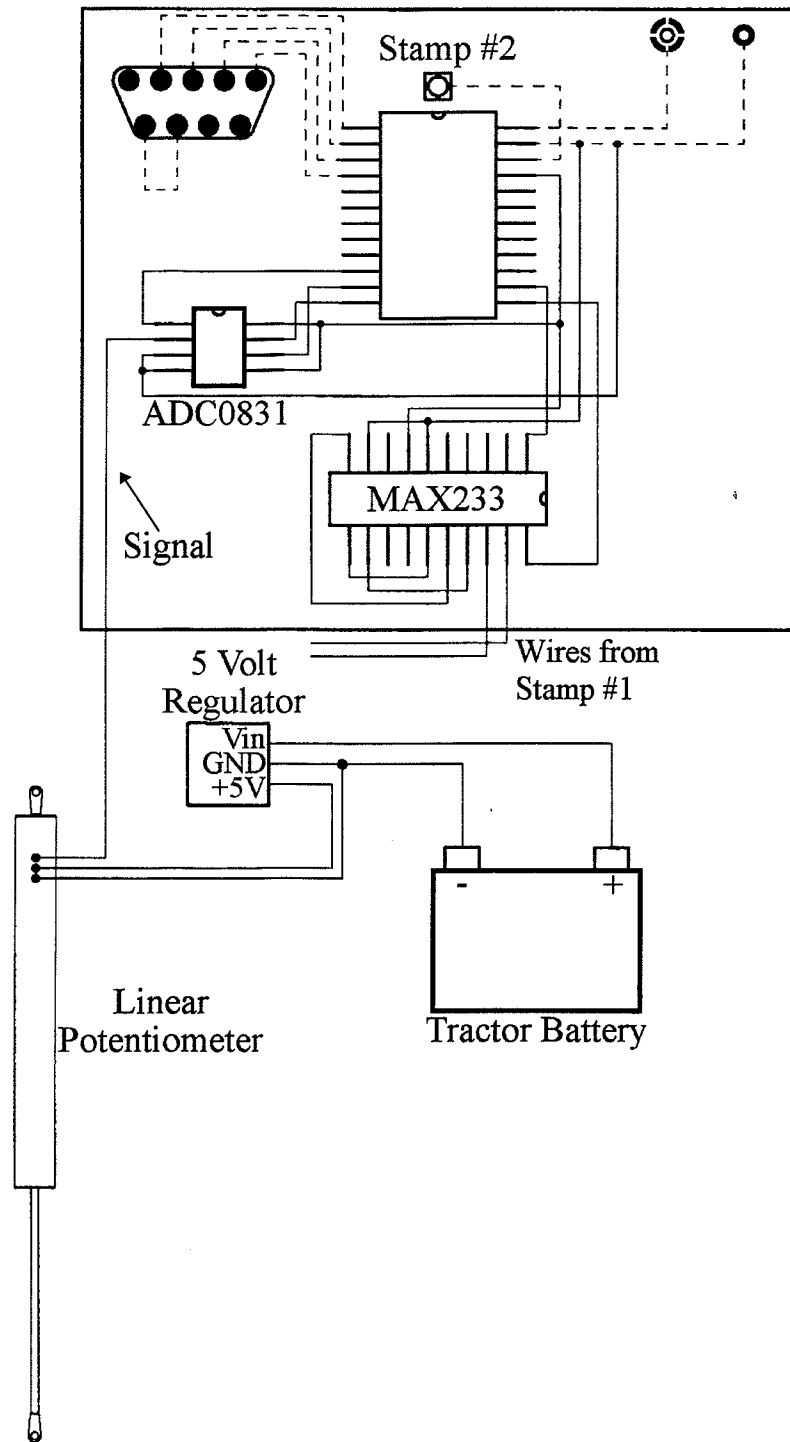


Figure 5.8: Schematic of position system with PARALLAX computer and A/D IC chip.

5.3.4 DCV: Hydraulic System

The spreader's DCV solenoids need a power source capable of outputting +12 Vdc with a minimum current of 3.4 amps to operate properly. This power requirement exceeds the power provided by the computer's output signal (+5 Vdc @ 0.020 amps). This situation required the design of an electrical circuit to match the power output signal of the computer to the valve's solenoid signal.

Activation of the valve's solenoids is accomplished by sending a computer supplied +5 Vdc signal on one of its I/O lines which is sent through a voltage circuit to charge one of the valve's solenoids. Specifically, the computer signal is delivered on either P14 or P10 of the Stamp #2 computer to one of two voltage circuits which incorporate each pair of solenoid lead wires to respectively lower or raise the spreader's gate. The two voltage circuits shown in Figure 5.9 acts as switches to operate the solenoids. The two individual voltage circuits are placed on one circuit board shown in Figure 5.10.

P14 connects to Input 1 of the Valve Signal screw terminal on the circuit board. P10 connects to Input 2 of the Valve Signal and the computer's GND pin is connected to the Ground of the Valve Signal screw terminal on the circuit board. The two voltage circuits each consists of a network of resistors and transistors. This network of electrical components limit the current draw of the computer. It is important to do this because the computer can only supply a maximum of 0.020 amps on any one I/O line. A current draw in excess of this

amount will irreversibly damage the computer's IC. That protected signal is sent to the MOSFET which converts the low level computer signal into a power signal capable of operating the DCV's solenoids. The network of 1.2 k Ω resistors and bipolar transistors (2N222 NPN) act as an isolator to limit the current draw from the computer, while the metal-oxide-semiconductor field-effect transistor (MOSFET), IRF 510 FET, steps up the computer power output signal.

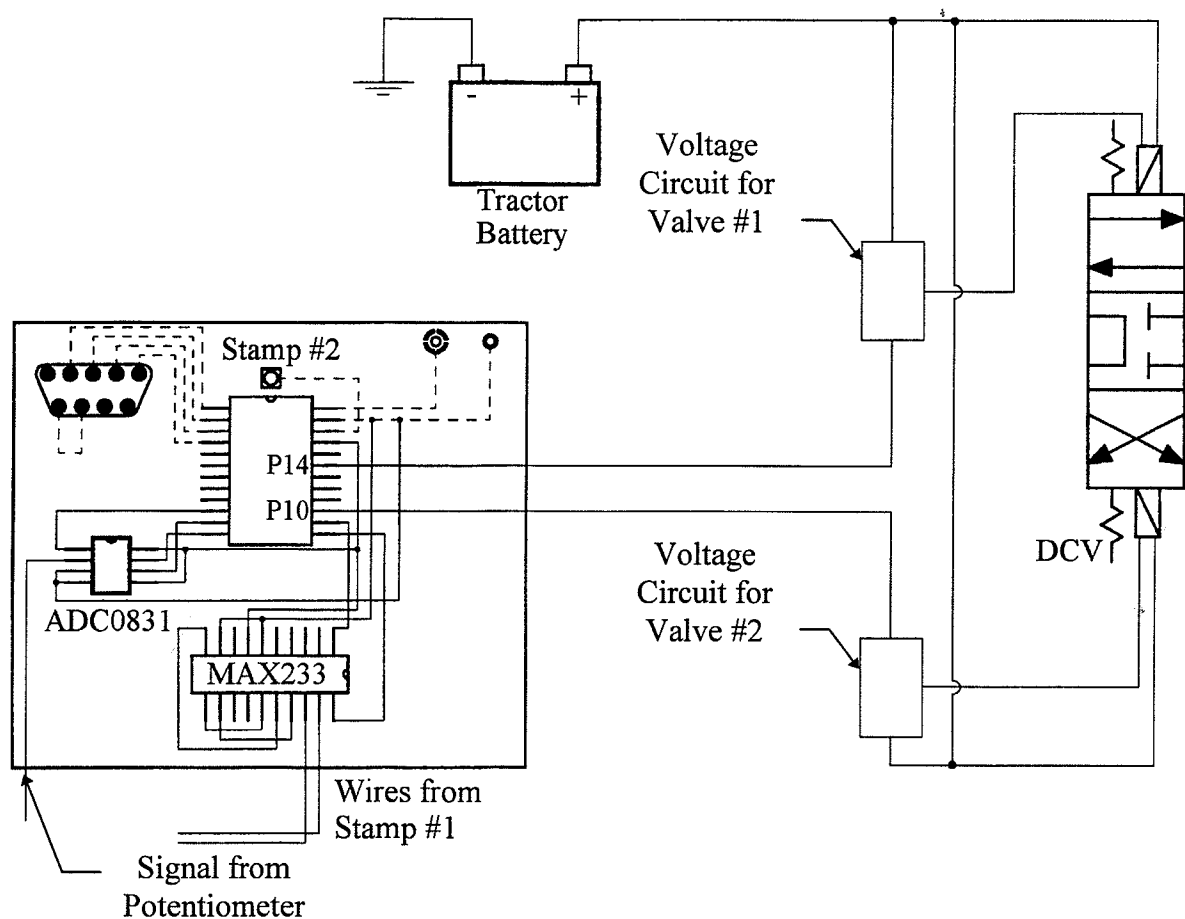


Figure 5.9: Schematic of DCV with voltage circuit and PARALLAX computer.

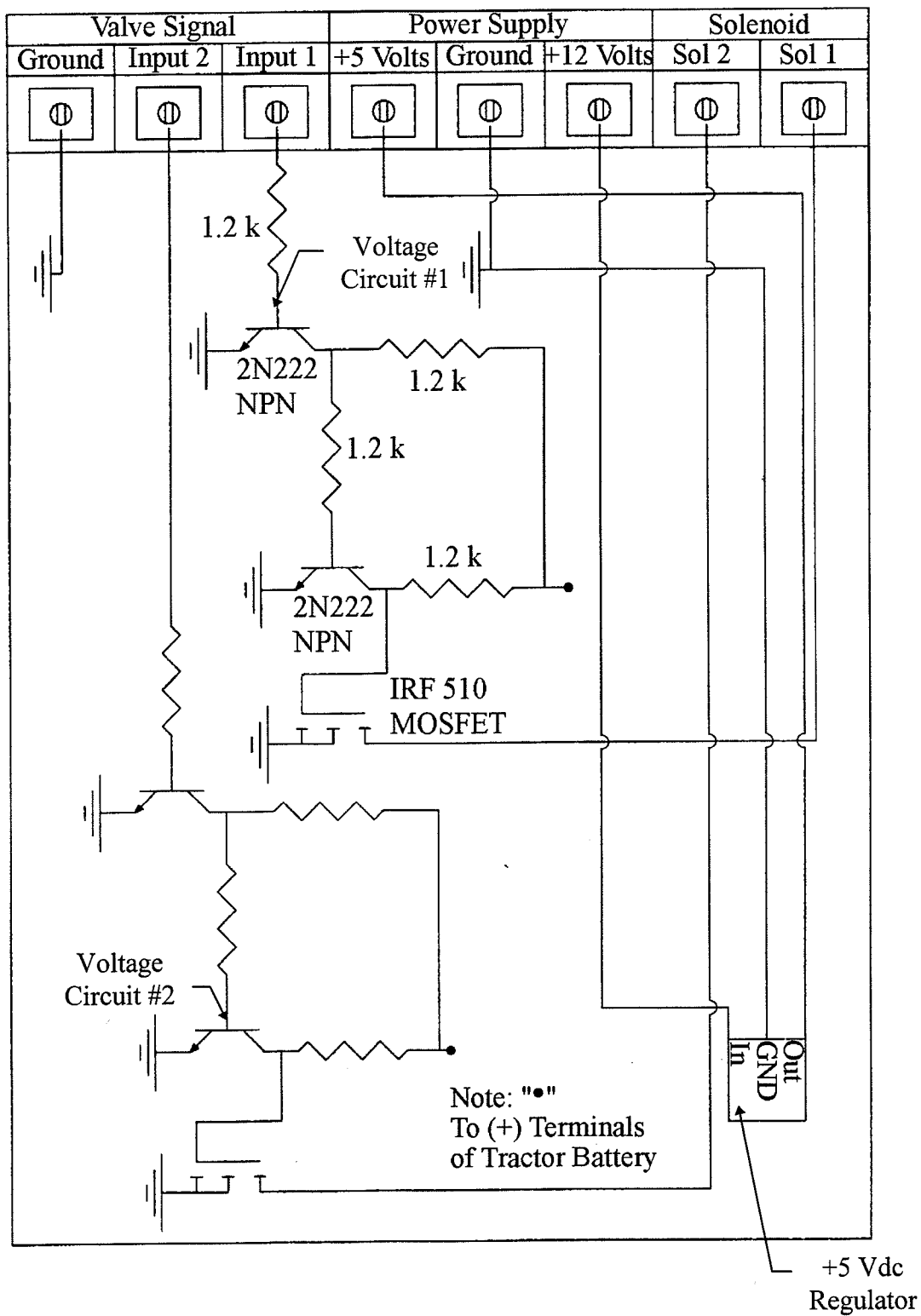


Figure 5.10: Schematic of controller circuit board.

To supply power to the circuits, two 16 AWG wires connected to the battery terminal are directly wired to the circuit at the solid dot ("•") locations in Figure 5.10. Output from the other lead wire getting connected to positive battery terminal (+).

This circuit board also incorporates the +5 Vdc fixed voltage regulator used to supply +5 Vdc to the linear potentiometer. This portion of the circuit board accommodates the +5 Volts, Ground, and +12 Volts wire connections between the tractor battery, voltage regulator, and potentiometer. The circuit board also employs a common voltage sink which is used as a common ground between the tractor battery, solenoids, voltage regulator, potentiometer, and the two computers. This configuration makes for neat wiring as well as consolidation of electrical components and voltage supplies and grounds.

5.3.5 Display System

The display system consists of a Vorne Industries, model 77/232, large digit display unit. The primary function of the unit is to accept RS232 serial communication input and output the input string on its 3.3 inch high LED alphanumeric 5 digit display. The display has a visibility range up to 100 feet and is powered by 120 Vac.

A female DB 9 pin connector is used to interface with the display's serial communication screw terminal strip. The serial in (+) terminal is connected to the #3 pin (transmit data) of the DB 9 connector by a 30AWG wire. Similarly, the serial in (-) is connected to the #5 pin

(signal ground) of the DB 9 connector by a 30 AWG wire. The female DB 9 connector of the display interfaces with male DB 9 connector which is attached to the Stamp #1 computer.

The male DB 9 connector is linked to the Stamp #1 computer via the MAXIM 233 IC. The application rate is sent to the display unit by first transmitting the rate in TTL form from the P9 I/O line of the computer to the #1 pin of the MAXIM IC. The TTL string is converted into RS232 by the MAXIM IC and sent out on the #18 pin of the IC. The #18 pin is connected to the #3 pin of the male DB 9 connector by a 30 AWG wire. The computer's GND pin is connected to the #5 pin of the DB 9 connector by a 30 AWG wire. Refer to Figure 5.11 for a schematic of the Stamp #1 Computer with the male DB 9 connector.

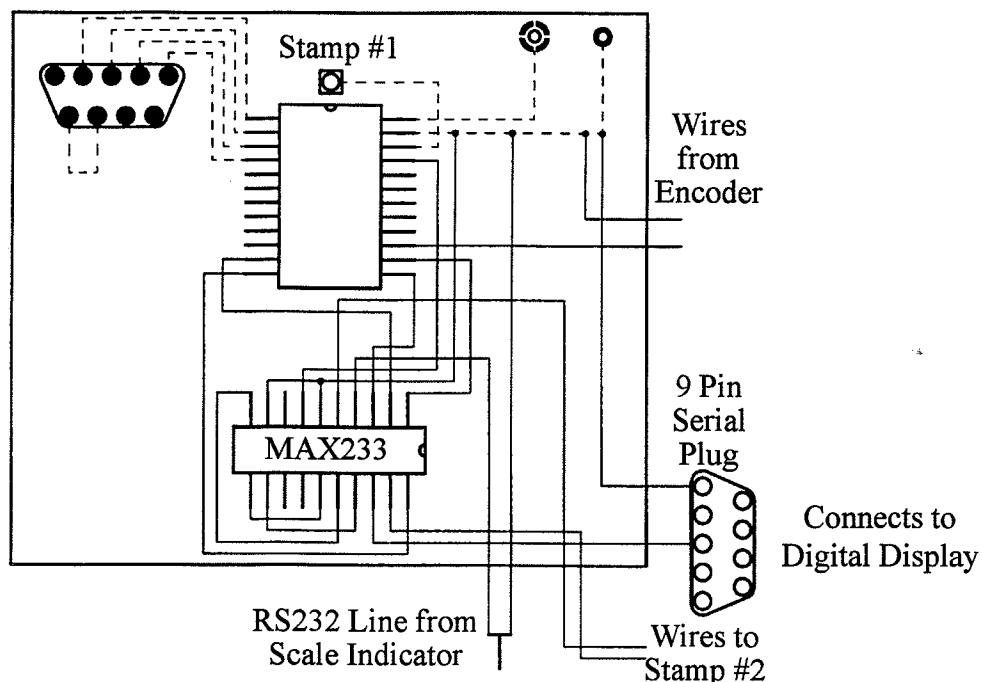


Figure 5.11: Schematic of display interface with PARALLAX computer.

5.4 The Complete Control System

Once all the subsystems were configured and laid out individually, it was important to combine all of the subsystems into a completely enclosed portable control system. This was done by putting the two computers and circuit board into a plastic hand held enclosure. All of the connections between the two computers and the circuit board were completed within the confines of the enclosure. All of the remaining connections between the computers or circuit board and the external instrumentation on the spreader or tractor were made by using three wire harnesses: spreader, tractor, and battery.

The spreader wire harness includes the seven wires from the linear resistor and the two solenoids from the DCV. The wire ends are soldered into the terminals of a 7 pin metal circular socket. The socket interfaces with a corresponding plug which is mounted on the enclosure with the wire ends connected to the Stamp #2 computers and voltage circuit. See Table 5.1 for a detailed listing of the spreader wire harness.

The tractor wire harness incorporates the six wires from the following: the Digi-Star RS232 weight signal, the encoder's indexed pulse signal, and the RS232 output signal to the display. The wire ends for all inputs and outputs are soldered into the terminals of a 7 pin metal circular plug. The plug interfaces with a corresponding socket which is mounted on the enclosure with the wire ends connected to the Stamp #1 Computer. See Table 5.1 for a detailed listing of the tractor wire harness.

The battery wire harness contains four wires leading from the battery terminals soldered to a 5 pin metal circular plug. The plug interfaces with a corresponding socket which is mounted on the enclosure with the wire ends connecting to the solenoid lead wire ends and voltage circuit +12 Vdc and Ground wire terminals. See Table 5.1 for a detailed listing of the spreader wire harness.

When the three wire harnesses are connected to the enclosure, the controller's internal circuitry is completed. The controller is now capable of the following: receiving the Digi-Star Indicator weight signal, counting encoder pulses, measure the gate position with the potentiometer, manipulating the flow of fluid in the hydraulic cylinder, and outputting a calculated application rate. Refer to Table 5.2 for specifications on the complete wiring diagram of the controller.

The controller was designed with a variety of purchased off-the-self electrical equipment. All of the subsystems and components were purchased through electrical component venders and wholesalers. The only two items within the controller required fabrication were the Zener diode voltage regulation circuit and the controller circuit board. However, all of the components used in the fabrication of these two items are commonly found electrical components sold by wholesalers.

SOURCE	CONNECTOR	TERMINAL	WIRE COLOR	CONNECTOR	JUNCTION
Spreader					
Pot. "+"	7 Terminal Plug	B	Red	7 Terminal Socket	5 Volts (Vol. Circuit)
Pot. "-"	7 Terminal Plug	E	Black	7 Terminal Socket	Ground (Vol. Circuit)
Pot. "Signal"	7 Terminal Plug	G	Yellow	7 Terminal Socket	ADC0831 "2"
Solenoid #1 "+"	7 Terminal Plug	A	Blue	7 Terminal Socket	Tractor Battery "+"
Solenoid #1 "-"	7 Terminal Plug	F	White	7 Terminal Socket	Sol #1
Solenoid #2 "+"	7 Terminal Plug	D	Green	7 Terminal Socket	Tractor Battery "+"
Solenoid #2 "-"	7 Terminal Plug	C	Orange	7 Terminal Socket	Sol #2
Tractor					
D.S. RS232 "+"	7 Terminal Socket	F	Blue	7 Terminal Plug	MAX233(1) "4"
D.S. RS232 "-"	7 Terminal Socket	A	White	7 Terminal Plug	Stamp#1 "VSS"
Encoder "+"	7 Terminal Socket	E	Red	7 Terminal Plug	Zener-Diode "A"
Encoder "-"	7 Terminal Socket	B	Green	7 Terminal Plug	Zener-Diode "B"
Display "+"	7 Terminal Socket	D	Yellow	7 Terminal Plug	MAX233(1) "18"
Display "-"	7 Terminal Socket	C	Black	7 Terminal Plug	Stamp#1 "VSS"
Battery					
Battery "+"	5 Terminal Plug	B	Red	5 Terminal Socket	12 Volts (Vol. Circuit)
Battery "+"	5 Terminal Plug	E	Blue	5 Terminal Socket	Tractor Battery "+"
Battery "+"	5 Terminal Plug	D	Green	5 Terminal Socket	Tractor Battery "+"
Battery "-"	5 Terminal Plug	C	Black	5 Terminal Socket	Ground (Vol. Circuit)

Table 5.1: Complete listing of the three wire harnesses.

SOURCE	JUNCTION	JUNCTION	JUNCTION	JUNCTION
RS232 Com.				
Stamp #1 "P6"	MAX233(1) "2"	MAX233(1) "5"	MAX233(2) "19"	Stamp #2 "P8"
Stamp #2 "P9"	MAX233(2) "1"	MAX233(2) "18"	MAX233(1) "19"	Stamp #1 "P7"
Weight Data				
D.S. RS232 "+"	MAX233(1) "4"	MAX233(1) "3"	Stamp #1 "P8"	
D.S. RS232 "-"	Stamp #1 "VSS"			
Speed Data				
Encoder "+"	Zener-Diode "A"	Zener-Diode "C"	Stamp #1 "P10"	
Encoder "-"	Zener-Diode "B"	Zener-Diode "D"	Stamp #1 "VSS"	
Gate Position				
Pot. "+"	5 V Reg. "Out"			
Pot. "-"	5 V Reg. "GND"			
Pot. "Signal"	ADC0831 "2"			
ADC0831 "3"	ADC0831 "4"	Stamp #2 "VSS"		
ADC0831 "8"	ADC0831 "5"	Stamp #2 "VDD"		
ADC0831 "1"	Stamp #2 "P5"			
ADC0831 "6"	Stamp #2 "P6"			
ADC0831 "7"	Stamp #2 "P7"			
DCV Control				
Stamp #2 "P10"	Signal Input "1"	Voltage Circuit	Sol #1	Sol #1 Lead Wire
Stamp #2 "P14"	Signal Input "2"	Voltage Circuit	Sol #2	Sol #2 Lead Wire
Stamp #2 "VSS"	Signal Input GND	Voltage Circuit		
Display				
Stamp #1 "P9"	MAX233(1) "1"	MAX233(1) "18"	Male DB 9 "3"	Female DB 9 "3"
Stamp #1 "VSS"	Male DB 9 "5"	Female DB 9 "5"	Display Serial "-"	Display Serial "+"

Table 5.2: Complete listing of the wiring diagram for the two computers and voltage circuit.

CHAPTER 6

PRELIMINARY SYSTEM RESPONSE AND OVERLAP TESTING

6.1 Load Cell Calibration

To insure the controller receives correct weight data from the load cells, the entire weighing system was calibrated. To do this, the spreader was filled to a predetermined weight and run through the self calibration routine programmed into the Digi-Star Scale Indicator. Two series of tests were performed to verify the static and dynamic response of the weighing system.

Preliminary spreader load capacity tests found the average spreader load was roughly 10,000 lb. Using this value as a basis and employing a factor of safety of 1.5, the spreader's maximum weight capacity was set for 15,000 lb. As part of the system calibration, the spreader was positioned on a certified platform scale with a 20 lb. resolution. The spreader was loaded with topsoil until the platform scale indicated 15,000 lb. The spreader's weighing system was calibrated by entering the reading from the platform scale into the Scale Indicator and initiating the calibration routine. Once the system verified the load and finished the routine, the weighing system calibration process was complete and set up for a maximum capacity of 15,000 lb.

6.2 Static Weight Test

Water was selected as the weighing medium for the static weight test. Water was used because it gives the most uniform loading within the spreader's tank. To prepare the spreader

for the static test, the tank must be completely water tight. Two 8 ft x 4ft, 3/8 inch thick plywood sheets were used to line the bottom portion of the spreader's tank. The plywood sheets rested on the side walls of the tank and on top of the auger. Large plastic sheets taped together with duct tape were laid over the plywood sheets and tank walls to act as a liner. A drum was plugged and calibrated for 55 gallons. This was done by filling it with a calibrated five gallon bucket. Using the weight conversion for one gallon of water (8.34 lb./gal), each drum had a net weight of 459 lb. when filled to the 55 gallon level. The drum was positioned over the center of the spreader tank on a wooden pallet that straddled the width of the spreader. The empty weight of the spreader with the drum and pallet were recorded and used as a tare weight. The drum was filled with water to the calibration level and emptied into the spreader. The net water weight of each drum was recorded until the spreader reached its maximum modified volumetric capacity of 990 gallons (8,257 lb.). The weight measured by the load cell system verses the actual water weight is plotted in Figure 6.1.

The results demonstrate a nonlinear relationship between the actual weight and the measured weights for values ranging from 0 to 1,800 lb., with relatively large error at smaller weight values. As the applied weight increases, the relationship becomes more linear and closer to the actual weight. Around 3,000 lb. the measured values have an error less than 5% with a decreasing error at larger weights. Since the spreader reached its volumetric capacity at 8,257 lb. (actual weight of water), it was impossible to test the weighing system up to the 15,000 lb capacity limit using this water filling technique. However, given the results and trends of the

measured data it is believed the weighing system is reasonably accurate and effective at weights up to the capacity limit of 15,000 lb.

To support this belief, a linear regression was performed on the measured load data and a weight value was extrapolated to the maximum weighing system capacity. The results indicated the predicted value was 14,828 lb. for a applied load of 15,000 lb. This results in a 1.15 % error, which is within the acceptable error range of the measured loading. Although the spreader will not likely be loaded to the 15,000 lb. capacity, the weighing system needed to be calibrated to an absolute weight value which would guarantee accurate weight measurement for all spreading conditions and various types of manure.

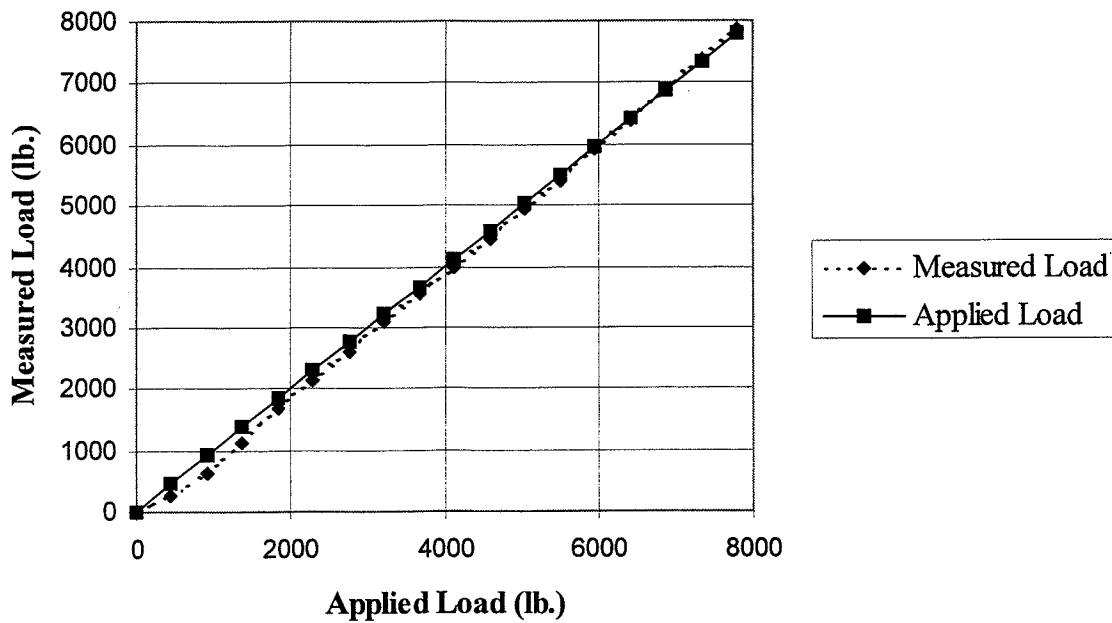


Figure 6.1: Static weight test results of the spreader's weighing system.

6.3 Dynamic Weight Test

To evaluate the weighing system under dynamic conditions, two tests were used to quantify the variation in the weight measurement data in two different driving situations. The spreader was loaded with manure to 12,200 lb. and driven on a mowed field in a straight line and in a curvilinear "S" pattern at various speeds (2.5, 4.0, and 7.5 miles/hour (mi/h)). A 4 Hz. weight measurement signal was collected from the Digi-Star Scale Indicator as the spreader was driven through the field without discharging any material. The average test S pattern was approximately 50 feet long and 20 feet wide. These S patterns were believed to encompass turns tighter than realized during normal spreading conditions.

The results in Table 6.1 show the weight measurement data under different driving conditions and different speeds. The Average Error is calculated by averaging the absolute value of the difference between the weight measurement and the 12,200 lb. static weight. The %Error is calculated by dividing the Average Error by 12,200 lb. and multiplying by 100.

The results indicate the variation in the weight data increase as the travel speed increases. The results also indicate the variation in the data is worse in the S pattern test than the Straight Line test. This suggests that curvilinear driving has a negative effect on the performance of the weighing system. However, since the %Error for the S pattern is less than 2% for a speed of 7.5 mi/h for driving conditions not likely to be seen in practice, there is little concern for this higher variation under these conditions.

Table 6.1: Dynamic weight test results.

	Speed (mi/h)	Straight Line	S Pattern
Average Error (lb.)	2.5	31.7	85.8
%Error	2.5	0.3	0.7
Average Error (lb.)	4.0	107.5	136.6
%Error	4.0	0.9	1.1
Average Error (lb.)	7.5	153.0	210.7
%Error	7.5	1.3	1.7

Similar tests were conducted by Loehr (1996) using a Figure 8 pattern that was 150 long and 60 feet wide done on blacktop driving at 4 mi/h. His results concluded that for a load of approximately 13,150 lb. there was an average error of 546.7 lb. which translated to an error of 4.1%. The results of the S pattern tests at 4 mi/h yield an error of 1.1%. This is almost an improvement of 400% over the system Loehr used. Although the test conditions differ because of the driving surface used in the tests, the shape of Loehr's Figure 8 and the S pattern is proportional. Dividing the length of each pattern by its width, there is a consistent 2.5 proportion between each of the test conditions. However, the turns performed in the S pattern had a radius of curvature more severe than what Loehr used to conduct his tests. Therefore, it appears that the five load cell system used with the Digi-Star Scale Indicator is better than the three load cell system configured without the Digi-Star Scale Indicator.

6.4 Dynamic Discharge and Overlap Testing

To validate the weighing system in dynamic situations, the system needed to be tested in on-the-go spreading conditions and compared to the actual weight discharged by the spreader. A

procedure was devised to approximate the system's accuracy and quantify the machine's spreading characteristics.

The test procedure involved spreading manure of various classifications based upon moisture content at different spreader gate heights. The manure is spread over a 49 ft. test course perpendicular to one row of 5 ft. x 7 ft. plastic sheets separated and held in place by 1 in. x 4 in. x 8 ft. wood borders (Figure 6.2). The row of sheets are set up in the middle of the total spreading area and are staked down with 6 inch long rods built into the wood borders.

The weight loss values of the weighing system are compared to an approximate weight value based upon the collected weight values. This is done by assuming the discharge collected on the single row of plastic sheets is 1/7th of the total amount of spread manure. The total captured weight must be approximated because the time required to spread manure on the sheets is less than the time required to extract and average weight data from the weighing system. It is impractical to capture all the weight discharged from the spreader in a time frame which allows the controller to extract data because the weight discharged is too great. This would have demanded a larger scale capacity for measuring the sheets and manpower for weight collection than was available. The sheet's 5 ft. x 7 ft. dimensions were selected based upon the test travel speed (2 mi/h) of the spreader. Since the auger design and speed has a tendency to cause a pulsing effect in the discharge pattern, it was important to capture the discharge over at least two auger cycles. By making the sheets 7 ft. wide, the sheets were

sure to capture two complete auger cycles of discharge on one sheet driving at the chosen test speed. Refer to Figure 6.2 for an illustration of the dynamic test procedure.

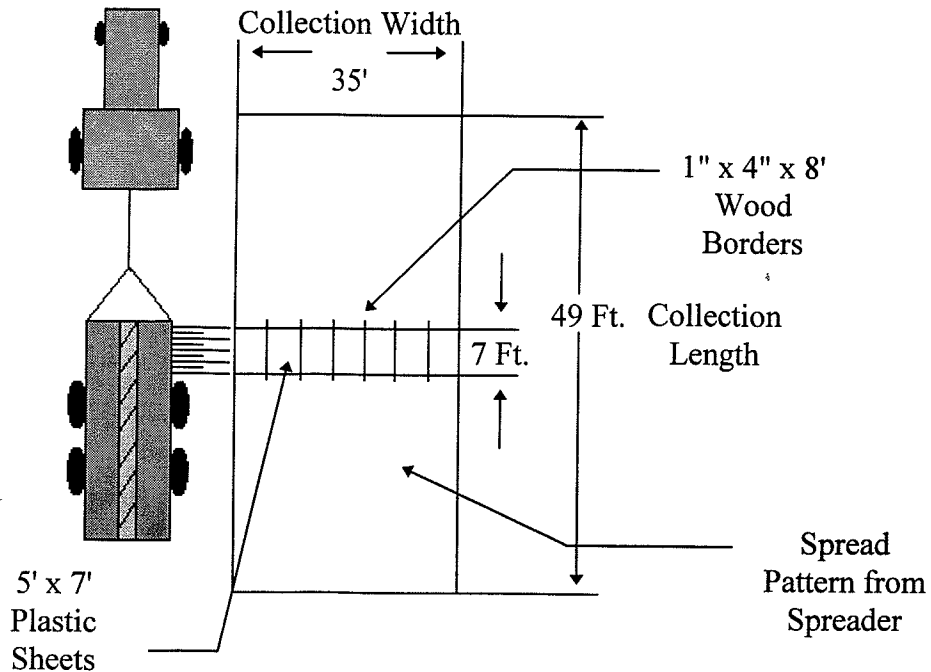


Figure 6.2: Illustration of dynamic and overlap test.

The results of the tests indicated the starting and ending weight values from the weighing system correlated with the approximated values of the recovered manure. Using the approximated discharge weight value as the true weight and the weighing system values as the measured weights, there was a range between 0.2% to 19.1% error. Although some of the tests yielded a rather high error, the average error of the tests was 7.0%.

The high error is most likely due to the assumption that the discharge is completely uniform. Bridging of manure within the spreader can cause temporary disruptions in the discharge rate which prevent manure from being ejected from the spreader. These momentary laps in the spreader's discharge has the ability to skew the values of the approximated weight values. Although bridging problems did arise during some of the tests, the results still demonstrated that the dynamic system was functional and capable of delivering accurately measured weights discharged. Refer to Spread Pattern Test Results in Appendix B for dynamic test results.

6.4.1 Spread Pattern Test Results

In addition to verifying the systems functionality and accuracy, the tests were structured to quantify the spreader's distribution pattern for manures with different moisture contents at different spreader gate settings. Low (35.0%), medium (61.2%), and high (78.5%) moisture content manures were spread at the following gate opening settings: 10, 8, and 6 inches. Each pair of conditions was replicated three times (total of 27 tests) and the results of the individual tests averaged. The results indicated some trends and variations in the spread pattern as well as the existence of bridging problems. Computer fitted plots of the spreader's average distribution patterns can be seen in Figures 6.3 - 6.8.

The trends of the tests indicate there are a few direct relationships between the varied spreading parameters and the spread pattern. Figures 6.3 - 6.5 show the spread width (see Figure 6.2) increases as the moisture content of the manure increases. These plots suggest

there is a linear relationship between the moisture content and the pattern spread width within the range tested. This information becomes useful when predicting spread widths for different types of manures. Refer to Spread Pattern Test Results in Appendix B for spread pattern information regarding the correlation between the moisture content and spread width.

Figures 6.3 - 6.5 also show an inverse relationship between the moisture content and the distribution peaks. As the moisture content of the manure increases, the distribution peak decreases. This data suggests that the manure's moisture level has a significant role in shaping the of spread pattern's distribution. The distribution curves in Figures 6.3 - 6.5 are labeled with the measured application rate in tons/acre (T/A).

Figures 6.6 - 6.8 illustrate an important trend concerning the gate opening and the discharge rate. Increases or decreases in gate height cause proportional increases or decreases in the discharge rate of the manure (tons/acre) for a given moisture level. Also, Figures 6.6 - 6.8 show trends that suggest changes in the tested range of gate height positions cause rather small changes in the shape of the distribution and only minor changes in the spread width. The distribution curves in Figures 6.6 - 6.8 are also labeled with the measured application rate in tons/acre (T/A).

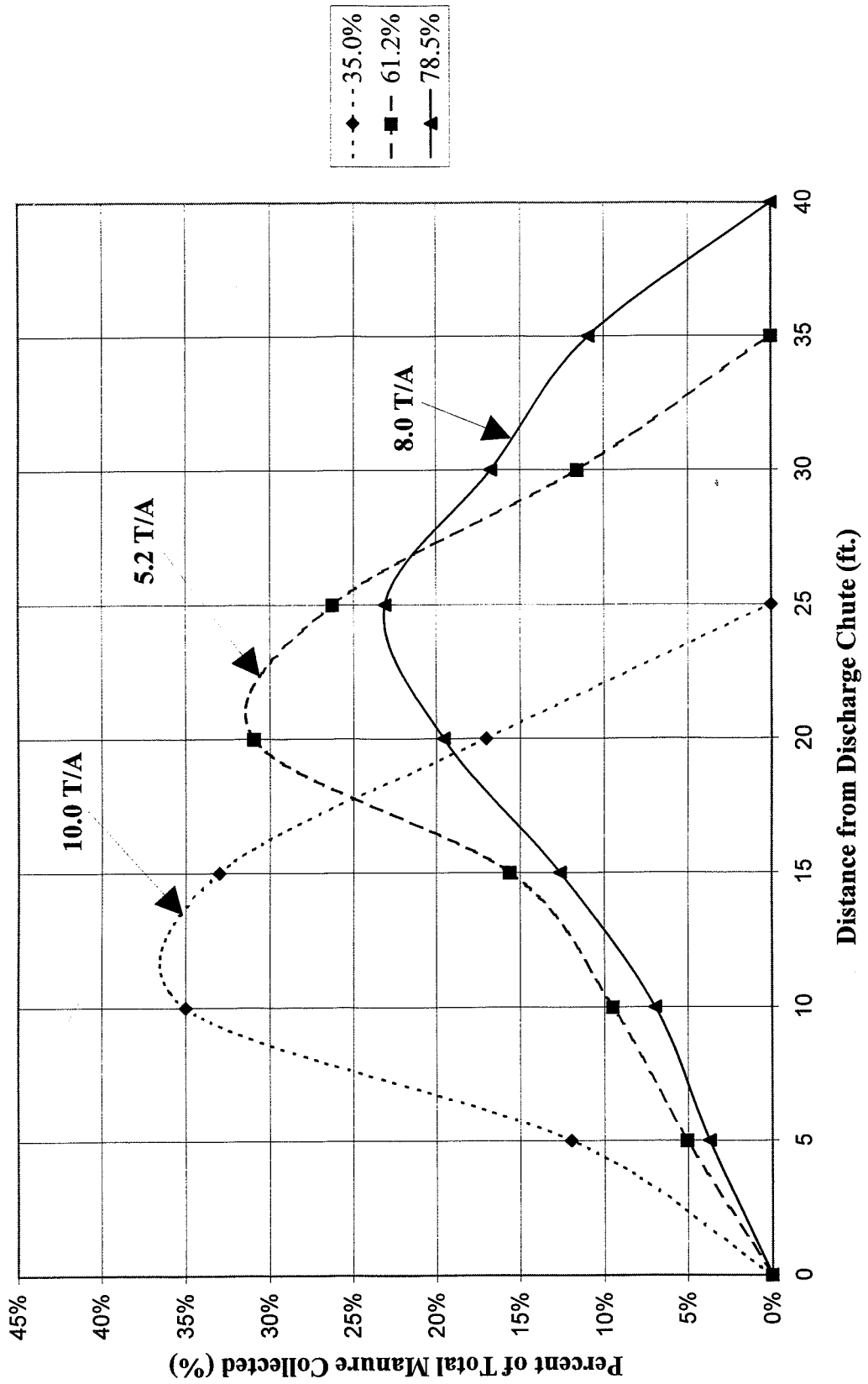


Figure 6.3: Plot of spread pattern for tested manures at an opening height of 10 inches.

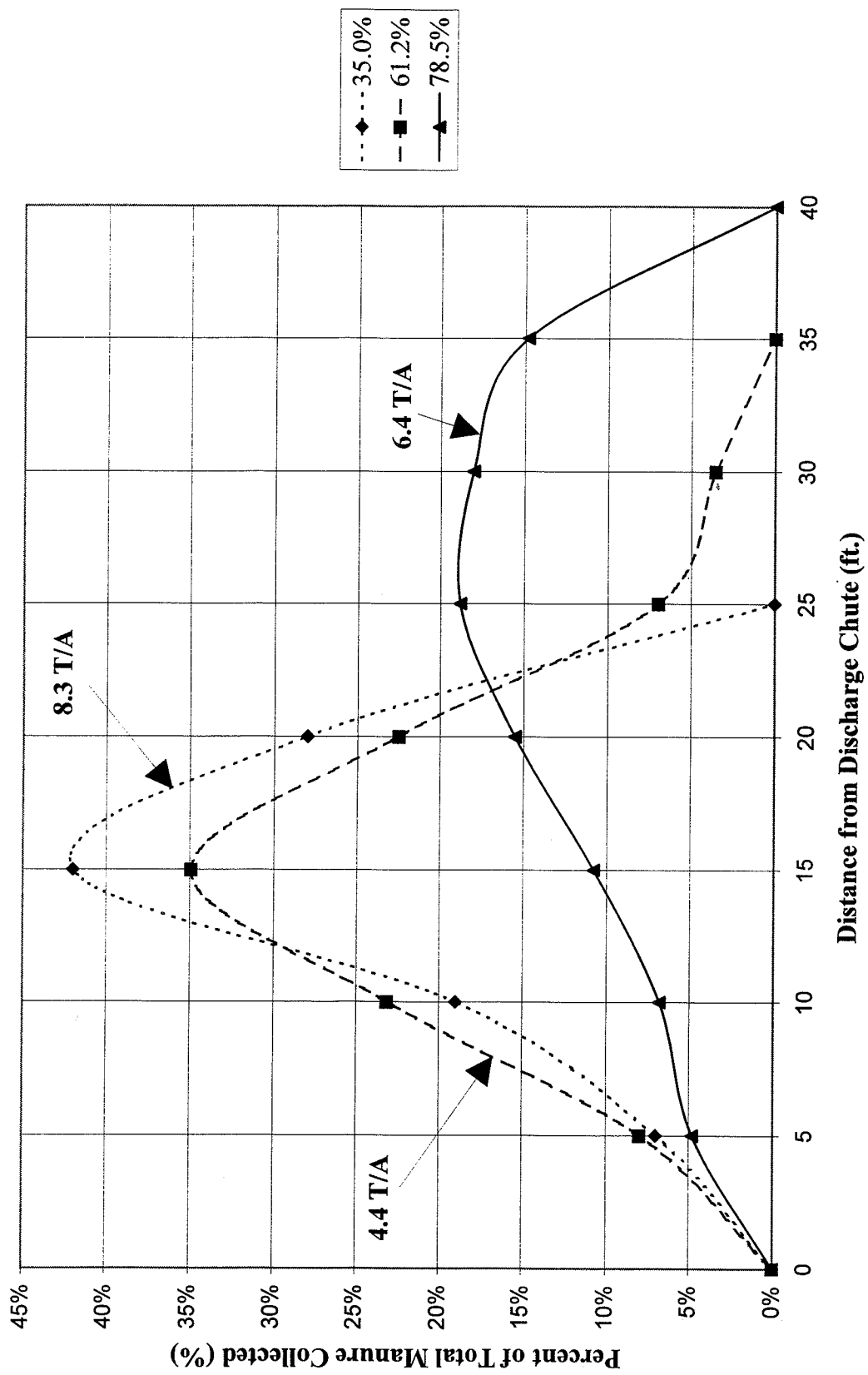


Figure 6.4: Plot of spread pattern for tested manures at an opening height of 8 inches.

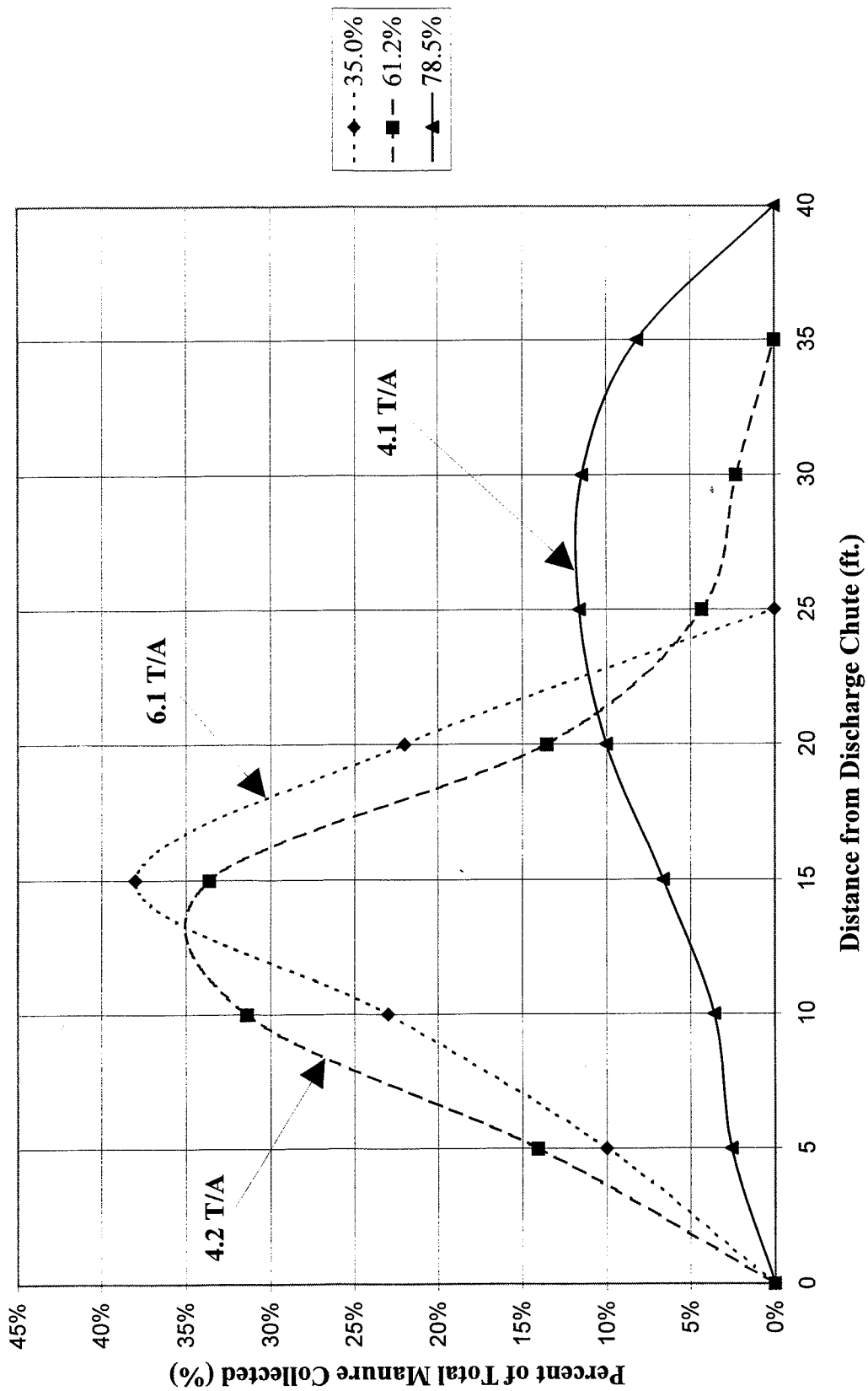


Figure 6.5: Plot of spread pattern for tested manures at an opening height of 6 inches.

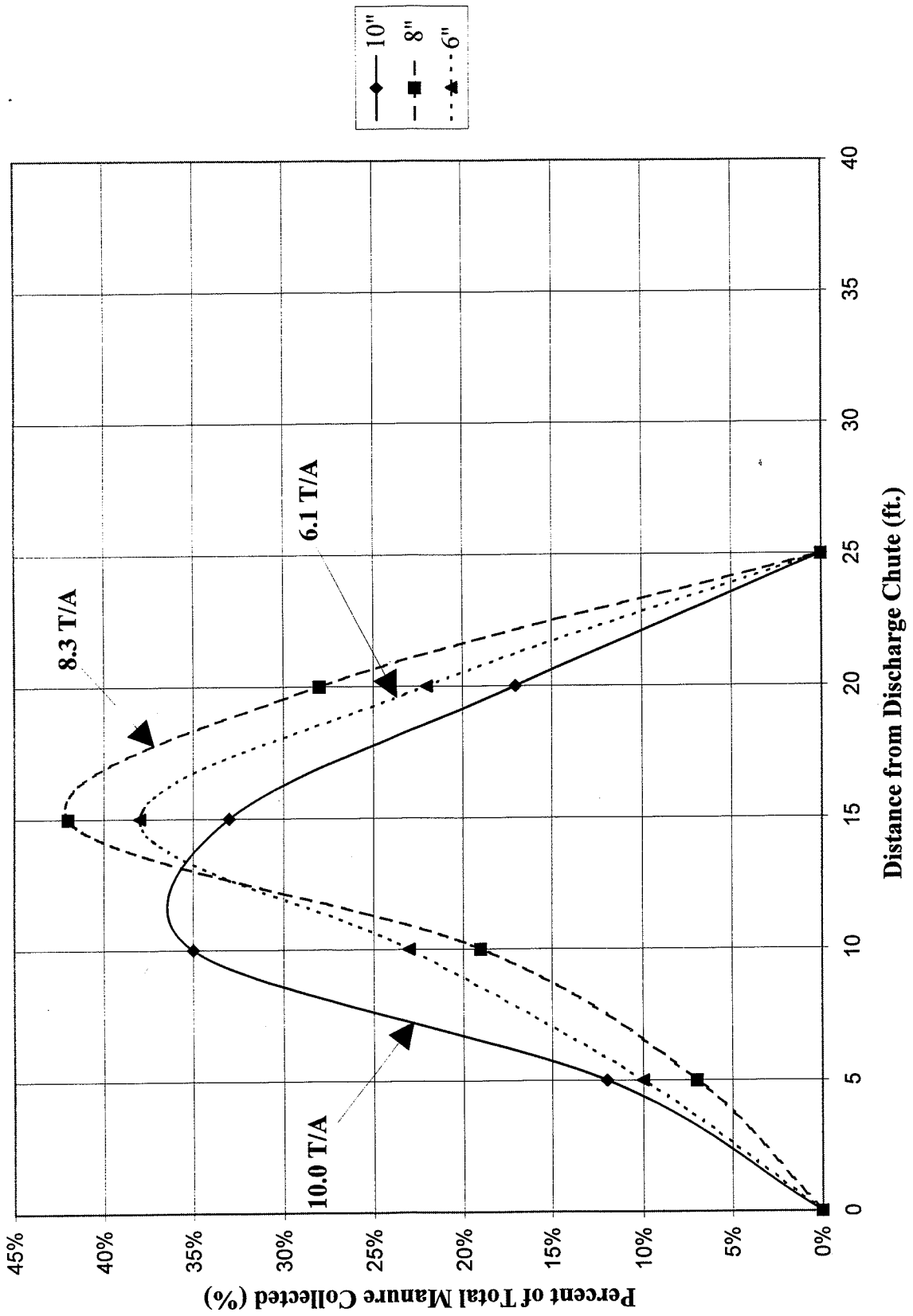


Figure 6.6: Plot of spread pattern for tested gate heights at a moisture content of 35.0%.

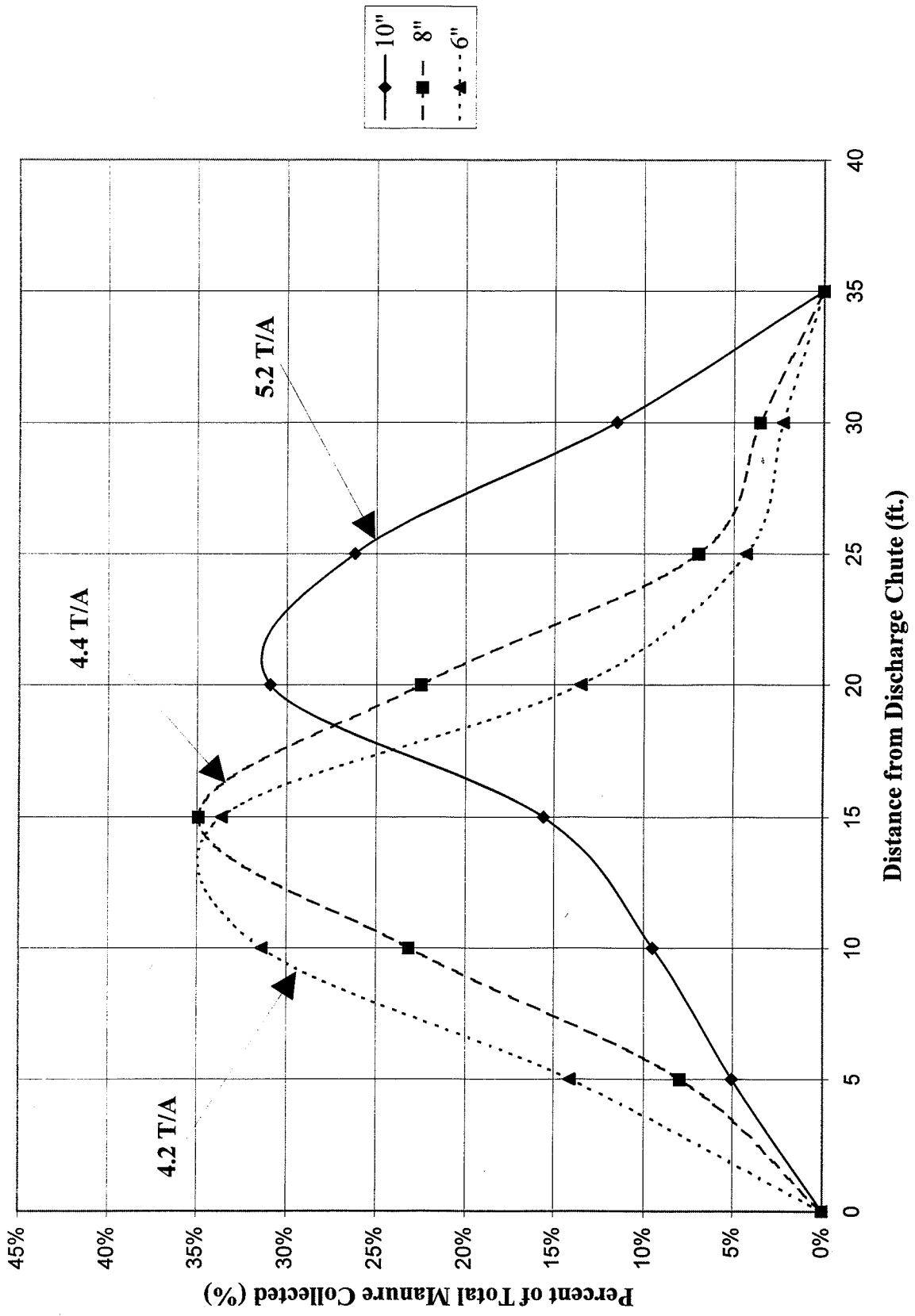


Figure 6.7: Plot of spread pattern for tested gate heights at a moisture content of 61.2%.

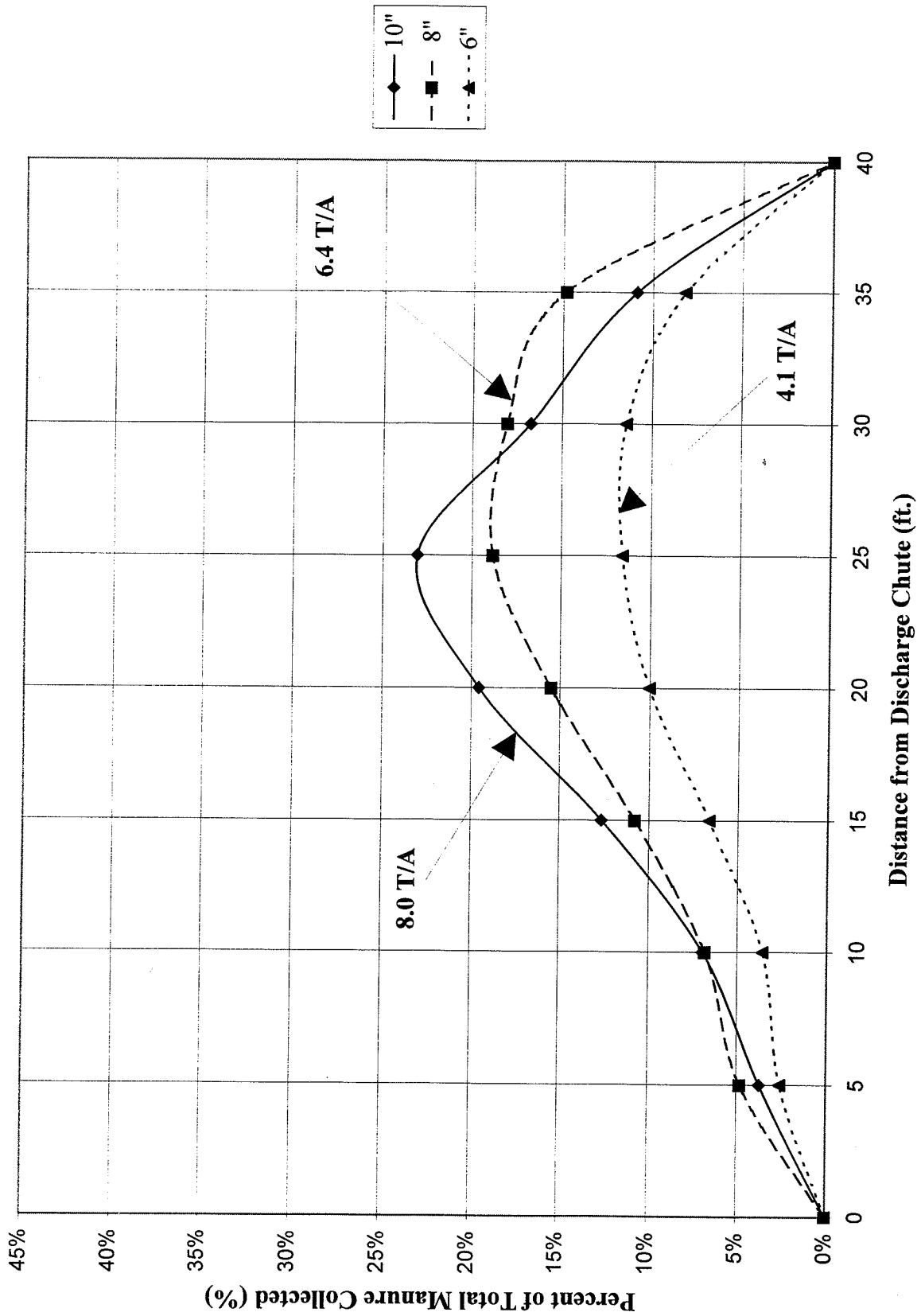


Figure 6.8: Plot of spread pattern for tested gate heights at a moisture content of 78.5%.

Variations in the data involve the shape of the distribution, discharge rate, and the gate height. For low moisture manures, the shape of the distribution seems to be independent of gate height (Figure 6.6). However, at higher moistures, the gate height appears to skew the distributions in either a lateral or longitudinal direction. For example, at the medium moisture tested (Figure 6.7), a gate height of 10 inches skews the distribution peak to the right compared to the 6 or 8 inch gate height. With high moisture manures (Figure 6.8), a gate height of 10 inches skews the distribution peak to the left of the smaller gate height peaks.

Another variation exists between the gate height and the discharge rate. Although the data supports a trend that the gate height is proportional to the collected discharge, the rate is not constant over the range of moisture levels. For instance in Figure 6.3, the 35.0%, 61.2%, and 78.5% moisture manures yield a collected discharge of 10.0, 5.2, and 8.0 tons/acre (T/A) respectively for a gate height opening of 10 inches. The major variation is the medium moisture manure discharge deviates from the expected 580 to 790 lb. range which is used to calculate the application rate (see Appendix B). The distributions for 8 and 6 inch gate heights (Figures 6.4 and 6.5) are similar to the above results with the low and high moistures having similar discharges while the medium moisture being consistently much lower.

Since the distributions are averaged from three tests, it is important to understand the trends and to try to explain the variations in the data. Given the fact that each moisture type was sequentially tested on different days, under changing wind conditions, it is conceivable the

weather had an influence on the shape of the pattern. This would very likely explain the skewed distribution for the medium moisture manure at a gate height of 10 inches (Figure 6.7). On the day those series of tests were run, the wind speed was an average of 9.41 miles/hour (mi/h) with peak wind speeds of 15.05 mi/h for tests involving the 6 and 8 inch gate height settings. During the time the 10 inch gate height tests were conducted, the wind speed increased to an average of 13.76 mi/h with peak wind speeds of 22.77 mi/h with minimal changes in direction. Given the fact that all of the tests were conducted into the direction of the wind, this increase in speed would likely explain the shift in the 10 inch distribution.

Besides the changing weather conditions, a bridging problem could have occurred which would have had disturbing effects on the amount and shape of the distributions. This would likely explain why the medium moisture manure had a considerably lower collected discharge relative to the other two moisture levels. Additionally, the bridging factor in combination with the changing wind conditions could explain the skewed distribution for the high moisture manure at 10 inches of gate height in Figure 6.8.

6.4.2 Overlap Test Results

The next step in the analysis was to determine the necessary distance to space the discharge intervals to achieve an appropriate uniform application. Since the tests showed the distributions had changed only slightly in response to changes in gate height, the tested gate height range was chosen as the operating range for the controller. Therefore, the test

distributions for all 3 gate heights tested were averaged for each moisture level and used as an approximate distribution for that particular moisture level. Refer to Figure 6.9 for an example of a generalized spread pattern plot for a moisture content of 61.2%. Refer to the Overlap Spread Pattern Plot in Appendix B for plots of the averaged distributions.

To simplify the analysis, any five foot section of the spread width containing less than 5% of the total manure was eliminated and the spread width was shortened by five feet. To further simplify matters, the percentage of manure within a five foot section was assumed to be equally distributed over the five foot section using one foot intervals. The five foot section percentages were divided by five and matched to the corresponding one foot intervals of the spread width. Refer to Figure 6.10 for an example of the discrete version of the generalized spread pattern distribution in Figure 6.9.

The discrete spread pattern was overlapped by identical discrete spread patterns using spread sheet software. The percentages were added together from one end of the original spread pattern to the other. The other pattern was offset at various distances in one direction until the most uniform discharge pattern was formed. The spread sheet analysis concluded that for the range of manures tested, a single overlap of 15 feet could be used to provide an uniform application within 12% of the total average application. The analysis assumes the operator will constantly spread in one direction and travel at the same speed for all discharge intervals. Refer to Figures 6.11 and 6.12 for an illustration of how the spread pattern overlap analysis is done and the resulting spread pattern produced within the overlapped range.

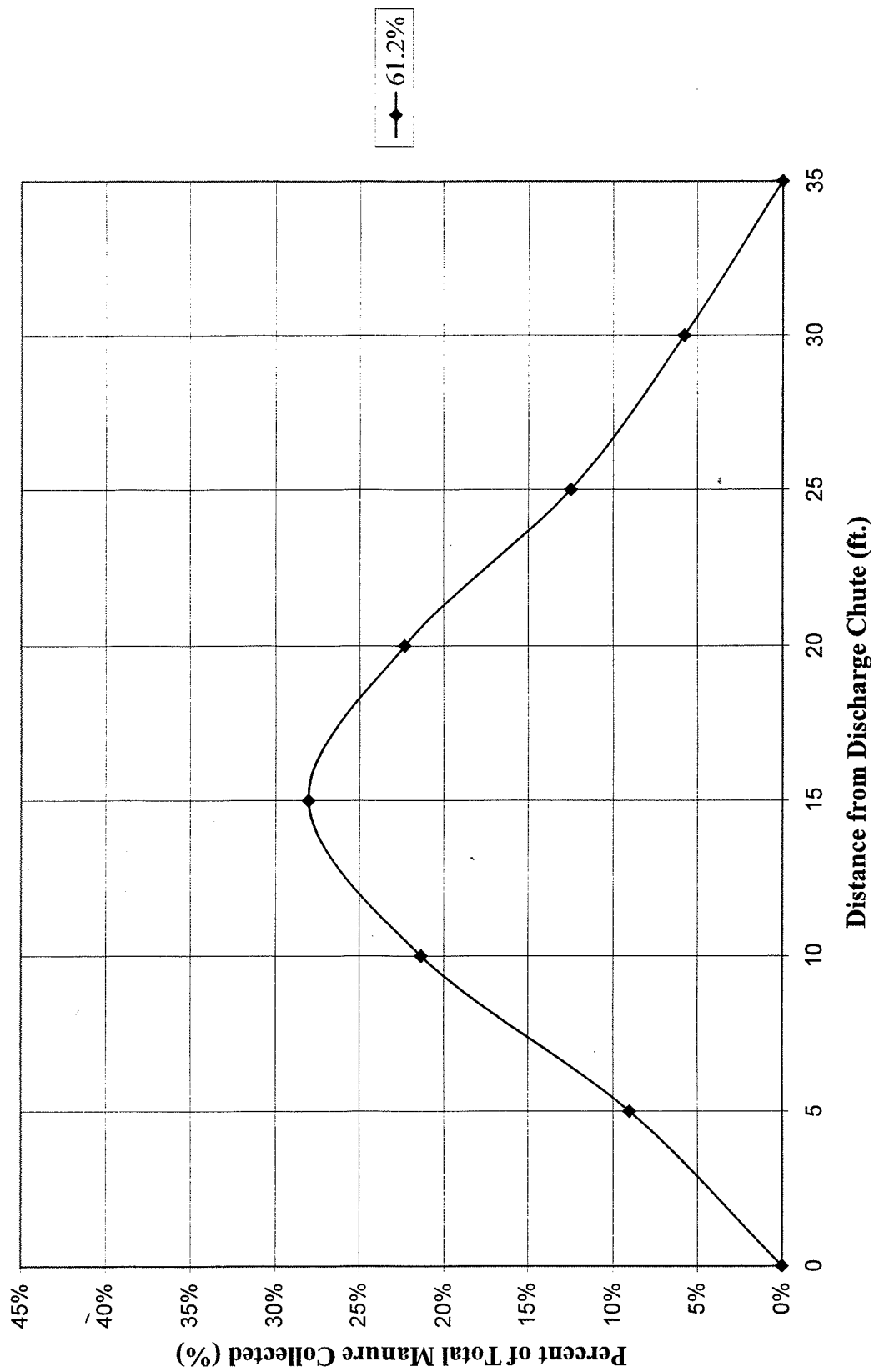


Figure 6.9: Plot of generalized spread pattern for a moisture content of 61.2%.

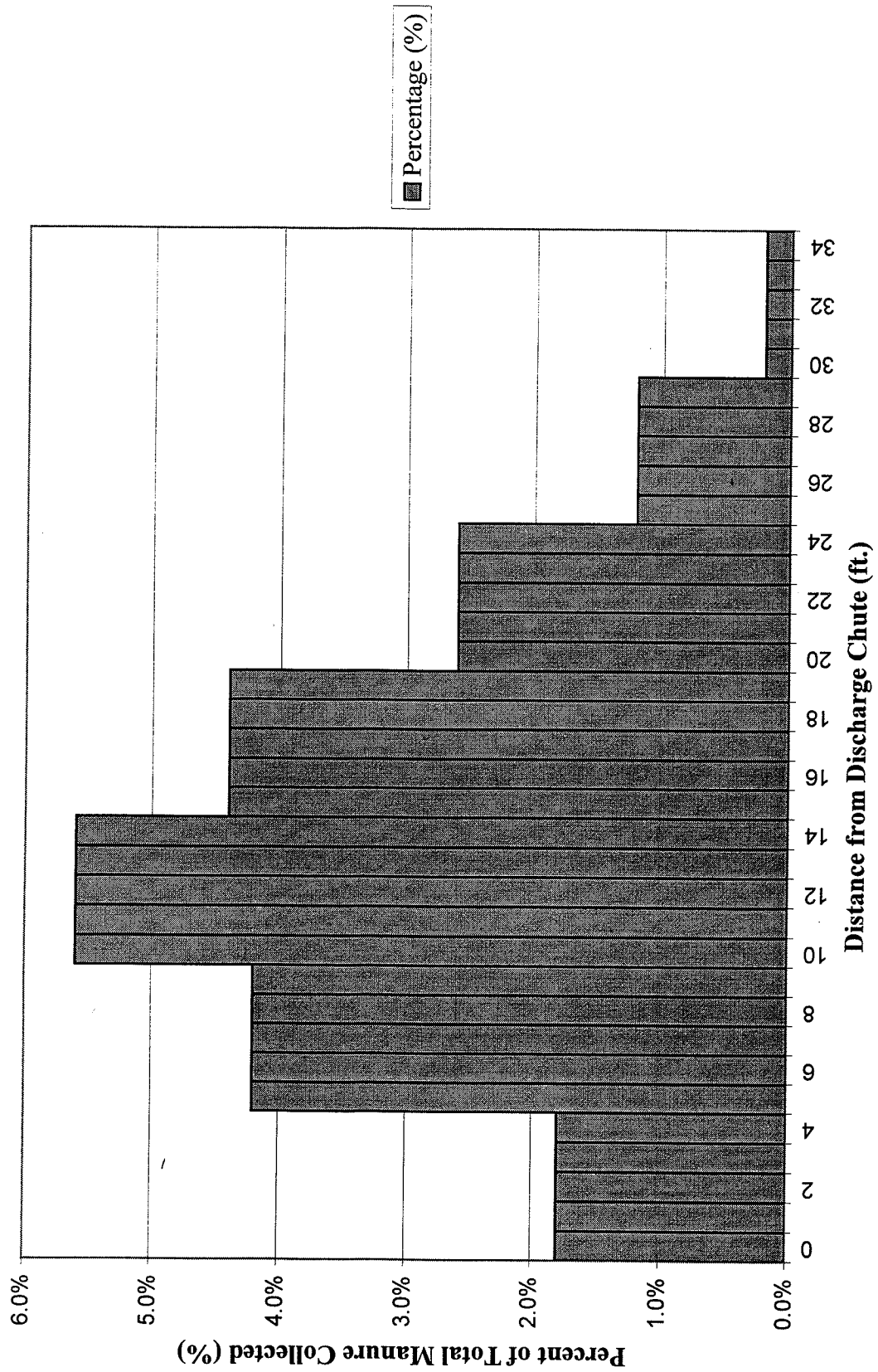


Figure 6.10: Plot of generalized discrete spread pattern for a moisture content of 61.2%.

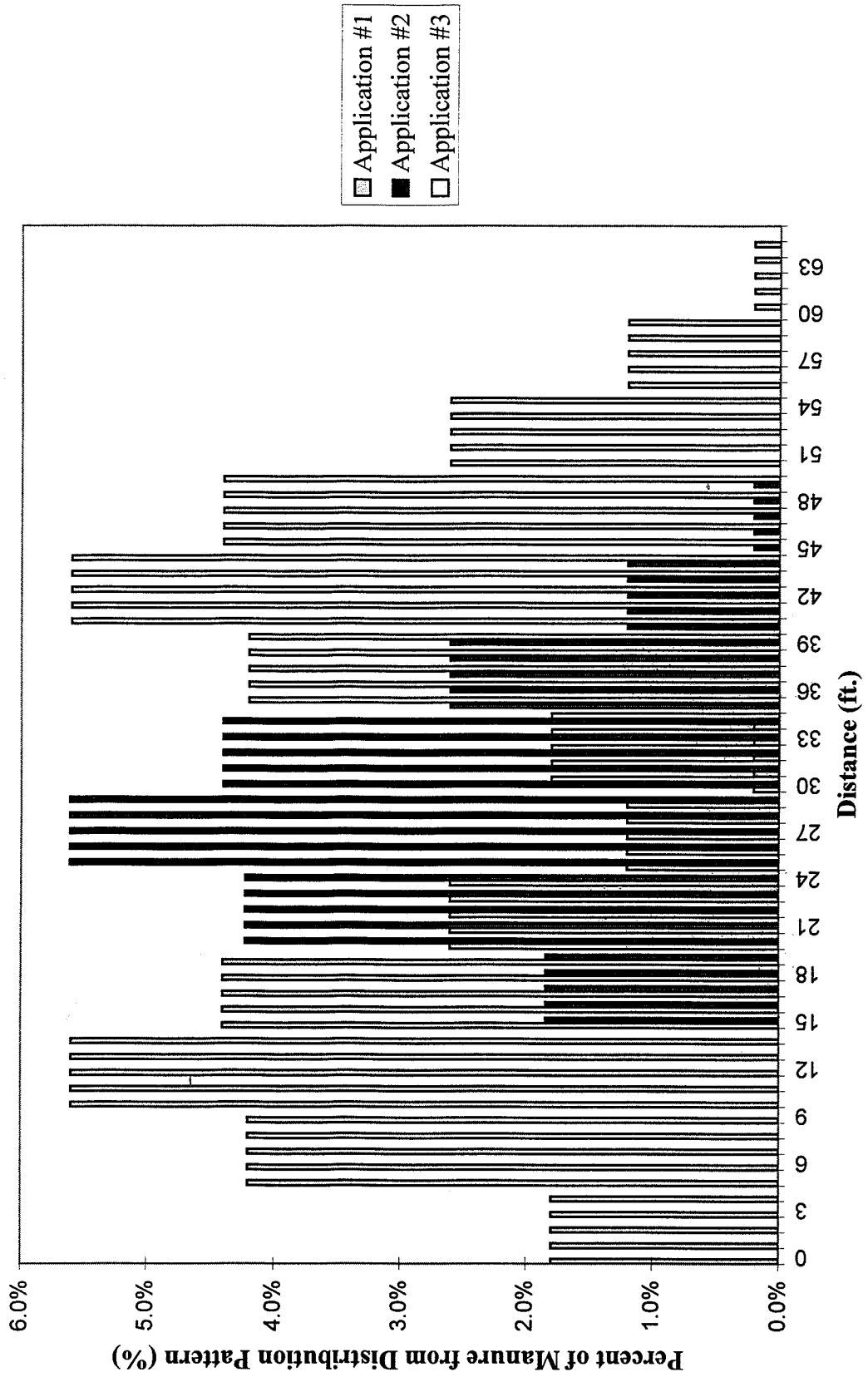


Figure 6.11: Plot of discrete overlap pattern when overlapped twice.

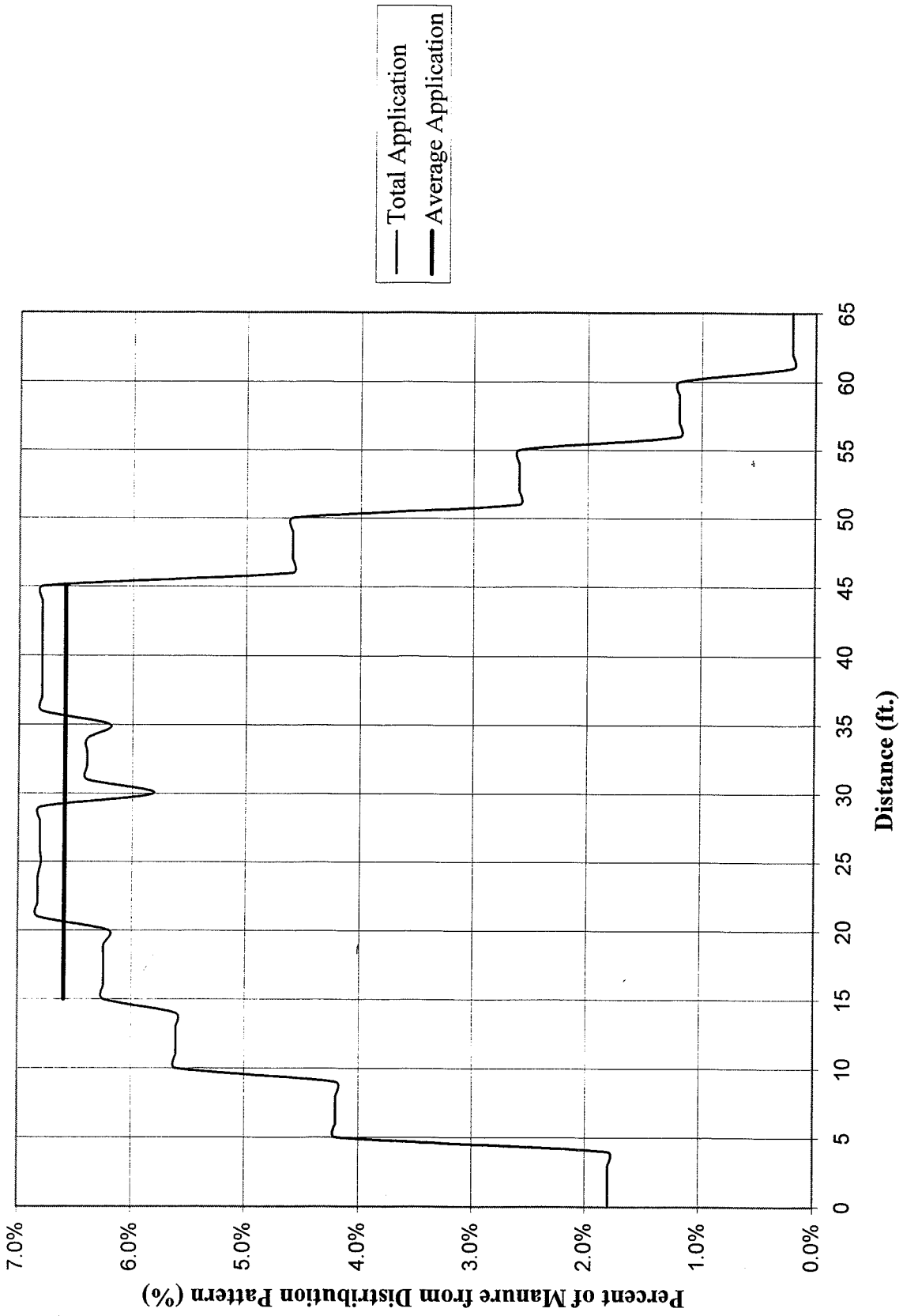


Figure 6.12: Plot of resulting spread pattern distribution when overlapped twice.

CHAPTER 7

CONTROLLER THEORY, DESIGN, AND TEST RESULTS

7.1 Controller Theory

Since the spread pattern tests showed changes in the tested gate height range only caused changes in the discharge rate and not the overall pattern, the gate was used to control the spreader's discharge rate. Therefore, the controller's output would involve manipulating the gate position. To do this effectively, the spreader's discharge system would have to be tested and modeled in order to program the controller.

7.1.1 Discharge Testing

To test the discharge system, the spreader was loaded from 11,000 to 12,000 lb. with manure of relatively high moisture content (81.3%). The manure was discharged with the spreader operating at the required 540 RPM PTO speed with the gate positioned at the following heights: 16, 12, 10, 8, and 6 inches. The spreader's load was statically discharged twice at each gate position for 50 seconds. Four weight samples from the Digi-Star Scale Indicator were taken over a period of one second. The four samples were averaged and used as one weight value. After waiting one second, four more samples were taken over a one second period and averaged.

Because of the way the data is sampled and averaged, the weight data was sampled every two seconds. Weight samples are sent from the controller through the RS232 male DB 9 plug

(see Figure 5.11) to the serial port of a laptop computer. Communications software, called Telix, is used to collect the serial weight data and save it to a file.

Since each set of test data exhibited a linear discharge, a linear regression was performed on the data to derive a discharge rate per unit time for each gate position. The two individual discharge rates for each gate position were both averaged to arrive at an average discharge rate for a given gate position. The averaged values were used in a linear regression analysis to develop an average discharge rate over the whole gate opening range (0 to 16 inches). The results of the tests are shown in Table 7.1. Refer to Discharge Data and Discharge Plots in Appendix C for the regression results for the individual sets of data and a regression plot of the averaged values.

Table 7.1: Linear regression of averaged static discharge data.

Gate Height inches	Averaged Discharge Rate (A) lb./sec	Linear Regression of Discharge Rate (B) lb./sec	Error abs(A-B) (C) lb.	% Error (C/A)•100
0	0.0	0.0	0.0	0.0
6	103.7	97.6	6.1	6.3
8	131.5	130.1	1.4	1.1
10	150.2	162.6	12.4	7.6
12	203.7	195.2	8.5	4.4
16	218.8	260.2	41.4	15.9

7.1.2 Controller Process Modeling

The data and the plot of the averaged data indicated there were some nonlinear interactions between the gate height opening and the discharge rate at the highest gate position. However,

since the spread pattern tests verified the spread pattern is unaffected within the 6 to 10 inch working range, a linear regression was performed without the extreme gate position of 16 inches. The results of this regression yielded a discharge rate of 16.24 lb./sec per inch of gate height with a correlation factor of 0.9942. This analysis concluded the spreader's discharge system could be modeled as an integration process.

An integration process is a control theory term used to describe a proportional relationship between a process' output and its input. In this case, the process output is the discharge rate (lb./sec) and the process input is the gate height (inches). The process' proportionality constant is the calculated slope from the regression analysis of averaged discharge rates (16.24 lb./sec•inch). The process output is calculated by multiplying the process input by the proportionality constant. Therefore, the spreader's discharge rate is calculated by multiplying the gate height by the proportionality constant. For example, if the gate height opening were 6 inches, the spreader would discharge manure at a rate of 97.44 lb./sec (6 inches•16.24 lb./sec•inch).

7.2 Controller Design

The next step in developing a controller is to devise a method that will control the process output. Due to the large magnitude of the sensor measurement values and application rate calculations, the controller has very few computer resources remaining to perform control calculations. This limitation prompted the use of a proportional (P) type controller to manipulate the gate height.

A P controller is the least complex method of controlling a process' output. It uses the system error to calculate the adjustments to the process. The system error, E_n , is computed by the summing junction and is the difference between the commanded or desired output, R_n , and the process output, C_n . The P controller takes E_n and multiplies it by the controller gain, K_c , to derive the necessary process input, M_n , to bring the system output to the desired level. The controller's output is called a manipulation. This manipulation is the input into the process and will cause the process output to change. By placing the P controller in series with (or cascading it with) the spreader's discharge process within a continuous loop, a closed-loop control system is formed. Figure 7.1 is a block diagram illustrating the closed-loop control system.

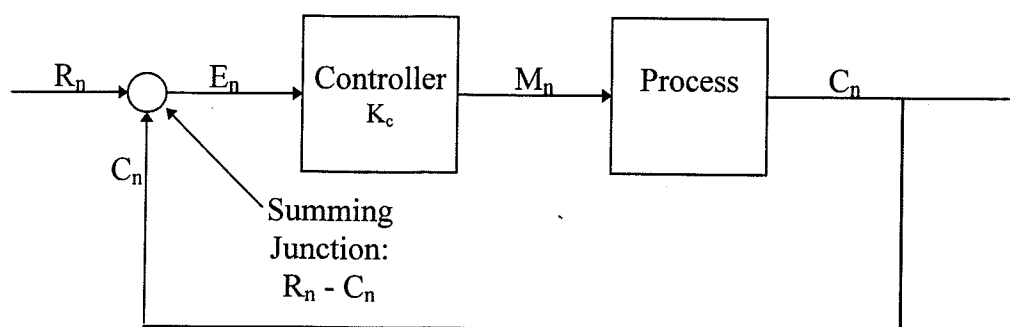


Figure 7.1: Block diagram illustration of closed-loop control system.

To model and analyze the feedback closed-loop system, mathematical equations are used to describe the discrete controller and process' characteristics. These equations are called transfer functions and they are defined as the ratio of its output to its input with all initial conditions assumed to be zero (Bollinger and Duffie, 1989). The discrete transfer functions

can be obtained from difference equations by using the backward-shift operator B, which is defined such that

$$By_n \equiv y_{n-1}$$

$$B^2y_n \equiv y_{n-2}$$

$$B^jy_n \equiv y_{n-j}$$

It should be noted that the B operator is not a variable, so no numerical variables should be assigned to it (Bollinger and Duffie, 1989). Therefore the process' transfer function can be described as a function of the B operator such that

$$G_p(B) = \frac{C_n}{M_n}$$

Similarly, the controller's transfer function can be described as a function of the B operator such that:

$$G_c(B) = \frac{M_n}{E_n}$$

Using this type of notation and analysis, the process can be mathematically described as an integral process taking the form:

$$G_p(B) = \frac{C_n}{M_n} = \frac{KTB}{1-B}$$

where K is the process' proportional constant and T, the sample period, is the time between controller executions (Bollinger and Duffie, 1989). See Derivation of Control Equations in Appendix D for derivation of $G_p(B)$. Since the PARRALAX Stamp computers can only perform integer computations, K is assigned to be 16 which is the rounded integer value of the calculated 16.24 lb./sec•inch discharge rate of the spreader gate.

To assign T a value, the weighing system response had to be assessed. The weighing system gave accurate results in the dynamic tests described in Chapter 6, Section 4.1 measuring the discharge over an approximate 16 second time period. This method of weight measurement captures the start and end values that approximate a discharge trend or a discharge per unit time. Therefore, the same type of measurement scheme would be used in the design of the controller.

By dividing the dynamic test sample period by four, the computer is programmed to measure a discharge trend that encompasses at least two auger cycles. This is important due to the pulsing conditions that arise with each cycle of the auger. This 4 second sample period captures the weight loss over two complete auger cycles. This sample period is able to reduce the pulsing effects and give a more representative discharge rate than if a shorter time period were used due to the dynamic ground effects on the weight data. On the other hand, the time period can not be made too much longer because it will decrease the accuracy of the control system. Since an accurate trend needed to be measured while maintaining the systems integrity, a sample period of 4 seconds was assigned to T. Therefore, the process' transfer function, G_p , is written as:

$$G_p(B) = \frac{C_n}{M_n} = \frac{KTB}{1-B} = \frac{16 \frac{lb}{sec \cdot inch} \cdot 4 sec \cdot B}{1-B} = \frac{64 \frac{lb}{inch} \cdot B}{1-B}$$

Specifically, the computer samples the weight at 4 Hz and averages the four values. The computer pauses for 3 seconds and samples the weight again at 4 Hz and averages the second

set of values. The second average value is subtracted from the first. This discharge value is divided by 4 seconds to yield a discharge rate per second.

The controller has a less complicated transfer function. Since it only takes the error, E_n , and multiplies it by a controller gain, K_c , to arrive at the controller output, the transfer function, G_c , only has one term and is written such that:

$$G_c = \frac{M_n}{E_n} = K_c$$

In designing the optimum closed-loop control system, it sometimes helps to simplify the entire system using all of its individual transfer functions. When working with control systems, the desired relationship is the single transfer function, $G(B)$, that describes the whole system in terms of its inputs and outputs. Since this is a single input/single output cascade control system, the two individual transfer functions, $G_c(B)$ and $G_p(B)$, can be multiplied to arrive at $G(B)$ which is written as

$$G(B) = \frac{C_n}{R_n} = \frac{G_c(B)G_p(B)}{1 + G_c(B)G_p(B)}$$

See Derivation of Control Equations in Appendix D for derivation of $G(B)$. Since the P controller controls the system output, C_n , by multiplying E_n by K_c , the optimum P controller in theory would always manipulate C_n to equal R_n . To implement this type of controller, it would require K_c to have a value that would always properly correct for E_n . This type of controller is called a "dead-beat" controller, because it yields a system response that equals

the command input. More specifically, since the controller operates in a discrete time domain with sample periods, a dead-beat controller yields a system response that equals the command input one sample period later. Therefore, the desired closed-loop transfer function, $G_d(B)$, for this type of system is

$$G_d(B) = \frac{C_n}{R_n} = B$$

Using $G_d(B)$ as the desired transfer function, G_c can be mathematically determined for dead-beat response.

$$G_c(B) = \frac{1}{G_p(B)} \frac{G_d(B)}{[1 - G_d(B)]} = \frac{B}{\frac{KTB}{1-B}(1-B)} = \frac{1}{KT} = \frac{1}{64 \frac{lb}{inch}} = 0.0156 \frac{inch}{lb}$$

Since G_c was calculated to be 0.0156 inches/lb. and G_c is equal to the controller gain K_c , then K_c must equal 0.0156 inches/lb. See Derivation of Control Equations in Appendix D for derivation of $G_c(B)$.

According to control theory, if K_c is set below 0.0156 the system response will require more than one time period to reach the desired response. On the other hand, if K_c is set above 0.0156 than the system response will over-shoot the desired response and take more than one sample period to reach the desired response. With the control parameters calculated, the control system can be completely described by the closed-loop block diagram illustrated in Figure 7.2.

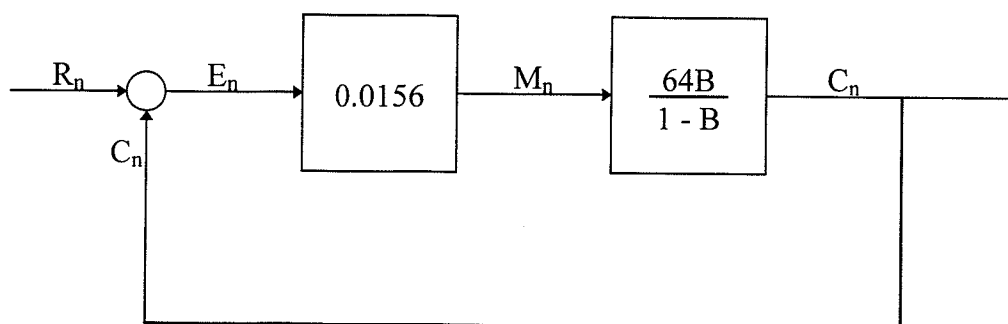


Figure 7.2: Complete closed-loop block diagram.

For the computer to calculate M_n using K_c , an integer form of 0.0156 had to be formulated. To do this the value was multiplied by 1000, rounded down, and programmed into the controller. The number was rounded down in efforts to be conservative on the value so the system response would not over-shoot the desired response. This integer K_c value is multiplied by E_n and divided by 10 to calculate the number of inches the gate must travel to correct the error with 2 decimal places of precision.

7.3 Controller Programming Logic

With the controller parameters defined, programming code needed to be developed to dictate the controller's mathematical, I/O, and logic operations. Since there are two computers handling separate tasks, the programming logic needed to be specific about each operation. The passing of information from computer to computer and the data retrieval of sensor measurements are very critical parts of the controller's success. Although there are probably many ways to program the controller, Figures 7.3a and 7.3b represent the flow chart used in programming the controller.

Figure 7.3a illustrates how the programming code is structured for the Stamp #1 computer. The program starts using two loops. The first loop is to read in four weight values from the indicator's printer port, and the second loop is used to run through the first loop again to collect pulses from the encoder and another set of weight values. At the start of the first loop, four weight values are read in at 4 Hz, averaged, and set to a value (w(1)). After this, the computer pauses for 2 seconds and reads in the encoder pulses for 1 second. The pulses are used to calculate the ground speed (Speed) in ft/sec. The program directs the computer through the second loop where it reads in four more weight values at 4 Hz, averages them, and assigns the averaged weight value to a variable (w(2)).

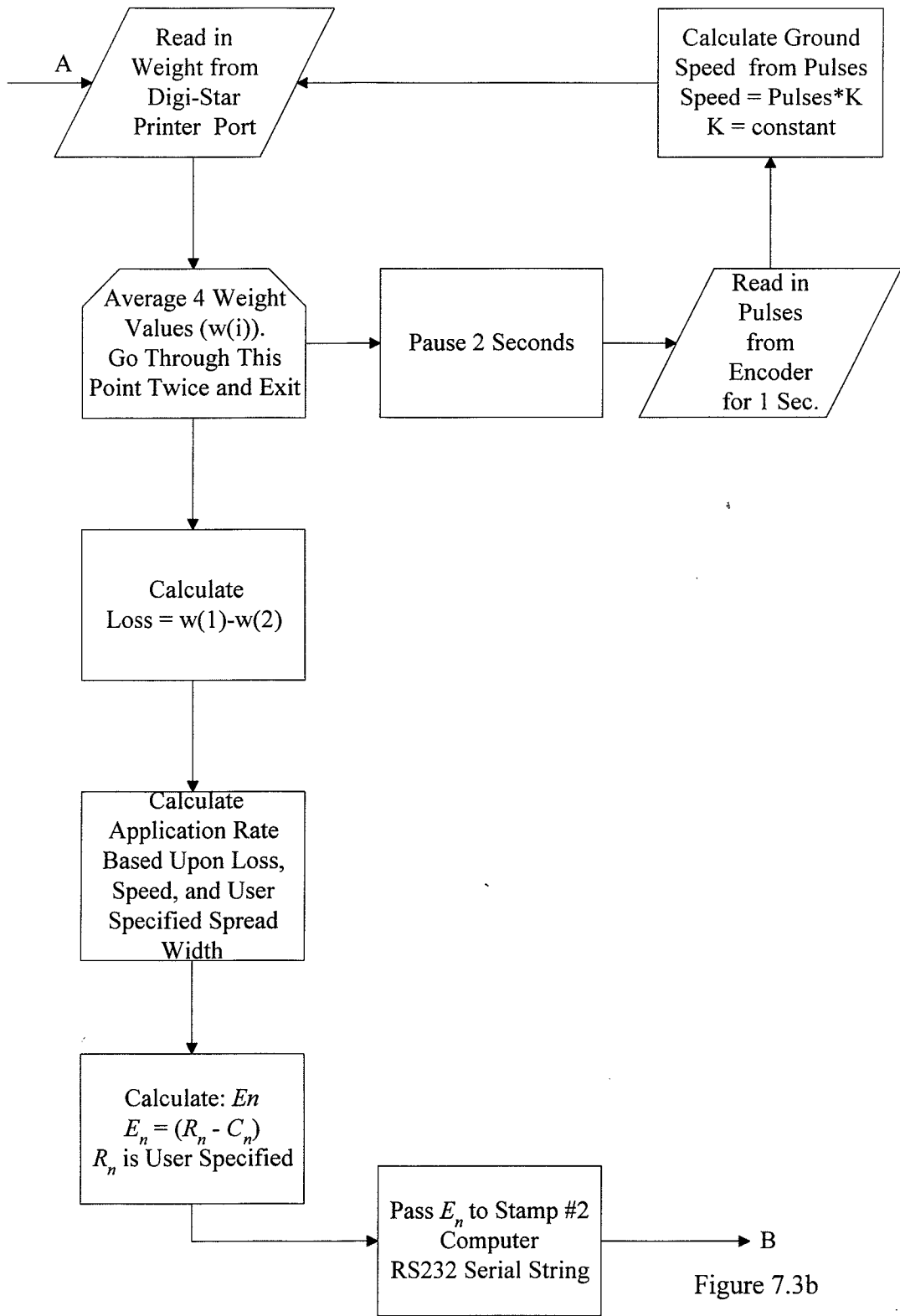


Figure 7.3b

Figure 7.3a: Flow chart for Stamp #1 computer.

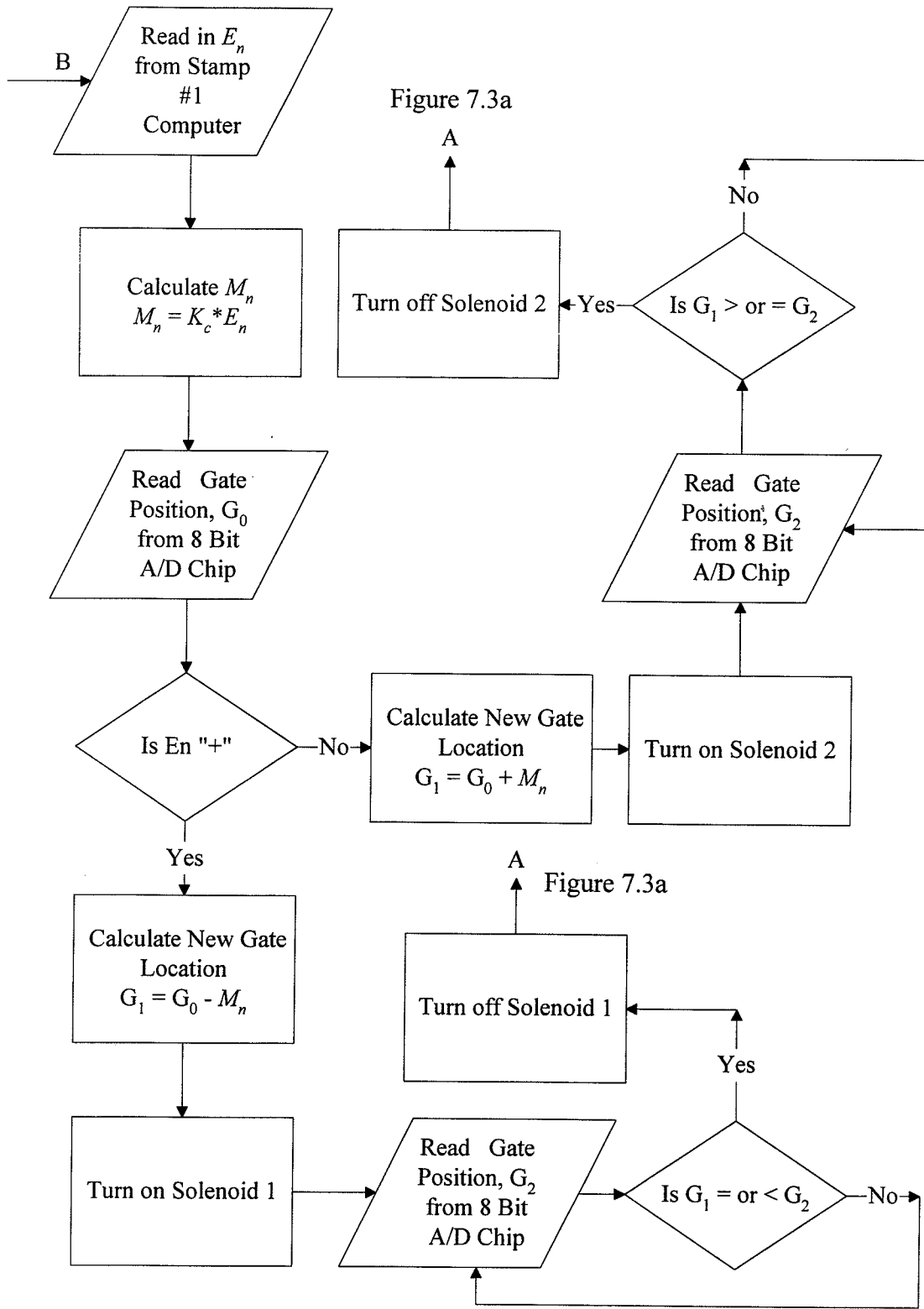


Figure 7.3b: Flow chart for Stamp #2 computer.

The computer subtracts $w(2)$ from $w(1)$ to arrive at a discharge weight (Loss) over a 4 second interval. With the discharge weight (Loss) and the ground speed (Speed) defined, the computer calculates the measured application rate using a previously entered user-specified spread width value. The measured application rate is assigned to a variable, C_n , and is subtracted from the user-specified command application rate, R_n . The error, E_n , is calculated by subtracting the measured system application rate from the command application rate. If E_n is greater than or less than $\pm 5\%$ of the commanded application rate, the value is passed to the Stamp #2 computer which is represented by location B in Figure 7.3b. Otherwise, if E_n is within $\pm 5\%$ of the commanded application rate, the Stamp #1 computer starts to take weight and speed data again instead of passing E_n to the Stamp #2 computer.

Once E_n has been received by Stamp #2, the computer calculates the required manipulation, M_n , in gate position. The computer reads in the current gate position, G_0 , from the 8 bit A/D converter IC chip which is interfaced with the linear potentiometer. If E_n is positive, the computer subtracts M_n from G_0 to arrive at the new gate position, G_1 . However, if G_1 is lower than the 6 inch gate opening, G_1 is set to the digital 8 bit 6 inch gate position. Solenoid #1 is activated which causes the gate opening to decrease in height. While the gate is moving downward, the gate position is being read, G_2 , and checked against G_1 . The computer continues to operate the solenoid until G_2 is less than or equal to G_1 . When this condition is met, Stamp #2 passes a logic operator, 1, to location A in Figure 7.3a, which acts as a switch to turn on Stamp #1 and begin collecting weight data and perform application rate calculations.

If E_n is negative, however, the computer goes through a slightly different process. Instead of subtracting M_n from G_0 to arrive at G_1 , it adds M_n to G_0 to arrive at G_1 . However, if G_1 is higher than the 10 inch gate opening, G_1 is set to the digital 8 bit 10 inch gate position. This will cause the computer to activate Solenoid #2 instead of Solenoid #1, which will cause the gate to move up not down. While the gate is moving upward, the gate position, G_2 , is being read and checked against G_1 . The computer will continue to operate the solenoid until G_2 is greater than or equal to G_1 . When this condition is met, Stamp #2 passes a logic operator to location A in Figure 7.3a returning control to Stamp #1.

The control system never terminates since it is programmed to run in a continuous closed-loop. Stamp #1 is working while Stamp #2 waits for data transmission from Stamp #1. Likewise, when Stamp #2 is working, Stamp #1 is waiting for data transmission from Stamp #2. The only way to terminate the continuous loop is to interrupt the power supply to either or both computers. If a power loss occurs in the Stamp #1 computer, the Stamp #2 computer will be suspended in a constant waiting mode until power is restored to Stamp #1 and data is transmitted. If Stamp #2 loses power, both computers must be reset since Stamp #1 initiates the data exchange. If both computers lose power, power must be restored to both computers within a 4 second period to assure the data transmission will take place and the continuous loop can begin again.

7.4 Controller Test Results

To verify the functionality of the P controller, two tests were devised to establish the experimental controller gain, K_c , and the system's robustness to dynamic conditions. In the first test, the controller was evaluated under static conditions in which the spreader's load was discharged into a pile using different values of K_c . The second experiment tested the controller's ability to regulate the discharge rate as the spreader moved through the field using different values of K_c . In both tests, the spreader's gate was initially opened to its maximum height to test the systems ability to recognize and correct for large discharge errors.

7.4.1 Static Test Results

Using the calculated K_c value of 0.015 as a basis for the static tests, the controller was programmed at values above and below 0.015 to evaluate the controller's sensitivity to different values for the control parameter. The purpose of these tests was to find the optimum K_c value under static conditions and use it as a starting value for the dynamic tests.

Fresh dairy manure which possessed a fairly uniform consistency and high moisture content was used for all of the static tests. By approximating the moisture content of the manure, a distance of 40 feet was programmed into the controller for the user-specified spread width. This spread width dimension was used because the tests would only measure the application rate applied in one single pass without any overlap. To simulate dynamic conditions in the static tests, the encoder was removed and a value of 3 ft/sec was programmed into the controller for the speed input. An application rate of 10 tons/acre was programmed into the

controller as the command rate, R_n . The combination of these spreading parameters correspond to a discharge rate of 55 lb./sec or 220 lb. per 4 seconds. Therefore, the control system was programmed to regulate a 220 lb. discharge ($\pm 5\%$) every sample period for a total run time of 88 seconds. The controller was programmed using the following K_c values: 0.017, 0.016, 0.014, 0.013, 0.012, and 0.010 inch/lb. Each K_c value was tested twice and the average of the absolute error (command - output) was calculated for each run. The two average error values for each K_c were averaged and used as a basis of evaluating the system's response for the tested value. The percent error for each controller gain is determined by dividing the averaged error value for both tests by the desired value of 220 lb. and multiplying by 100.

Figures 7.4a and 7.4b represent the results of the static system using a K_c of 0.017 inch/lb. In both tests, the system demonstrates very good ability to adjust for the large initial discharge after the system is first turned on. Both tests, however, suggest K_c is set too high due to the constant oscillation about the command line of 220 lb. The average output and error for the two test were 219.0 and 38.4 lb. respectively. Using the average error as a basis for the overall system accuracy, there is a 17.5% error of the commanded 220 lb.

Figures 7.5a and 7.5b illustrate how the system responded when K_c was set to 0.016 inch/lb. It appears the system does not respond to the initial discharge as well as when K_c was set at 0.017. In both cases, the discharge is still more than desired up to 3 sample periods after starting. The overall results conclude the value for K_c is still set too high, which is causing

the oscillation of the system output. Although there still is an oscillation pattern about the command line, the magnitude of the oscillating response appears to be slightly less than before. The average output and error for both tests were 225.8 and 37.9 lb. respectively, which translates to a 17.2% error.

The next series of tests used a K_c value of 0.014 inch/lb., which proved to be beneficial. The results of the tests which are shown in Figures 7.6a and 7.6b, confirm that K_c was set too high in the previous tests. Although there is still some oscillation about the command line, the frequency and magnitude of the oscillations are not as large with higher values. In both cases, the initial discharge was near the command, so the system did not recognize an oversized discharge until the second sample period. However, in Figure 7.6a the control system did a very good job in bringing the discharge down to just below the -5% command line. In Figure 7.6b, the control system brought the discharge slightly below the command. The overall results of the tests showed the system was responding better with decreasing K_c values. The average output and error for both tests were 235.9 and 37.0 lb. respectively which translates to a 16.8% error.

Figures 7.7a and 7.7b represent the system response when K_c is set to 0.013 inch/lb. There is a rather dramatic improvement in the system output, with a major reduction in the magnitude of the oscillation pattern. However, there does not seem to be any change in the frequency of the pattern compared to tests results with K_c set at 0.014. In both tests, the controller demonstrates good ability to correct for the large initial discharges (at 8 seconds in Figure

7.7a and at 4 seconds in Figure 7.7b). The overall results of the tests showed the system was improving with decreasing K_c values. The average output and error for both tests were 226.6 and 23.1 lb. respectively, which translates to a 10.5% error.

When K_c was stepped down to 0.012 inch/lb., the system response of the control system became worse. In both tests, the results indicate the system response becomes more random and the magnitude of the output is beginning to increase with decreasing K_c . In Figure 7.8a, the controller demonstrates very good ability to control the initial discharge, but in Figure 7.8b, the controller does not correct the discharge rate adequately. In Figure 7.8b, the system output at the later sample periods suggest the lower value might be causing the system to begin oscillating again. Overall, the results are worse than the previous results when using a K_c of 0.012. The average output and error for both tests were 227.2 and 36.6 lb. respectively, which translates to a 16.6% error.

Since the previous tests indicated the system response was worsening, a K_c of 0.010 inch/lb. was used in efforts to save time and prove that lower values would cause poorer system response. The results in Figures 7.9a and 7.9b demonstrated this is indeed true. In both tests, the controller did a very poor job in correcting for the initial discharge. The system response has a more profound oscillation pattern with a larger magnitude of system output than the two previous K_c values. The average output and error for both tests were 233.6 and 52.08 lb. respectively, which translates to a 23.7% error. From these test results, it was determined that any value under 0.010 inch/lb. would render unsatisfactory results.

The static test results can be summarized in Figure 7.10 and Table 7.2, which shows the optimum K_c value to be 0.013 inch/lb. Figure 7.10 illustrates that based upon the integer K_c values tested, 0.013 has the lowest average error. Although not all values were tested, the trend of the results suggest there is a rather steep decrease in improvement which levels off when starting from the optimum moving to higher values. As the values decrease from the optimum, there appears to be an equal decrease in system response which continues to escalate. The overall results show there is a nonlinear relationship between the average error and K_c . Table 7.2 lists the average output and the average error. In all of the tests the controller demonstrates a high repeatability in the system output. This is based upon the fact that the average error values for each test for a given controller gain are all within 14.5 lb. of each other.

An additional note concerning the test results is that all of the data points in Figures 7.4a - 7.9b represent individual discrete system responses. The points have been joined by a line to more clearly illustrate the presence or absence of the oscillation pattern. They are not to be interpreted as a continuous system response.

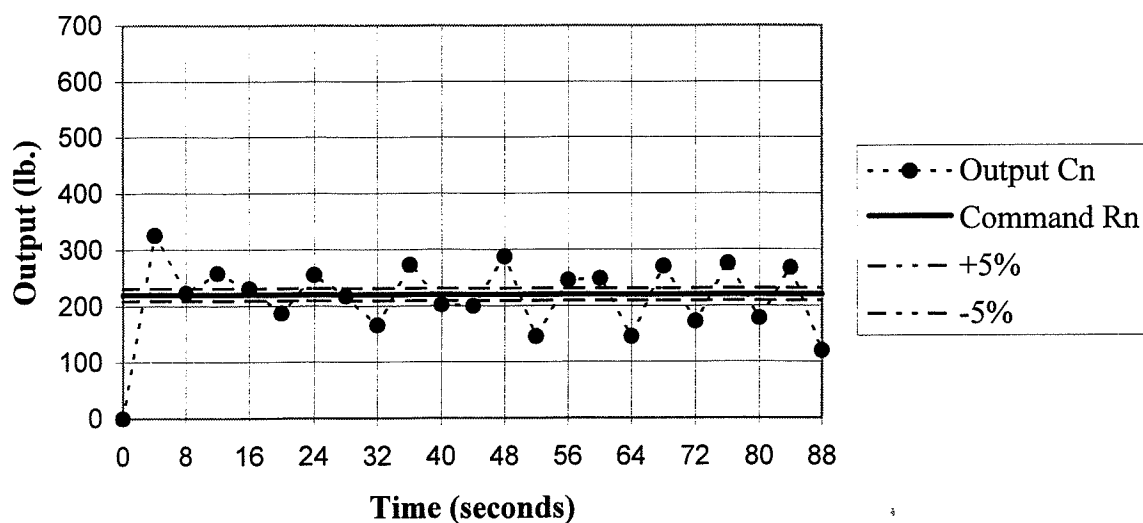


Figure 7.4a: Test #1: System response to static control test using a K_c of 0.017 inch/lb.

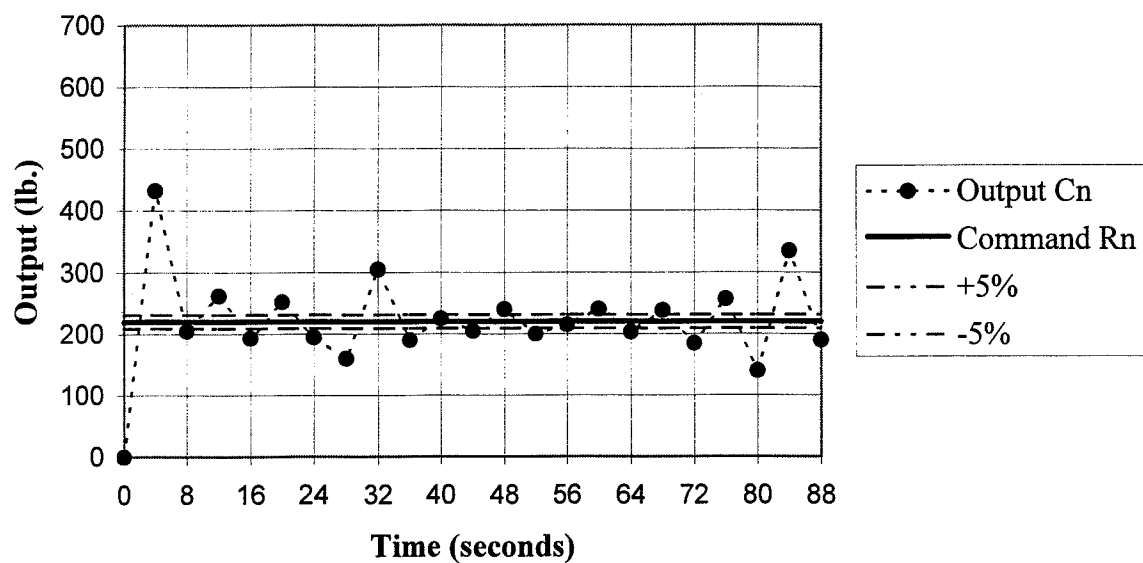


Figure 7.4b: Test #2: System response to static control test using a K_c of 0.017 inch/lb.

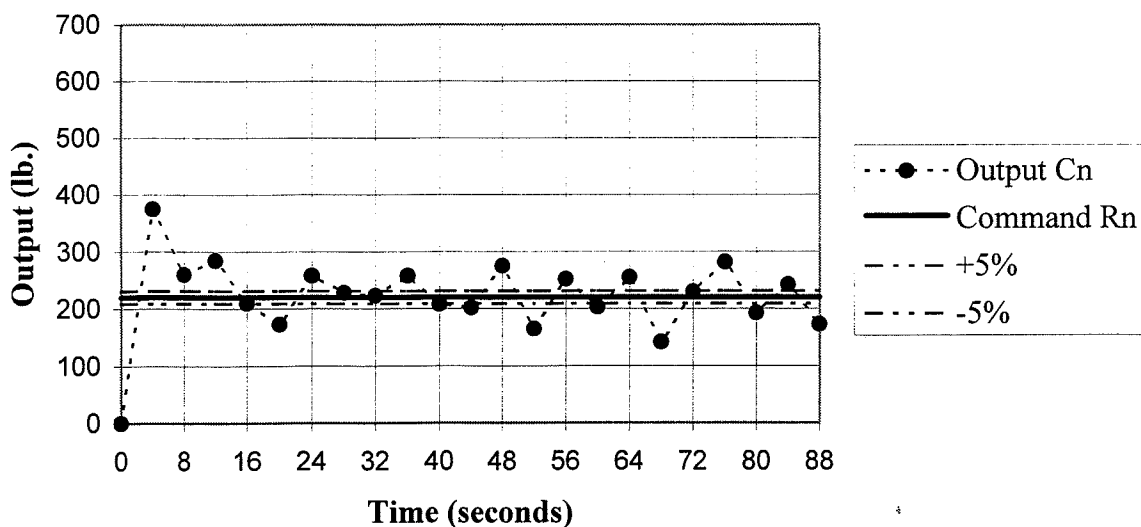


Figure 7.5a: Test #1: System response to static control test using a K_c of 0.016 inch/lb.

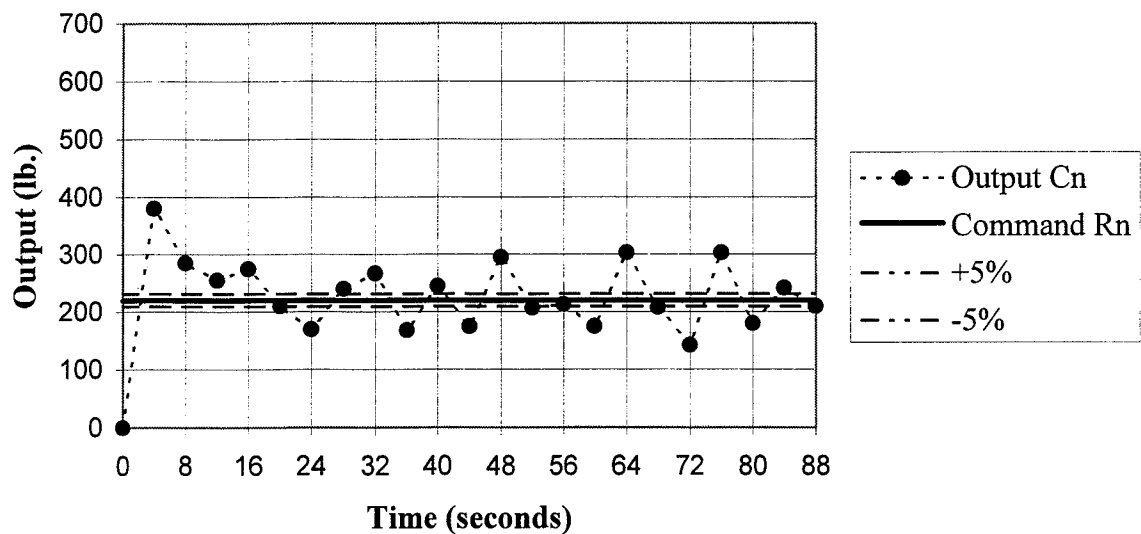


Figure 7.5b: Test #2: System response to static control test using a K_c of 0.016 inch/lb.

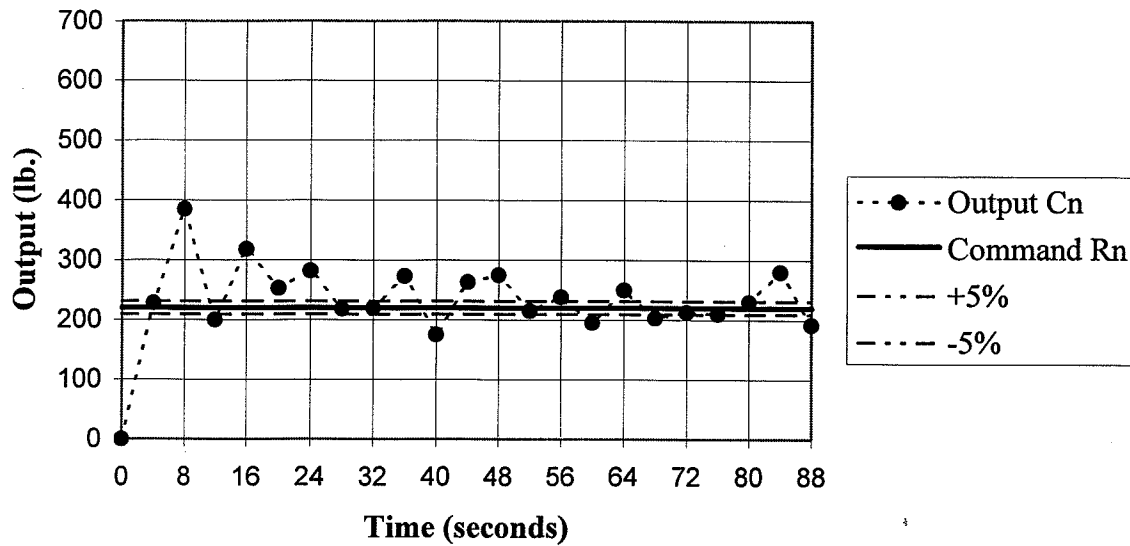


Figure 7.6a: Test #1: System response to static control test using a K_c of 0.014 inch/lb.

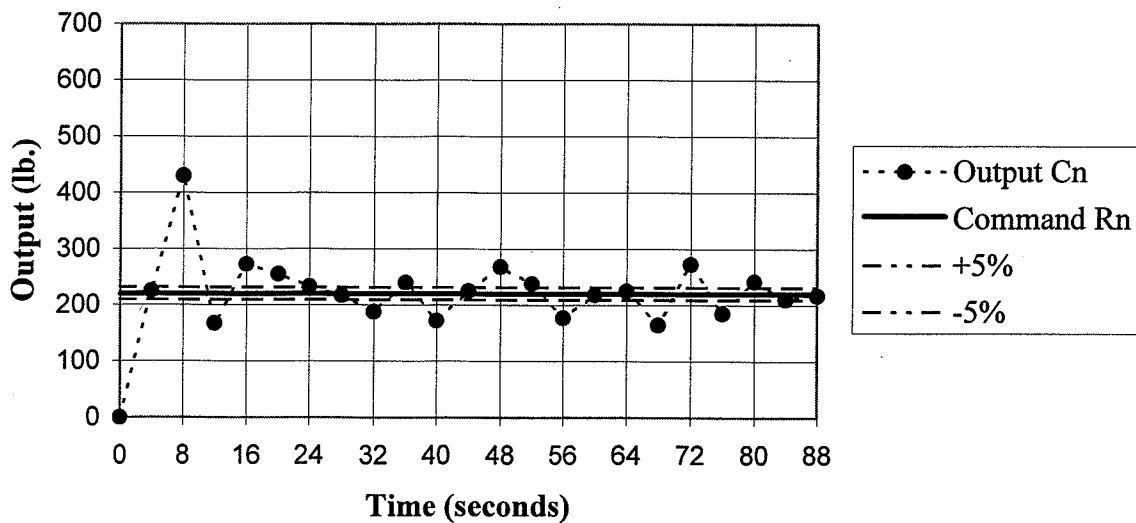


Figure 7.6b: Test #2: System response to static control test using a K_c of 0.014 inch/lb.

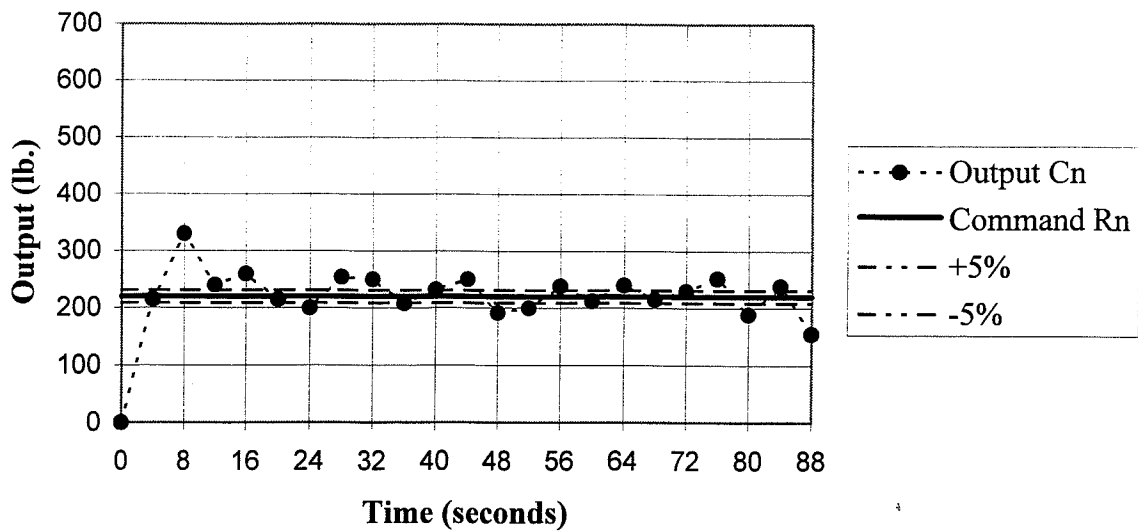


Figure 7.7a: Test #1: System response to static control test using a K_c of 0.013 inch/lb.

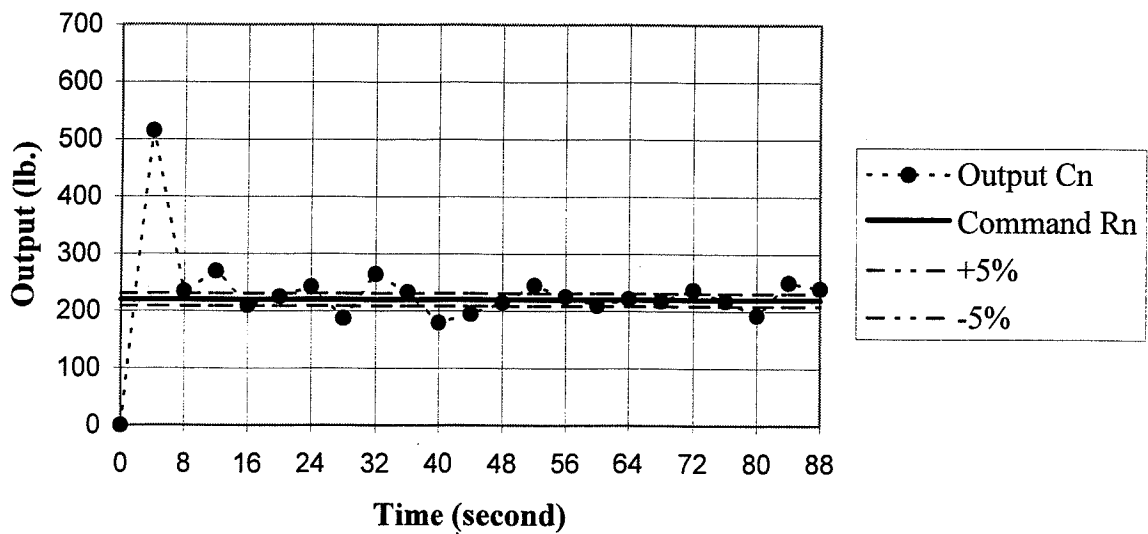


Figure 7.7b: Test #2: System response to static control test using a K_c of 0.013 inch/lb.

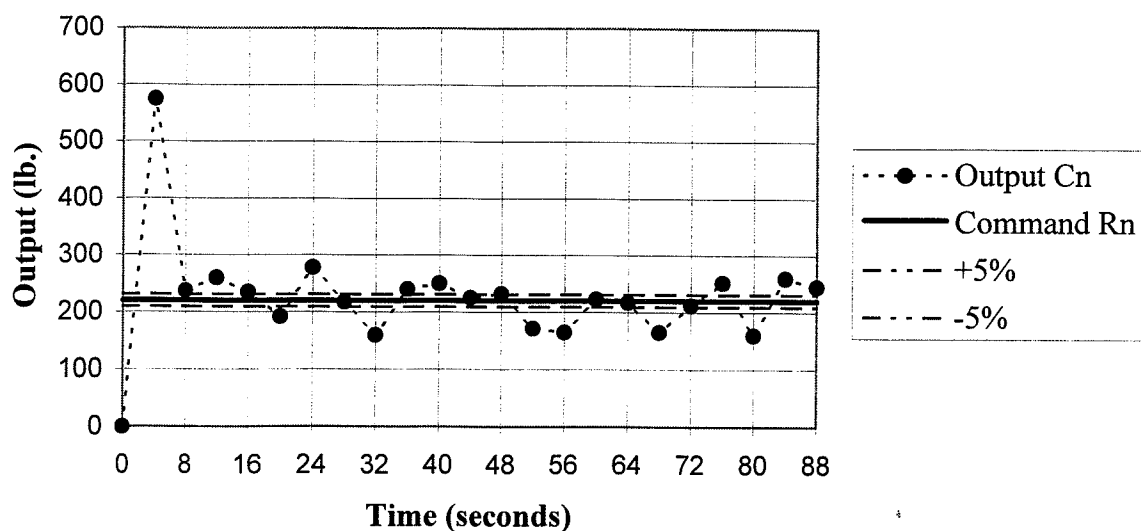


Figure 7.8a: Test #1: System response to static control test using a K_c of 0.012 inch/lb.

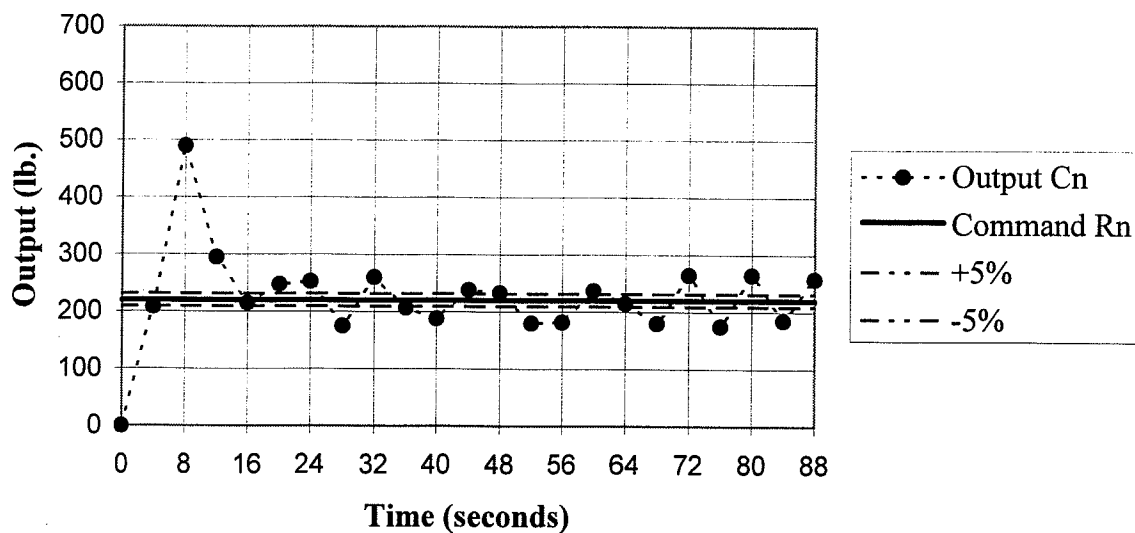


Figure 7.8b: Test #2: System response to static control test using a K_c of 0.012 inch/lb.

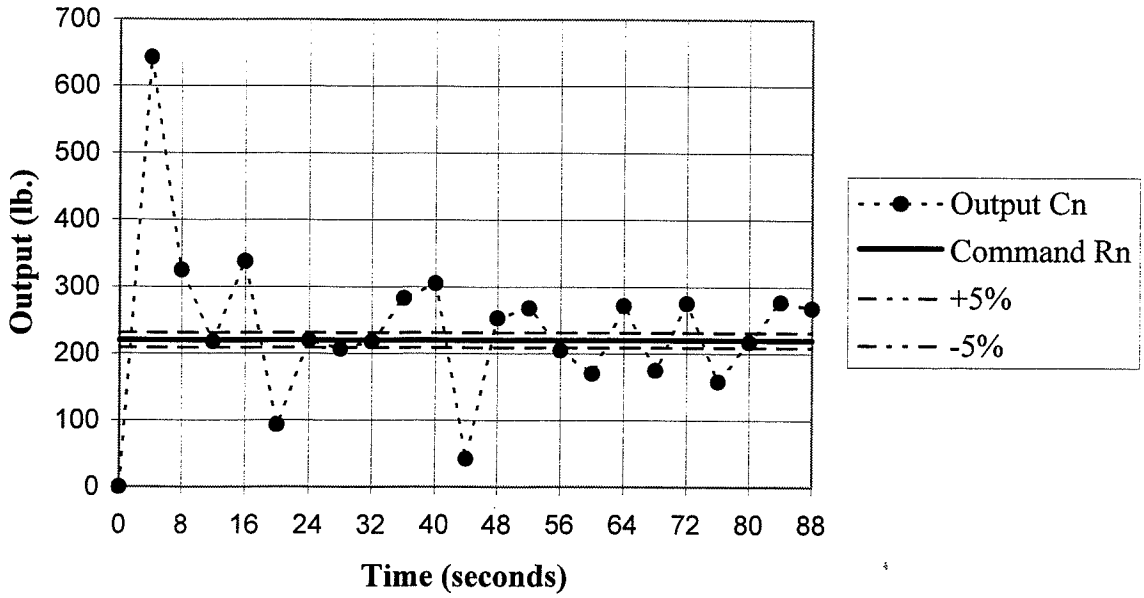


Figure 7.9a: Test #1: System response to static control test using a K_c of 0.010 inch/lb.

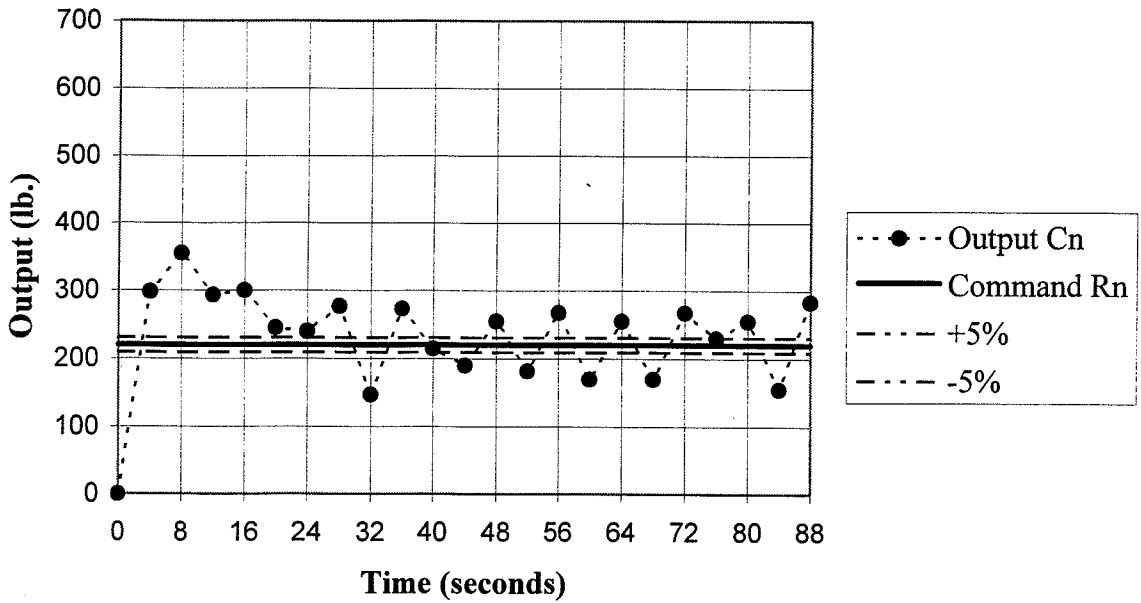


Figure 7.9b: Test #2: System response to static control test using a K_c of 0.010 inch/lb.

Table 7.2: Summary of static controller test results.

Controller Constant, K_c (inch/lb.)	0.017	0.016	0.014	0.013	0.012	0.010
Average Output Test #1 (lb.)	217.2	224.6	242.3	228.6	219.0	228.0
Average Output Test #2 (lb.)	220.7	227.0	229.4	224.6	235.4	239.2
Average Output for Both Tests (lb.)	219.0	225.8	235.9	226.6	227.2	233.6
Average Error Test #1 (lb.)	41.9 (19.0%)	34.2 (15.5%)	37.4 (17.0%)	27.1 (12.3%)	29.3 (13.3%)	55.3 (25.1%)
Average Error Test #2 (lb.)	34.9 (15.9%)	41.5 (18.9%)	36.5 (16.6%)	19.2 (8.7%)	43.8 (19.9%)	48.7 (22.1%)
Average Error for Both Tests (lb.)	38.4 (17.5%)	37.9 (17.2%)	37.0 (16.8%)	23.1 (10.5%)	36.6 (16.6%)	52.1 (23.7%)

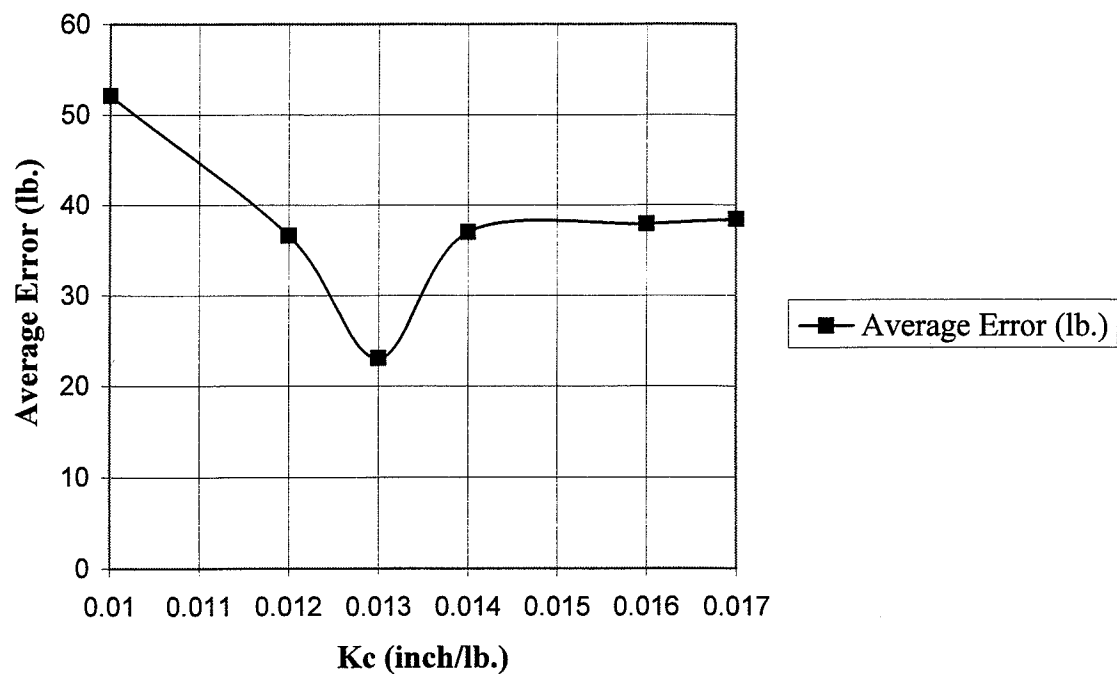


Figure 7.10 Plot of static control test results.

7.4.2 Dynamic Test Results

Believing the optimum static controller gain had been found, the next step was to apply it to dynamic conditions and determine how the system responds. Since the previous dynamic weighing tests were only approximations of the weighing system's accuracy, it was unknown how the control system would respond to the averaging of the instantaneous weight samples under dynamic conditions.

The purpose of the dynamic tests was to compare the dynamic results to the static results and determine what effects the force variation has on the controller. To test the controller under the same conditions present in the static tests, the same procedures were employed and the same type of manure was used. The encoder was inputting measured pulses for the controller to calculate the spreader's travel speed.

The tests were begun using the optimum K_c from the static tests. Figures 7.11a and 7.11b represent the dynamic system response using a K_c of 0.013 inch/lb. Both tests show the controller does an ineffective job of controlling the initial discharge. The results also show the same type of oscillation pattern illustrated in the static test when values of 0.017 and 0.016 (Figures 7.4a, 7.4b, 7.5a, and 7.5b) were used. The main difference was the magnitude of the dynamic oscillation patterns were almost 50% larger than the static results. This was the first indication the driving effects were having a negative impact on the controller functionality. The tests yielded an average output and average error of 224.6 and 58.3 lb. respectively, with a corresponding 26.5% error.

Figures 7.12a and 7.12b represent how the controller responded to a K_c of 0.012 inch/lb. In Figure 7.12b the controller demonstrates an improvement in its ability to correct for the initial discharge. The overall results of the two tests suggest a lessening of the oscillation pattern in magnitude and frequency. Although the results show an improvement in controller performance, the results also show the controller has more difficulty controlling the system output under dynamic conditions. The tests yielded an average output and average error of 227.2 and 47.8 lb. respectively, with a corresponding 21.7% error.

As K_c is lowered to 0.011 inch/lb., the system response improves. In Figures 7.13a and 7.13b, the controller demonstrates a marked improvement in correcting for the large initial discharge. Although the oscillation pattern still exists, the magnitude of the pattern has decreased by roughly 30%. Figure 7.13b suggests the frequency of the pattern has decreased which indicates the controller is working more effectively. The tests yielded an average output and average error of 231.7 and 44.1 lb. respectively, with a corresponding 20.0% error.

Figures 7.14a and 7.14b illustrate the dynamic system response when a K_c of 0.010 inch/lb. is used. Figure 7.14a shows the controller had difficulty in correcting for the initial discharge, while Figure 7.14b shows the controller had little difficulty. The resurgence of the oscillation pattern in Figure 7.14b is the same type of trend which appeared in the static results for a K_c of 0.012 and 0.010 (Figures 7.8a, 7.8b, 7.9a, and 7.9b). The tests yielded an average output and average error of 237.9 and 52.6 lb. respectively, with a corresponding 23.9% error. Due

to the repeated high error results and the reappearance of the oscillation pattern in Figures 7.14a and 7.14b, no more dynamic tests were performed.

The dynamic test results can be summarized in Figure 7.15 and Table 7.3, which shows the optimum K_c equal to 0.011 inch/lb. with the lowest average error. Although not many values were tested, the trend of the results suggest there is an optimum between 0.010 and 0.012. The overall results show there is again a nonlinear relationship between the average error and K_c . Table 7.3 lists the average output and average error for all dynamic tests. In all of the tests the controller demonstrates a high repeatability in the system output. This is based upon the fact that the average error values for each test for a given controller gain are all within 15.2 lb. of each other. Based upon these tests, using the optimum K_c of 0.011 for dynamic conditions, the control system will operate with 20.0% error.

Again, all of the data points in Figures 7.11a - 7.14b represent individual discrete system responses. The points have been joined by a line to more clearly illustrate the presence or absence of the oscillation pattern. They are not to be interpreted as a continuous system response.

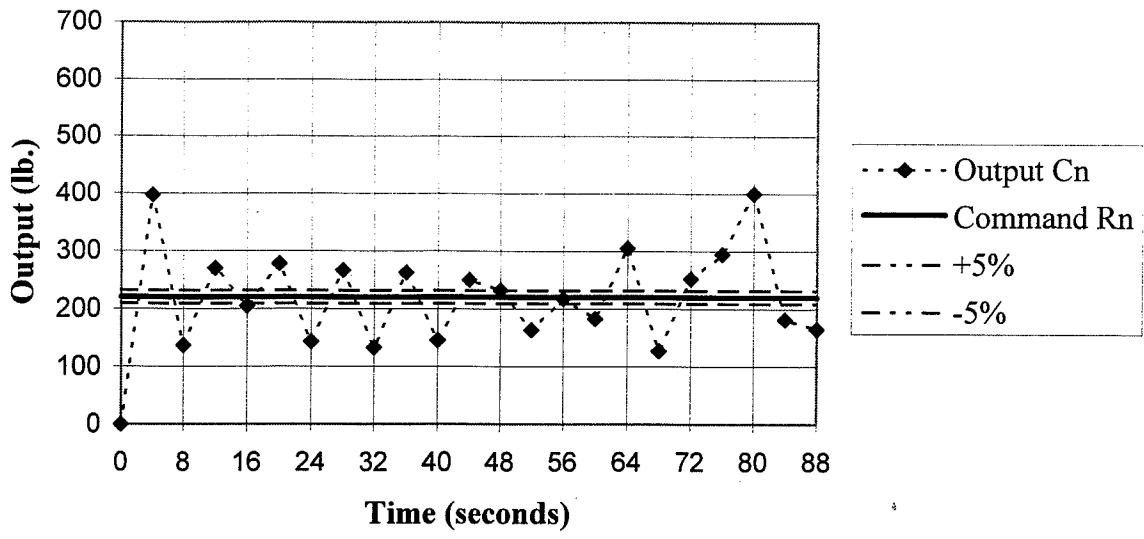


Figure 7.11a: Test #1: System response to dynamic test using a K_c of 0.013 inch/lb.

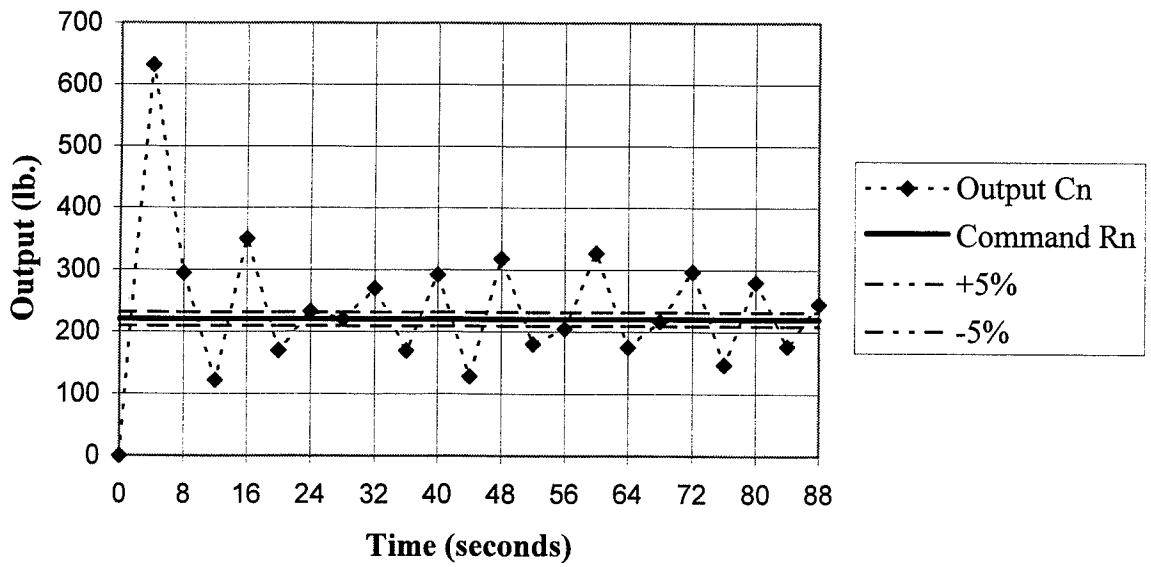


Figure 7.11b: Test #2: System response to dynamic test using a K_c of 0.013 inch/lb.

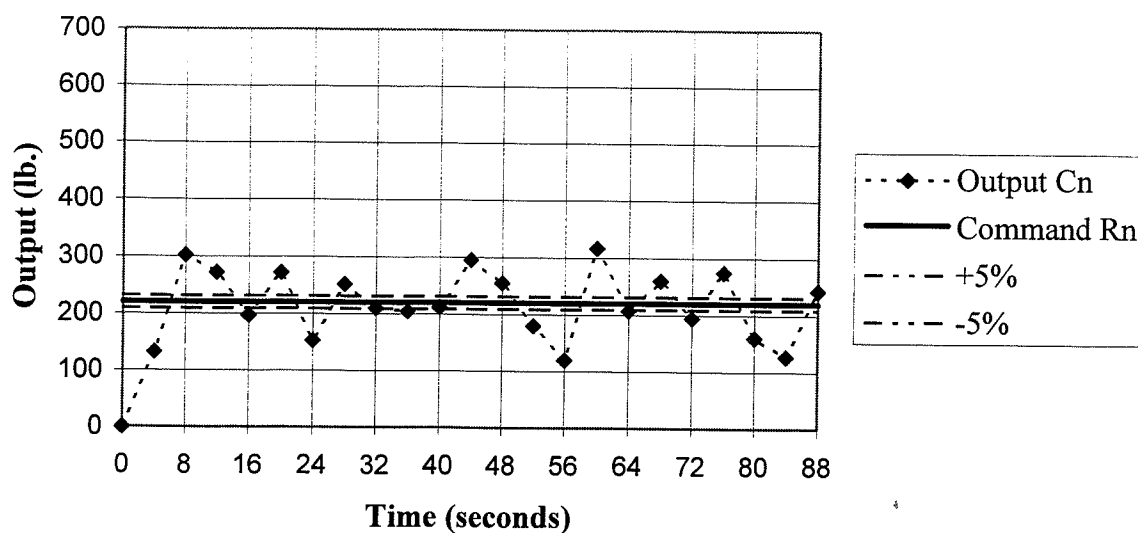


Figure 7.12a: Test #1: System response to dynamic test using a K_c of 0.012 inch/lb.

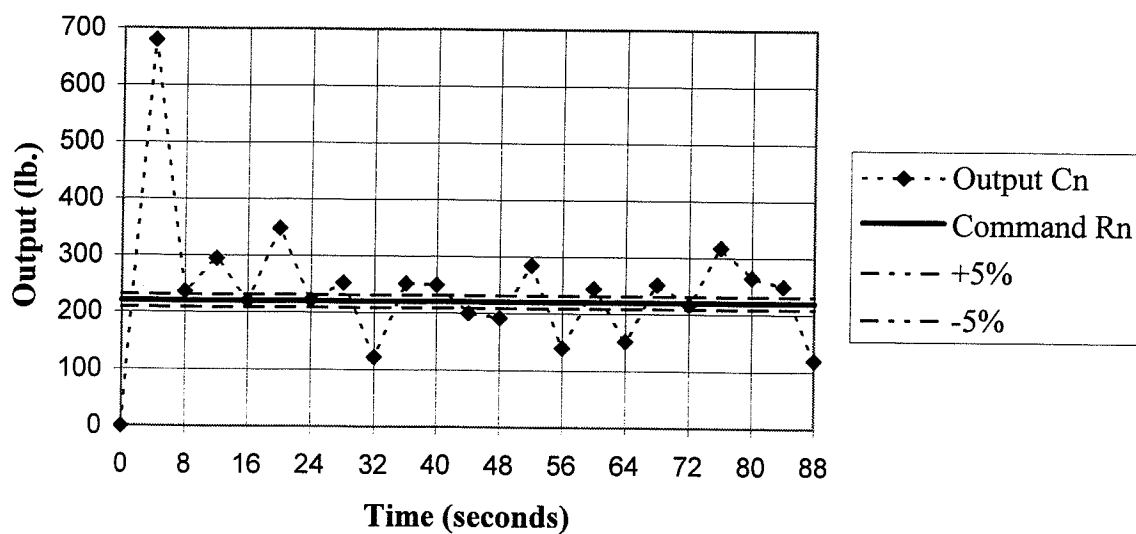


Figure 7.12b: Test #2: System response to dynamic test using a K_c of 0.012 inch/lb.

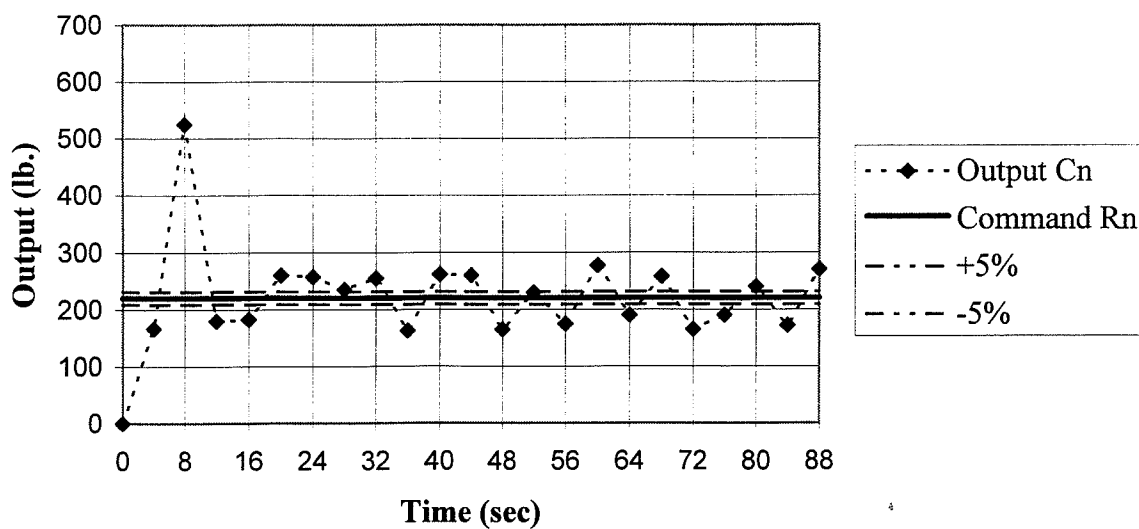


Figure 7.13a: Test #1: System response to dynamic test using a K_c of 0.011 inch/lb.

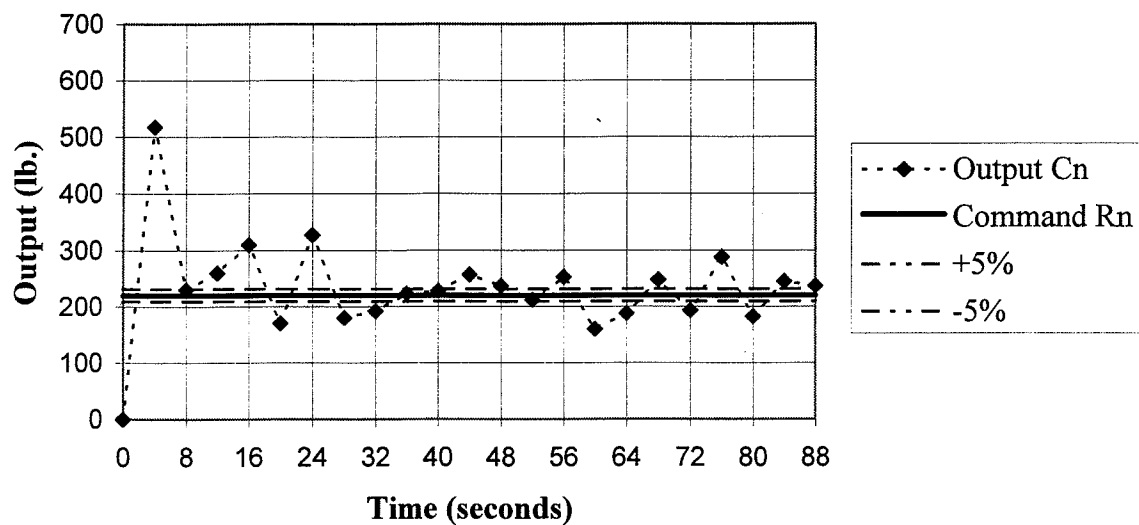


Figure 7.13b: Test #2: System response to dynamic test using a K_c of 0.011 inch/lb.

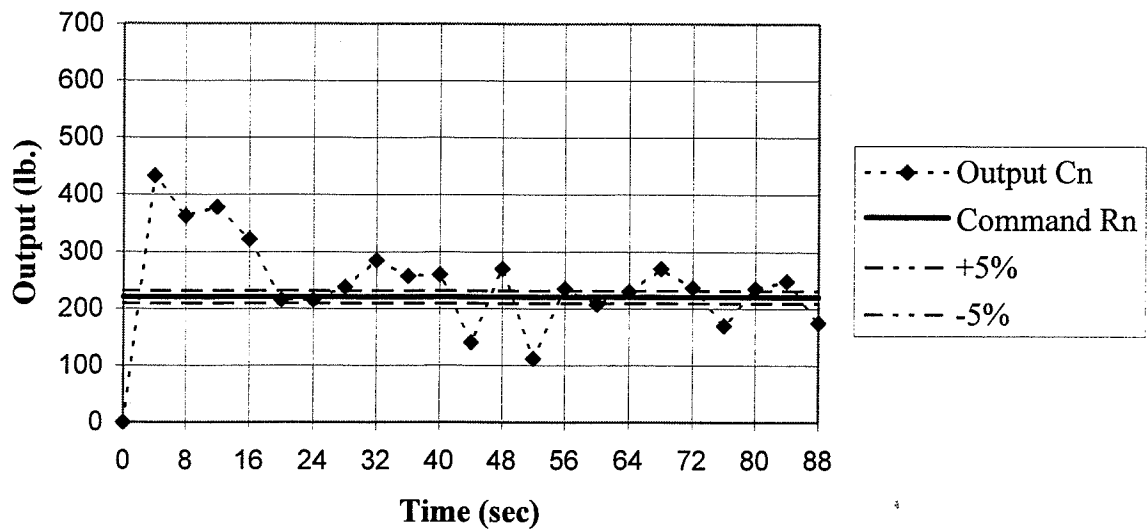


Figure 7.14a: Test #1: System response to dynamic test using a K_c of 0.010 inch/lb.

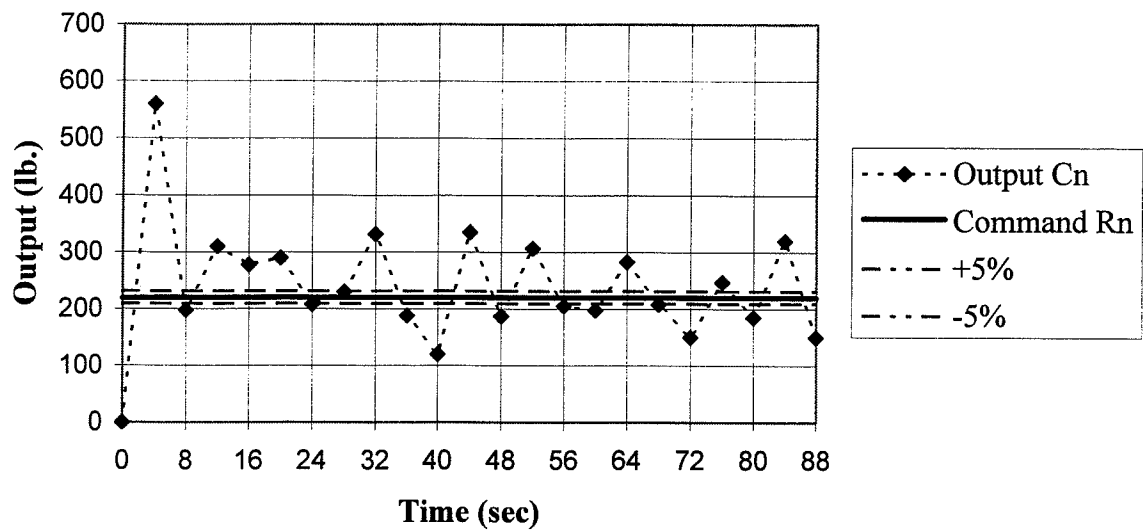


Figure 7.14b: Test #2: System response to dynamic test using a K_c of 0.010 inch/lb.

Table 7.3: Summary of dynamic controller test results.

Controller Constant, K_c (inch/lb.)	0.013	0.012	0.011	0.010
Average Output Test #1 (lb.)	219.7	224.2	233.9	241.0
Average Output Test #2 (lb.)	229.4	230.2	229.5	234.7
Average Output for Both Tests (lb.)	224.6	227.2	231.7	237.9
Average Error Test #1 (lb.)	58.6 (26.6%)	47.5 (21.6%)	51.7 (23.5%)	50.2 (22.8%)
Average Error Test #2 (lb.)	57.9 (26.3%)	48.1 (21.9%)	36.5 (16.6%)	55.0 (25.0%)
Average Error for Both Tests (lb.)	58.3 (26.5%)	47.8 (21.7%)	44.1 (20.0%)	52.6 (23.9%)

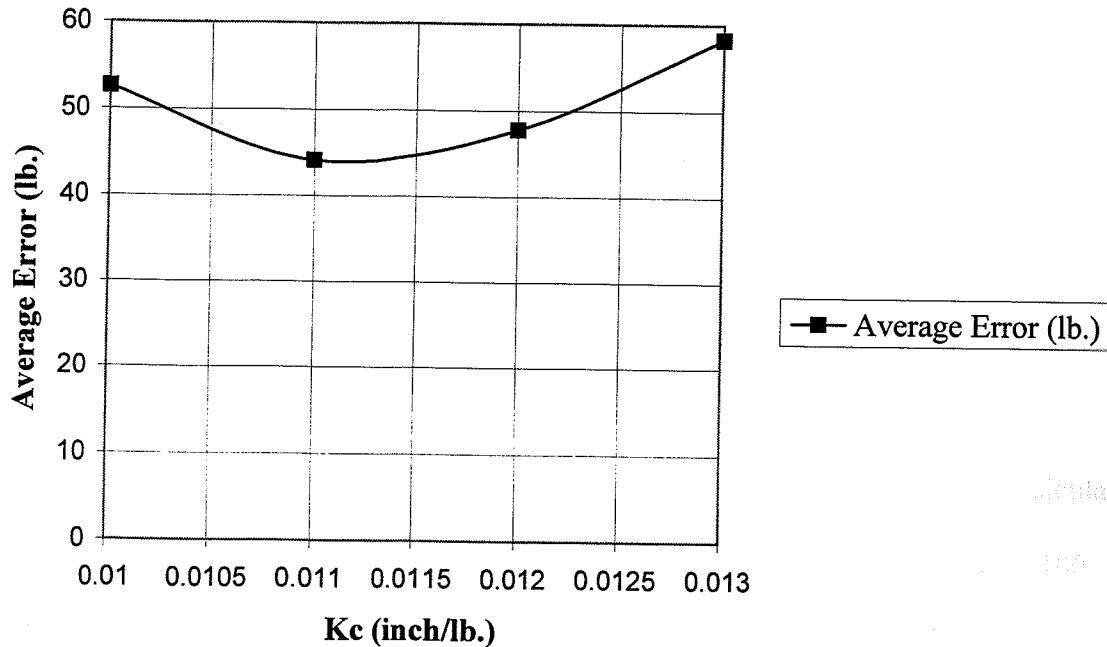


Figure 7.15: Plot of dynamic control test results.

7.5 Controller Precision

The microcomputer's limited integer mathematical capabilities did not compromise the controller's precision. By multiplying a sensor input by 10, one decimal point of precision can be gained in the next calculation involving the inputted term. Likewise, if a sensor's input is multiplied by 100, two decimal points of precision could be gained in the following calculation. The only adverse effect to increasing the precision level of the calculations is the memory required to perform the calculations with larger integer terms. However, if the proper inputs are scaled, the memory demands are only a small concern. For example, consider the following floating point application rate calculation for a discharge of 55 lb./sec, a ground speed of 3 ft/sec, and a spread width of 40 ft.

$$55 \frac{lb}{sec} \cdot \frac{1 \text{ sec}}{3 \text{ ft}} = 18.33 \frac{lb}{ft}$$

$$18.33 \frac{lb}{ft} \cdot \frac{1}{40 \text{ ft}} = 0.46 \frac{lb}{ft^2}$$

$$0.46 \frac{lb}{ft^2} \cdot 21.78 \frac{\frac{tons}{acre}}{\frac{lb}{ft^2}} = 10.02 \frac{tons}{acre}$$

By carrying out each portion of the calculation to two decimal places, the calculated application rate is 10.02 tons/acre. If the 55 lb./sec discharge rate is multiplied by 100, the same level of precision can be obtained with only a slight error in the calculated application rate. An example of how the controller performs the application rate calculation using a 100x scaling follows.

$$5500 \frac{lb}{sec} \cdot \frac{1 \text{ sec}}{3 \text{ ft}} = 1833 \frac{lb}{ft}$$

$$1833 \frac{lb}{ft} \cdot \frac{1}{40 \text{ ft}} = 45 \frac{lb}{ft^2}$$

$$45 \frac{lb}{ft^2} \cdot 22 \frac{\frac{tons}{acre}}{\frac{lb}{ft^2}} = 990 \frac{tons}{acre} = 9.90 \frac{tons}{acre}$$

The controller calculates the application rate to be 990 tons/acre, which is 9.90 tons/acre scaled by 100. This only amounts to a 1.20% error between the calculated integer rate and the floating point rate. If all of the other necessary inputs or variables are scaled properly, the desired level of precision can be carried throughout the entire controller operation. Although this will require more memory, the controller can be programmed to manage its memory resources. A 100x scaling was used when programming the controller, which rendered the controller's precision to two decimal places.

CHAPTER 8

CONCLUSIONS

8.1 Spreader Performance

The spread pattern tests helped to quantify the spread pattern as well as yield valuable information regarding the spreader's distribution for various types of manure. The important findings were: devising a correlation between the moisture content of the manure and the pattern's spread width, deriving a general distribution curve and an overlap dimension for different classes of manure, and identifying bridging problems which occur due to the design of the spreader's discharge system.

By collecting the spreader's discharge on plastic sheets as it was operated through a field, the spread patterns for low (35.0%), medium (61.2%), and high (78.5%) moisture manures were quantified for different spreader gate height openings of 10, 8, and 6 inches. In analyzing the spread pattern distributions, it was apparent the spread width of each pattern varied with the moisture content. As the moisture level increased, the spread width dimension also increased. The results of the spread pattern tests were used to develop a linear correlation between the moisture content and the spread width. The spread width was statistically determined to vary with moisture content using the following equation:

$$\text{Spread Width} = 0.348 (\text{feet}/\%) \cdot \text{Moisture Content (wet basis)} + 13.079 (\text{feet})$$

Averaging the tests results of each different combination of spreading parameters yielded representative spread pattern distributions for each moisture content level. These representative distributions were used to derive an individual overlap dimension for the various classes of tested manures. Numerical manipulation of these distributions for each manure class all resulted in a 15 foot overlap dimension. Although the pattern's spread width can be calculated using the previous equation, the 15 foot overlap dimension is a more significant number in terms of achieving an uniform application.

This dimension is to be used as a guideline in spacing the discharge intervals when spreading manure in the field. Specifically, adherence of the 15 foot overlap can approach an uniform application within 12% for the tested manures. This value is essential for calculating the spreader's measured on-the-go application rate. Although the spread width varied with moisture content, it is important to note the spread width did not change for varied spreader gate height openings (10 to 6 inches). This was an important finding used in the overlap analysis and the design of the controller.

The other important piece of information discovered during the course of the spread pattern tests was the occurrence of bridging in the spreader's operation. It is believed these momentary disruptions in the spreader's discharge were directly linked to the variations found in the spread distributions. Bridging exists due to the physical interaction between the manure and the spreader's discharge system. Although there were only slight occurrence of bridging in fresh manures, bridging was a major problem when spreading intermediate to dry

manures. This problem can only be addressed with the proper redesign of the discharge system. Until the spreader manufacture makes the revisions, this problem will remain inherent in the spreader's operation and cause irregularities in the spread distributions.

8.2 Controller Performance

The controller demonstrated reliability and gave repeatable results. The overall mechanical and electrical performance of the various sensors and control components proved to be very adequate under field conditions encountered. The spreader's modified mechanical designs withstood over 150 hours of field testing without showing any signs of wear or fatigue, while the weight, speed, and position sensors consistently gave accurate measurements. The microcomputers used in the controller design demonstrated they were capable of inputting and processing the sensor's measurements as well as having an effective means of developing and programming the controller's logic code.

The controller tested under static conditions with a controller gain, K_c , of 0.013 inch/lb. was able to control the spreader's discharge rate of fresh manure within 10.5%. Being satisfied with the preliminary static results, the controller was tested under dynamic conditions using the same K_c value. This value proved to be too high, since it caused unacceptable oscillations about the commanded discharge rate. Lower values of K_c were tested and the results indicated a K_c value of 0.011 inch/lb. was near the optimal value. The controller under dynamic conditions experienced a 20.0% error.

These test results indicate dynamic field forces degrade the controller's accuracy by a factor of 1.9. The use of two different K_c values for static and dynamic conditions supports this idea. Using lower values of K_c causes the gate height manipulations to be less, which causes less dramatic change in the discharge rate. This helps to better regulate the spreader's discharge when the controller is measuring larger weight fluctuations due to measured ground forces. Assume the discharge is relatively constant ($\pm 10\%$) under static conditions, the controller will only control for the small fluctuations in the discharge within a certain band of error. Assuming the same discharge parameters under dynamic conditions, the controller must control fluctuations of about 1.9 times as much ($\pm 19\%$) because of the ground forces. Moving the gate less for the calculated manipulation enables the controller to dampen out a portion of the ground forces when controlling the spreader's discharge. However, lowering K_c does not effectively remove all the dynamic weight fluctuations to increase the accuracy to that of static conditions.

Although the controller did not meet the project accuracy goal of $\pm 5\%$ under dynamic field conditions, this research demonstrated off-the-self technology could be incorporated into a manure spreader to measure and control its discharge rate. It also quantified the spreader pattern for various manures, which helped to develop a 15 foot overlap dimension operators can use to spread manure to insure an uniform application rate.

CHAPTER 9

RECOMMEDATIONS FOR FUTURE RESEARCH

9.1 Spreader Recommendations

To lessen the occurrence of irregularities in the spread pattern distribution, the most advisable thing would be to eliminate or reduce the bridging effect. One way to do this is to introduce one or two auger(s) into the discharge system. The auger(s) should be placed near and parallel to the side wall(s) of the V-bottom tank. This would prevent the manure from getting stuck on the tank wall(s) and provide a continuous flow of manure to the expellers. This multiple auger discharge system is currently offered on side discharge spreader's offered by other manufactures. Reduction of the bridging depends on the number of augers added to the current discharge system.

Another way to improve the uniformity of the spread pattern is to look at a different ways of expelling the manure. Although this spreader gives a consistent spread width within the tested 10 to 6 inch gate height opening range, the spread width varies non-linearly with the gate height opening. To combat this interaction, a second gate could be placed at the exit of the discharge chute. This gate would limit the amount of manure exposed to the expeller by sliding forward and backward over the opening. This way, the vertical gate could be placed in a stationary position while the horizontal gate could control the amount of manure expelled from the spreader. A second way to alter the discharge pattern would be to move the discharge chute from the side of the machine to the rear of the machine. Additionally, replace the horizontal expeller with two sets of vertical expellers. This configuration with a

vertical gate preceding the set of expellers would more likely give an uniform semicircular discharge. The presence of an overlap dimension would still have to be employed, but the uniformity could be greatly improved.

9.2 Controller Recommendations

Although it did not cause any significant problems with the controller function, the current speed system should be improved. The interaction between the spreader's wheel and the input wheel can be easily altered by dirt and debris that becomes attached to the input wheel. The build up of material makes for a noncircular circumference, which changes the 10 to 1 ratio between the two wheels. To hold the relationship nearly constant, a perforated disk or sprocket should be used in conjunction with a magnetic reluctance pick-up which was described in Chapter 3. This will yield a constant relationship between the size of the disk or sprocket and the spreader's wheel. Just as with the current system, it will not be able to adjust for radius fluctuations. This is why an average rolling radius value will still have to be used.

To improve controller results, another control scheme should be employed. Although a P controller is the simplest to employ, it is not suitable for every control application. Even though the spreading discharge tests concluded the spreader's discharge system could be modeled as an integer process model, the model did not include the presence of disturbances in the form of bridging. To design a controller to combat this, a proportional-integer (PI) controller should be designed. This type of controller uses the present error and the error from one previous sample period to calculate the corrective manipulation. Since part of the

controller is proportional, part of the manipulation will be purely proportional. The other part of the manipulation will be proportional to the time integral of the error.

The PI controller is very effective when disturbance rejection is desired. The system response with a PI controller will reduce the oscillation pattern that was consistently present in all of the test results. In addition to reducing the oscillation error, the PI controller guarantees zero steady state error. This means that if the spreader had a constant discharge rate, the outputted discharge rate would be controlled to exactly match the commanded discharge rate after so many time periods. The responsiveness of the matching would depend on the values used for K_p and K_i , the proportional constant and the integral constant respectively.

The only downfall to using this type of controller is the system response to step inputs is not as quick and responsive as a dead-beat controller. This would be seen when the system is first turned on and made to correct for the large initial discharge rate in the static and dynamic tests. Given the P controller results, the initial control manipulations could be sacrificed for an overall improvement in system accuracy.

To implement the PI controller, the existing controller configuration involving the two microcomputers would have to be altered. Because the PI controller requires the current as well as the past system error, the controller would have to store the previous error value for future calculations. This requires the addition of another microcomputer. Since the current

design has both computers running at maximum memory capacity, another computer is needed to help divide each computer's tasks and reduce the memory required.

The proposed PI design would not be much different than the current design. The Stamp #1 computer would only handle the weight input, averaging calculations, and output to Stamp #2 computer. Stamp #2 would be responsible for measuring the speed and calculating the application rate and system error. It would also pass the system error to Stamp #3. Stamp #3 would input the error and calculate the PI manipulation using the newly inputted error and the stored error from the previous sample period. Based upon this calculation, it would measure and control the gate height.

With this design, more memory is allocated to each computer to perform more demanding tasks. This will help to reduce the ground force effect of the measured weight data. With more memory available, the Stamp #1 computer could be programmed to do more averaging of the weight data or introduce back averaging of the data which was found effective in previous research by Loehr (1996).

A final recommendation for future research would be to use a limiting orifice on the hydraulic line between the gate cylinder and the DCV. By slowing down the velocity of the gate, the controller would have enough time to accurately check the gate position and turn off the valve to prevent any further cylinder movement. This would remove a set of logic

conditions in the controllers programming, which would increase the processing speed of the controller and insure the gate is moved to the correct control position.

REFERENCES

Bollinger, J., and Duffie, N. 1989. Computer Control of Machines and Processes. New York: Addison Wesley.

Dorf, R., and Smith, R. 1992. Circuits, Devices, and Systems. 5th ed. New York: Wiley and Sons.

Ess, D. R., and Morgan, M. T. 1996. Sensors for Tomorrow's Precision Agriculture. In International Off-Highway & Powerplant Congress & Exposition, 9611760. Warrendale, PA: SAE

Smith, G., and Willrich, T. 1972. Agricultural Practices and Water Quality. Ames, Iowa.: The Iowa State University Press.

Kurtz, J.A., and Neher, N. 1995. Protecting and improving water quality through better manure management in Wisconsin. Wisconsin Department of Natural Resources, Animal Waste Advisory Committee. Madison, WI.

Loehr, R. 1996. Development of Systems to Accurately Measure Application Rate of Waste Spreaders. MS, thesis, University of Wisconsin - Madison, 1996.

Norwak P. 1994. Natural Resources Report, Fall 1994. University of Wisconsin - Madison School of Natural Resources.

NPM-Nutrient and Pest Management. 1993. The Bottom Line: An Economic Summary of Nutrient and Pest Management Practices. University of Wisconsin - Extension. Madison, WI.

NPM- Nutrient and Pest Management. 1994. Nutrient Management: Practices for Wisconsin Corn Production and Water Quality Protection. University of Wisconsin - Extension, Madison, WI.

Smith, J. 1994. Tough Decisions: Regulators tackle ag-related water pollution. Natural Resources Report. UW-Madison School of Natural Resources. Madison, WI.

Sturgal, S. 1996. Personal Interview. UW-Extension Nutrient and Pest Management Program. Madison, WI.

Sheingold, D., ed. 1980. Transducer Interfacing Handbook. Norwood, Mass.: Analog Devices.

WDATCP. WA/0045, 1996. Wisconsin 1996 Agricultural Statistics.

APPENDIX A

ZENER-DIODE VOLTAGE REGULATOR CALCULATIONS

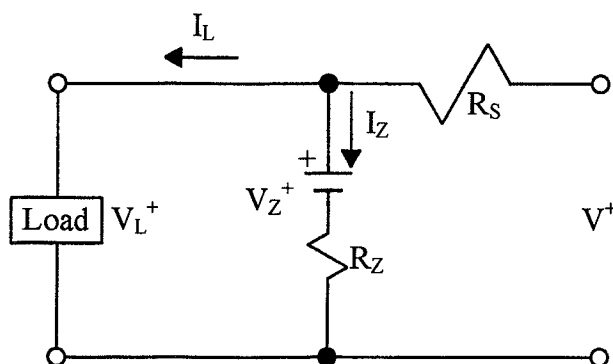


Figure A-1: Performance of a voltage regulator.

The encoder draws a current varying from 45 to 36 mA at a nominal voltage of 12 Vdc. A regulator consists of $R_s = 390 \Omega$ and a Zener-diode represented by $V_Z = 4.3 \text{ Vdc}$ and $R_Z = 37 \Omega$ (Figure #1). For $I_L = 15 \text{ mA}$, it is desired to determine the variation in DC input voltage V^+ which would correspond to maximum threshold voltage (5 Vdc) of the PARRALAX Stamp computer.

To place the diode well into the Zener breakdown region, it is suggested to use a minimum current $I_{Z(\min)} = 0.1 I_L = 0.1 \times 45 = 4.5 \text{ mA}$. Then

$$V_L = V_Z + I_Z R_Z = 4.3 + 0.0045 \cdot 37 = 4.5V$$

APPENDIX A

ZENER-DIODE VOLTAGE REGULATOR CALCULATIONS CONT.

and

$$V^+ = V_L + (I_L + I_Z)R_S$$
$$V^+ = 4.47 + (0.0150 + 0.0045)390 = 12.1V$$

If V_L increases to the 5.0 V threshold limit then

$$I_Z' = \frac{V_L' - V_Z}{R_Z} = \frac{5.0 - 4.3}{37} = 0.0189A$$

and

$$V^{+'} = V_L' + (I_L + I_Z')R_S$$
$$V^{+'} = 5.0 + (0.0150 + 0.0189)390 = 18.2V$$

Conclusion: For a change in V^+ of 6.1 V, there is only a 0.7 V change in V_L . Therefore, the computer's pulse processing circuit is protected for a maximum tractor battery output voltage of 18.2 Vdc.

APPENDIX B

SPREAD PATTERN TEST RESULTS

Dynamic Weight Test Results:

Table #1: Dynamic weight test results.

Moisture Content (%)	Gate Height (in.)	Estimated (lb.)	Discharged (lb.)	%Error
35.0	10	738.1	750	2%
35.0	10	578.8	580	0%
35.0	10	680.0	690	1%
35.0	8	679.1	680	0%
35.0	8	474.2	500	5%
35.0	8	469.4	500	7%
35.0	6	428.4	450	5%
35.0	6	354.2	370	4%
35.0	6	392.7	420	7%
61.2	10	389.1	420	8%
61.2	10	404.7	420	4%
61.2	10	382.9	400	4%
61.2	8	306.0	340	11%
61.2	8	326.2	370	13%
61.2	8	298.3	330	11%
61.2	6	297.6	340	14%
61.2	6	275.9	320	16%
61.2	6	285.4	340	19%
78.5	10	786.5	810	3%
78.5	10	669.1	630	-6%
78.5	10	697.4	700	0%
78.5	8	569.5	610	7%
78.5	8	633.2	650	3%
78.5	8	477.5	480	0%
78.5	6	322.6	360	12%
78.5	6	349.6	390	12%
78.5	6	314.6	360	14%

APPENDIX B

SPREAD PATTERN TEST RESULTS CONT.

Linear Correlation of Moisture Content and Spread Width:

Appendix B Table #2: Correlation of moisture content and spread width.

Moisture Content (%)	Maximum Spread Width (ft.)
35.0	25
61.2	35
78.5	40
Regression Variables	Regression Values ¹
Slope	0.348
Intercept	13.079
Correlation (R)	0.997

Appendix B Table #3: Calculated spread width distances using regression information.

Moisture (%)	Spread Width (ft)
30	23.5
35	25.3
40	27.0
45	28.7
50	30.5
55	32.2
60	33.9
65	35.7
70	37.4
75	39.2
80	40.9
85	42.6

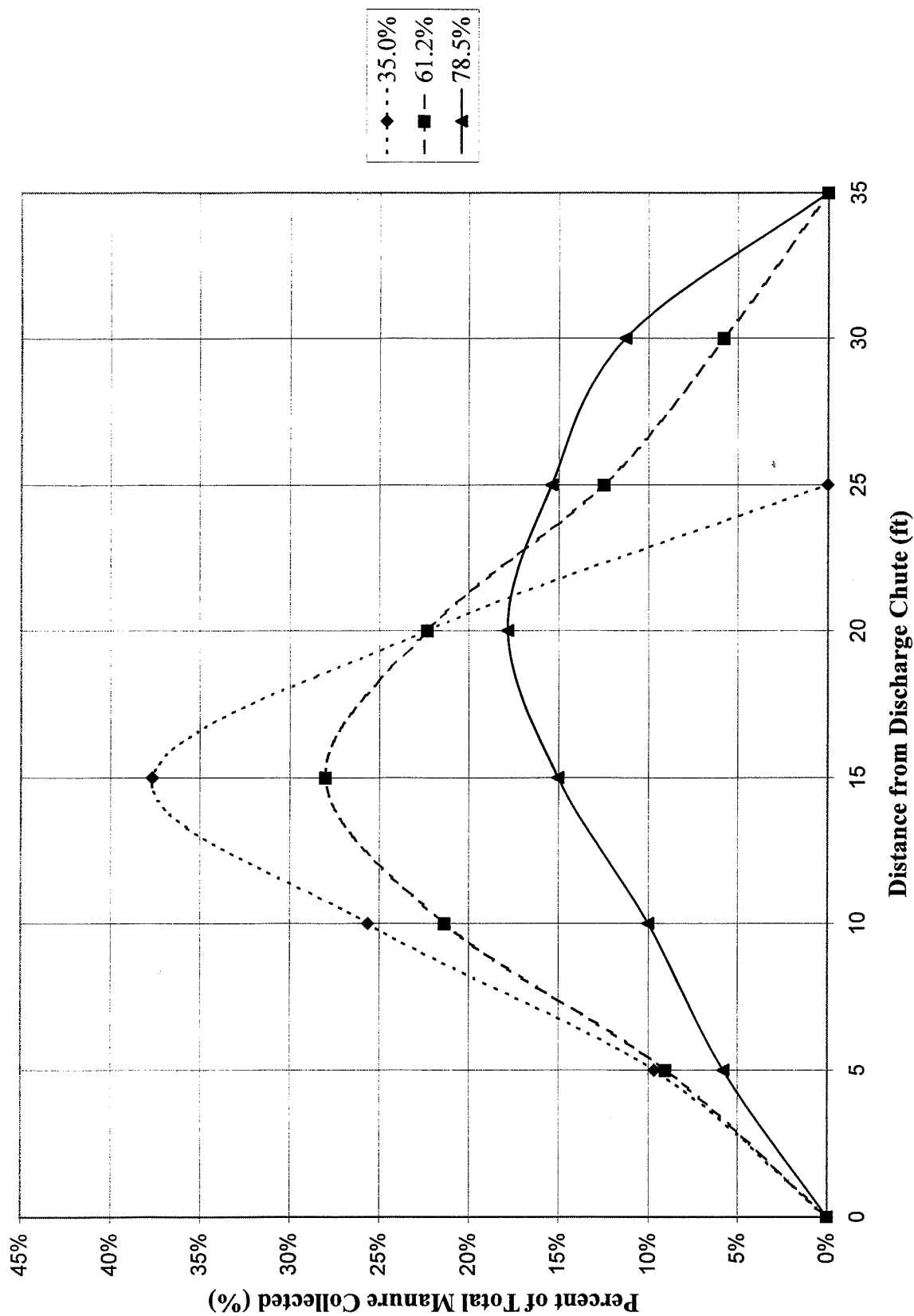


Figure B-1: Overlap plot of spread patterns for tested gate height range for various manure moisture contents used to develop 15 foot overlap dimension.

APPENDIX C

DISCHARGE DATA FOR FRESH MANURE

Linear Regression Information:

Appendix C Table #1: Linear regression data from discharge test using fresh manure.

Discharge Opening Height (Test #)	Discharge Rate (lb./sec)	Correlation for Test (R)
16 (1)	225.9	0.9990
16 (2)	211.7	0.9988
12 (1)	205.0	0.9997
12 (2)	202.4	0.9998
10 (1)	145.3	0.9997
10 (2)	155.3	0.9999
8 (1)	129.2	0.9997
8 (2)	133.8	0.9999
6 (1)	105.3	0.9998
6 (2)	102.1	0.9995

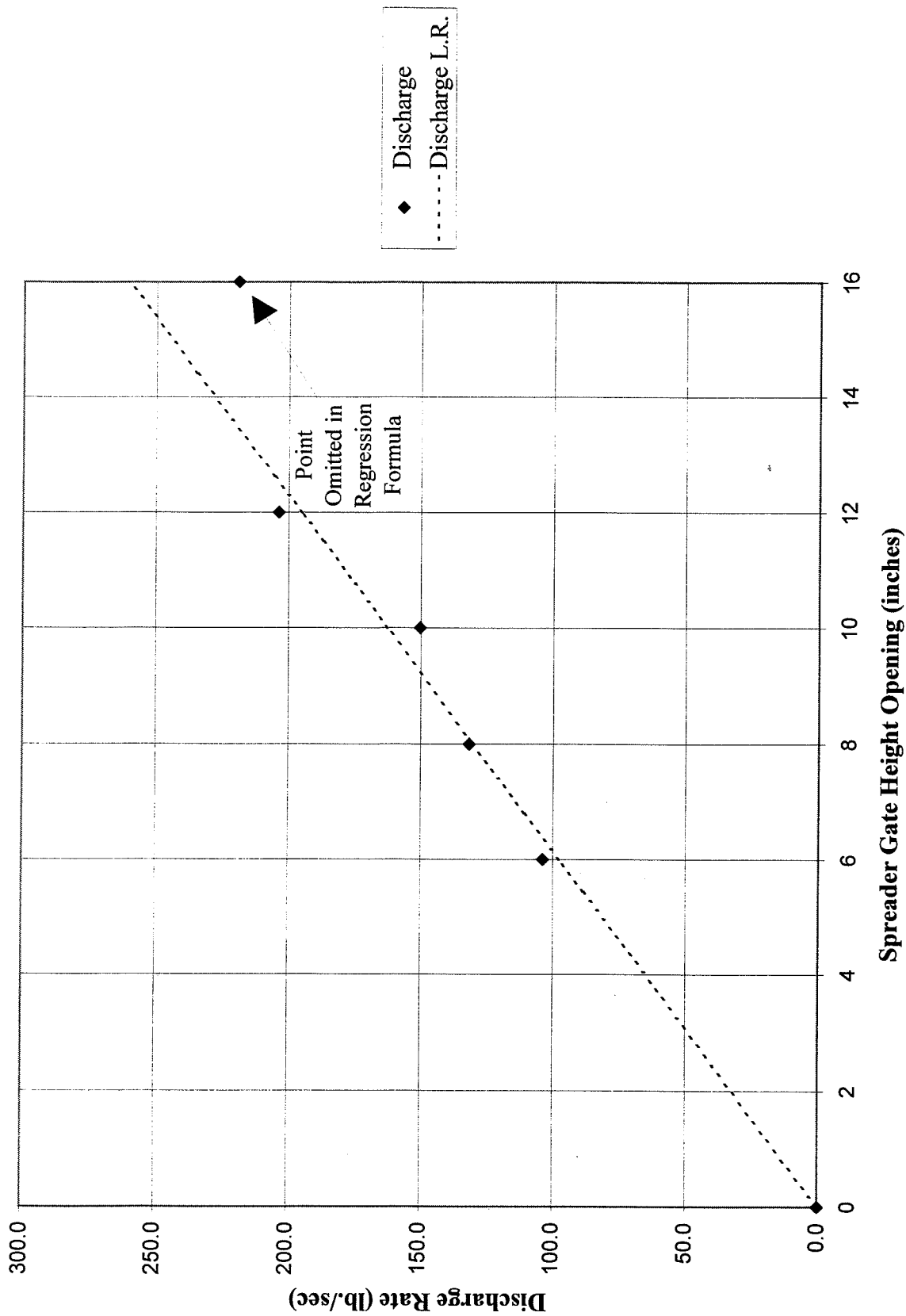


Figure C-1: Plot of linear regression of average discharge rates for fresh manure.

APPENDIX D

DERIVATIONS OF CONTROL EQUATIONS

Derivation of $G_p(B)$:

An example of an integer process to be controlled is described by

$$\frac{dc(t)}{dt} = Km(t)$$

where $m(t)$ is the manipulated process input variable, $c(t)$ is the process output variable, and K is a system constant. Assume that $c(0) = c_0$ at time = 0 and a constant input $m(t) = m_0$ for $0 \leq t \leq T$ is introduced. In this case,

$$c(T) = \int_{-\infty}^0 Km(t)dt + \int_0^T Km_0 dt$$

Integrating and using the initial conditions yields

$$c(T) = c_0 + Km_0T$$

Generalizing by the formal replacement of m_0 and c_0 with m_{n-1} and c_{n-1} respectively, and the replacement of $c(T)$ with c_n , produces the first order difference equation

$$c_n - c_{n-1} = K m_{n-1} T$$

Introduction of the B operator defined in Chapter 7 yields

$$c_n - Bc_n = KTBm_n \quad \text{or} \quad (1 - B)c_n = KTBm_n$$

Forming the ratio of output to input results in the discrete process transfer function

$$G_p(B) = \frac{c_n}{m_n} = \frac{KTB}{1 - B}$$

(Bollinger and Duffie, 1989)

APPENDIX D

DERIVATIONS OF CONTROL EQUATIONS CONT.

Derivation of $G(B)$:

The block diagram in Figure 7.1 can be used to obtain the closed-loop transfer function c_n/r_n and from it, the system difference equation. The closed-loop transfer function is:

$$G(B) = \frac{c_n}{r_n}$$

A step wise process shows the mathematics of how the complete transfer function is derived

$$c_n = G_p(B)m_n$$

$$c_n = G_c(B)G_p(B)e_n$$

Because $e_n = r_n - c_n$ at the sample times

$$c_n = G_c(B)G_p(B)(r_n - c_n)$$

Collecting like terms on opposite sides of the equation

$$c_n + G_c(B)G_p(B)c_n = G_c(B)G_p(B)r_n$$

Dividing through to get c_n in terms of r_n

$$c_n = \frac{G_c(B)G_p(B)}{1 + G_c(B)G_p(B)}r_n$$

The closed-loop transfer function is therefore:

$$G(B) = \frac{c_n}{r_n} = \frac{G_c(B)G_p(B)}{1 + G_c(B)G_p(B)}$$

(Bollinger and Duffie, 1989)

APPENDIX D

DERIVATIONS OF CONTROL EQUATIONS CONT.

Derivation of $G_c(B)$:

From the previous derivation of $G(B)$ it is known that the closed-loop transfer function is:

$$G(B) = \frac{G_c(B)G_p(B)}{1 + G_c(B)G_p(B)}$$

Multiplying the denominator of the right hand side by both sides of the equation yields

$$\{1 + G_c(B)G_p(B)\}G(B) = G_c(B)G_p(B)$$

Multiplying out both sides of the equation and collecting like terms yields

$$G_c(B)G_p(B) - G_c(B)G_p(B)G(B) = G(B)$$

Solving for $G_c(B)$ yields

$$G_c(B) = \frac{G(B)}{G_p(B) - G_p(B)G(B)}$$

Collecting $G(B)$ terms yields

$$G_c(B) = \frac{1}{G_p(B)} \frac{G(B)}{\{1 - G(B)\}}$$

Substituting values into the transfer function yields the result in the text.

$$G_c(B) = \frac{1}{G_p(B)} \frac{G_d(B)}{[1 - G_d(B)]} = \frac{B}{\frac{KTB}{1-B}} = \frac{1}{KT} = \frac{1}{64} \frac{lb}{inch} = 0.0156 \frac{inch}{lb}$$

(Bollinger and Duffie, 1989)

Approved: 

Richard J. Straub, Professor

Date: May 22 1997